Data analysis of estuarine dunes: Linking estuarine sand dune characteristics to environmental parameters

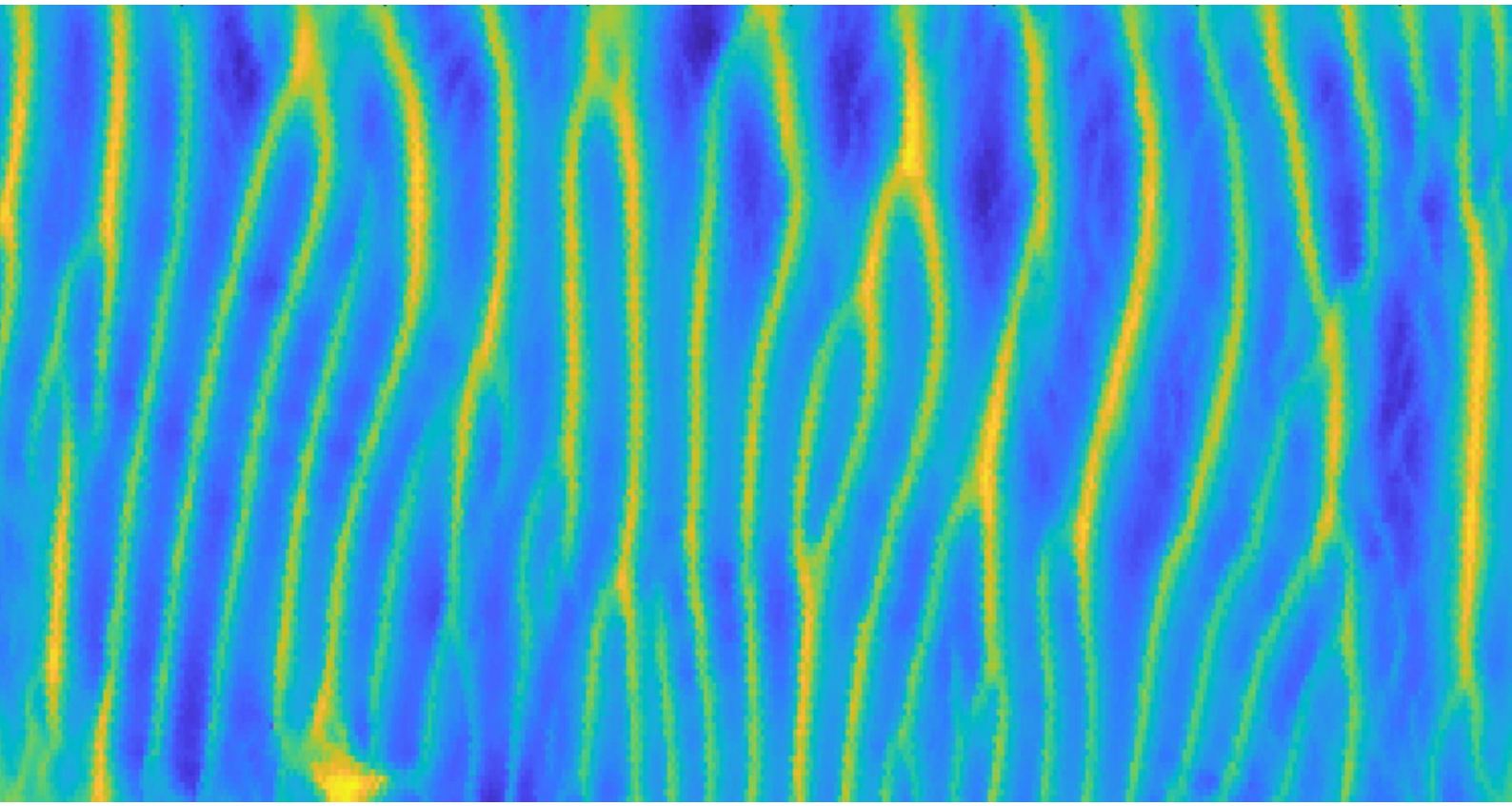

MSc Thesis

S.D. Muurman | August 2021

Final Version

UNIVERSITY OF TWENTE.

Colophon

This document is a Master Thesis to obtain a Master of Science in Civil Engineering and Management at the University of Twente.

Title:	Data analysis of estuarine dunes: Linking estuarine sand dune characteristics to environmental parameters.
Author:	Simon Dirk Muurman
Student number:	s1864777
Email:	s.d.muurman@student.utwente.nl
Version:	Final version
Date:	23-August-2021
University:	University of Twente Drienerlolaan 5 7522 NB, Enschede Faculty of Engineering Technology Department of Water Engineering and Management
Graduation committee	
Head of committee:	Prof.dr. S.J.M.H. Hulscher
Committee member:	Dr.ir. P.C. Roos
Daily supervisor:	Ir. L.R.Lokin
Daily supervisor:	Ir. W.M. van der Sande

Abstract

Estuaries form the transitional region between a river and the sea. Estuaries are important both from an economical and environmental standpoint. They are rich in intertidal area and biodiversity and form a gateway between the marine and the riverine environment, creating ideal harbor locations.

In estuaries, dunes are often found. Dunes are rhythmic features that exist on the bed. They can limit navigation depths and alter the flow structure and sediment transport. To better understand the dynamics of estuarine dunes, this study analyses the relation between dune characteristics and environmental parameters. The goal of the study is to explain the dune length, height and asymmetry based on the water depth, tidal asymmetry, river discharge and sediment grain size. To this extent, bed level and environmental data is available of the Western Scheldt and the Elbe estuary. Furthermore, the results of a hydrodynamic model of the Scheldt estuary are available to characterize the flow properties in the Western Scheldt.

In the Scheldt and Elbe estuary, the Antwerp and Hamburg port are located which are two of the three largest ports of Europe. The Western Scheldt is characterized by ebb and flood channels and a relatively weak influence of the river discharge. The Elbe estuary is characterized by a single channel and a significant discharge with a seasonal variation. Furthermore, the bed level data available for the Western Scheldt is extensive in space but scarce over time. The opposite holds for the Elbe where a smaller area of bed level data is available with a greater temporal resolution. The focus in the Western Scheldt is therefore set on the spatial variability of estuarine dunes and environmental parameters while the Elbe is mostly analysed for temporal correlations. In the Western Scheldt, three study sites are selected of which the bed level is mapped twice each in the period 2017-2019. In the Elbe, a single study location is selected where the bed level is measured 60 times in the period 2012-2014. The bed level of both estuaries is mapped using multibeam echosounders.

Dune characteristics are extracted from the bed level data using a developed bedform tracking tool. Environmental data is processed in order to obtain the average water depth, river discharge and flow velocity asymmetry prior to the bed level measurements.

The results of this study show a positive weak correlation between water depth and dune height in the Elbe study location, and water depth and dune length in the Western Scheldt. Since the dunes in the Elbe and Western Scheldt study locations exist in the same range of water depth, these obtained correlations were not able to explain the differences in dune length and height of the Elbe compared to the dunes of the Western Scheldt. Two study locations in the Western Scheldt showed differences in dune height and length. These dunes also exist in the same water depth range. Additionally, the median grain sizes of these study locations are very similar and can therefore not be used to explain differences in dune characteristics.

The most prominent finding in this study is the relation between dune asymmetry and the environmental conditions. In the Western Scheldt, a strong correlation is observed between the peak current asymmetry and the dune asymmetry. Study locations in ebb channels, where the velocity asymmetry is ebb directed, also showed dunes which are ebb-directed, and vice versa. In the Elbe, the dunes fluctuate over time, being asymmetric in landward and seaward direction. This fluctuation is also observed in the velocity asymmetry of the Elbe. Furthermore, in the Elbe, a strong correlation is found between the river discharge and the dune asymmetry. High discharge events cause the dunes to deform and be asymmetric in seaward direction. It is hypothesized that during low discharge events, the salinity gradient shifts further land inward, causing gravitational circulation in the study area. The hypothesis is that this gravitational circulation causes the dunes to grow asymmetric in landward direction during low discharge events.

Preface

This report is the result of my Master Thesis for the Master Civil Engineering with a specialization in River and Coastal Engineering. This research was conducted from February to August 2021 at the University of Twente under the supervision of Suzanne Hulscher, Pieter Roos, Lieke Lokin and Wessel van der Sande.

What better way than to spend the corona lockdown, where you are supposed to stay inside anyway, conducting a master thesis research project. It has not always been easy. Especially finding a way through the simultaneous abundance and scarcity of data. Therefore, I would like to thank my team of supervisors for guiding me through this process. A special thanks goes to Wessel and Lieke for meeting with me every Monday morning to review the progress of the previous week and to set the goal for the next week. It was very helpful to discuss ideas and to set the focus step by step.

Additionally, I would like to thank Jebbe van der Werf for providing me with the modelling result of an earlier study of his. The data of this model enabled me to dive deeper into the environmental characteristics of the Western Scheldt and compare them to those of the Elbe estuary. Without this dataset, a large part of my study would not have been possible.

Finally, I would like to thank my girlfriend, family, and friends. You guys were always ready to listen to struggles or successes even though estuarine morphology it is not your particular field of expertise.

I hope you enjoy reading.

Simon Muurman

Enschede, July 9, 2021

Content

1. Introduction

In this chapter, an introduction of the study is provided. First, the background information is described. Then, the research goal of the study is set up along with the posed research questions. Afterwards, the general methodology of the study is defined after which the structure of the report is elucidated.

1.1 Background

1.1.1 Estuaries

Estuaries are bodies of water that are partially enclosed by land and are characterized by the mixing of fresh river water with saline ocean water (Vilas et al., 2015). The term estuary is derived from Latin, where romans used the word “aestuarium” to refer to the tidal-influenced part of a river (Flemming, 2011). Estuaries form the transition between the marine and riverine environment and serve many economic and ecological purposes. Due to their transitional positioning between sea and land, estuaries are often used as harbour entrances. Think of the three busiest ports in Europe; the port of Rotterdam, Antwerp and Hamburg which are situated in the Rhine-Meuse, Scheldt, and Elbe estuary, respectively. Furthermore, the intertidal areas in estuaries form ecologically valuable habitats and the land surrounding an estuary is often densely populated (e.g. Leuven et al., 2019). All in all, estuaries are valuable regions both from an ecological viewpoint as well as an economical perspective

Estuaries form fluvial-marine transitions and are therefore influenced both by the forcing of the sea as well as by the forcing of the river, making them complex systems (Dalrymple & Choi, 2007). Since they form the transitional region between a river and the sea, estuaries have characteristics of both these environments. Estuaries resemble rivers since they have banks on both sides and flowing water that occasionally causes floods. On the other hand, estuaries are influenced by tides and saline water, which are typical marine characteristics (Savenije, 2012).

Hydrodynamic Forcing

The dominant hydrodynamic forcing in an estuary depends on the location in the estuary and ratio of the driving forces. Dalrymple & Choi (2007) give a schematic representation of the dominant forcing in an estuary (Figure 1). In Figure 1 can be seen that at the downstream end of the estuary, the oscillatory tidal currents are dominant in combination with the surface waves. At the upstream end, the unidirectional river forcing is dominant. These boundaries of riverine and marine dominated areas are however not constant. In the spring-neap cycle of the tide, the tidal forcing fluctuates resulting in a shifting marine-dominated area. The same holds for varying discharges resulting in a variable river dominated part.

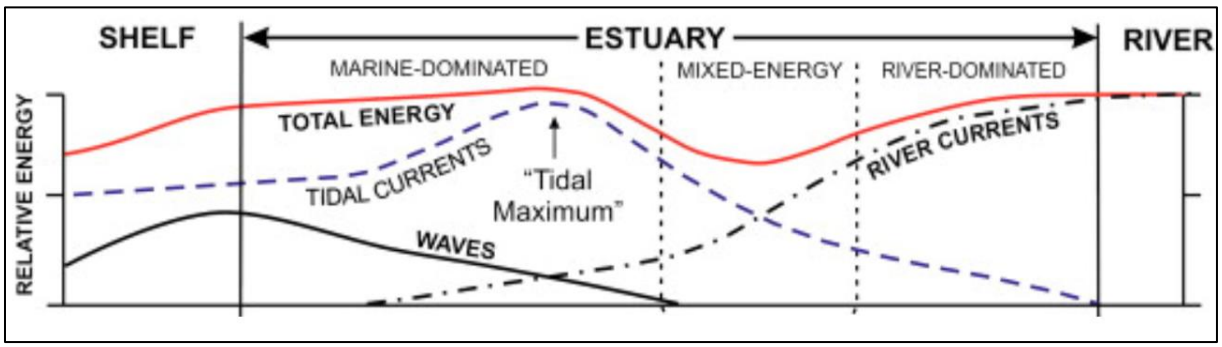

Figure 1: Schematic representation of dominant driving force transition in an (tide dominated) estuary (Dalrymple & Choi, 2007).

Hypersynchronous

A notable feature in Figure 1 is that the hydrodynamic forcing of the tidal current increases when moving upstream until the "tidal maximum". This is a characteristic of so-called hypersynchronous estuaries and is a result of the narrowing effect of an estuary. Naturally, estuaries have a funnel shape where the width of the estuary decreases "exponentially" when moving upstream (Langbein, 1963). A tidal wave entering this funnel shape is compressed into an exponentially smaller cross-section causing the tidal amplitude to increase. At a certain point, the added friction of the estuarine bathymetry will outweigh the narrowing effect and the tidal amplitude will decrease again (Dalrymple & Choi, 2007). In hyposynchronous estuaries, the dampening of the tidal wave caused by the friction already outweighs the amplification caused by narrowing effect of the estuarine mouth. In such a system, the tidal amplitude only decreases moving landward and no tidal maximum is present. Estuarine systems that are tide-dominated generally display a hypersynchronous behaviour (Dalrymple & Choi, 2007).

Gravitational circulation

A typical phenomenon inherent to estuaries is density- or salinity stratification. In estuaries, the denser saline water of the sea meets the less dense fresh water of the river. This density difference between the fresh and saline water tends to cause a stratification of the two layers. The degree to which this stratification occurs depends on the relation between the mixing induced by the tidal force, and the buoyancy force of the fresh water (Valle-Levinson, 2010). An overview of the different types of stratifications in estuaries is given in Figure 2, where the arrows indicate the relative strength of the tidal and river forcing. In general, a weak river forcing compared to the tidal forcing results in a weak stratification, and vice versa. Furthermore, due to the fresh river water meeting the saline sea water, a longitudinal salinity gradient is formed. This salinity gradient is simultaneously a density gradient since salt water is more dense than fresh water. As a result of a longitudinal density gradient, a baroclinic pressure gradient is found in estuaries. This pressure gradient in combination with a water level slope causes the water layers at the surface to flow seaward while the water near the bed tends to flow landward. This phenomenon is termed gravitational circulation and is typical for estuaries (Pritchard, 1952).

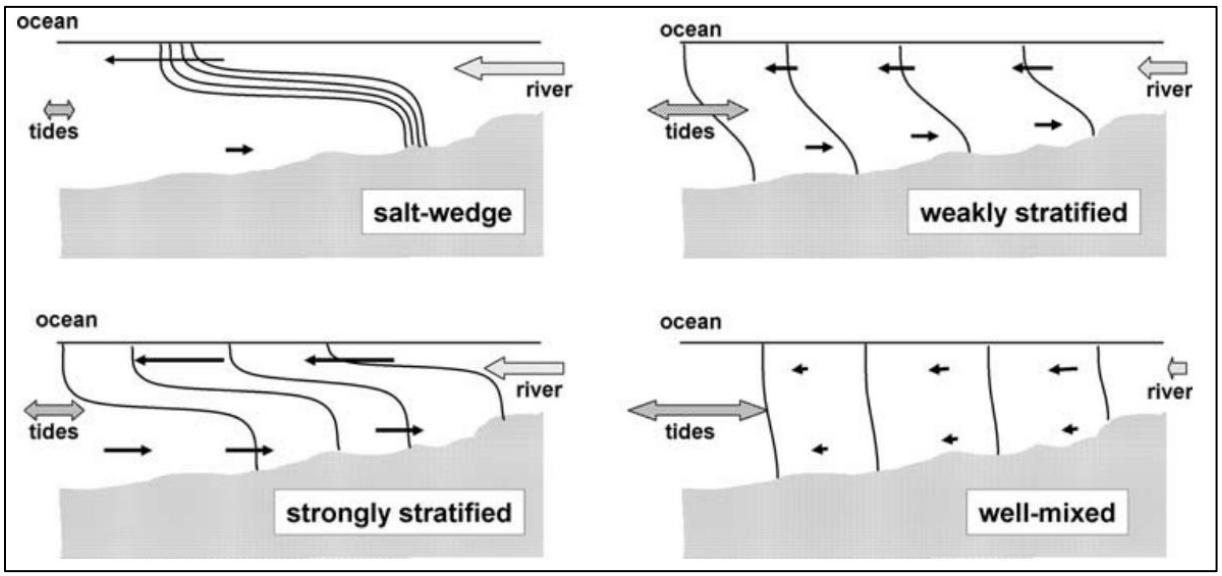

Figure 2: Density stratification in estuaries based on the ratio of tidal force and river discharge (Valle-Levinson, 2010).

Tidal asymmetry

The tidal forcing influencing an estuary is generated by the gravitational force of celestial bodies moving the water. A key factor is that the total tidal signal is composed of multiple tidal constituents resulting from (the interaction of) these celestial bodies and the overtides generated by non-linear friction effects (Dronkers, 1964; Gallo & Vinzon, 2005). These tidal constituents all have different frequencies and amplitudes, causing the total tidal signal to be a deformed sinusoid. An example of how a tidal constituent and its overtide can interact to form the tidal signal is given in Figure 3.

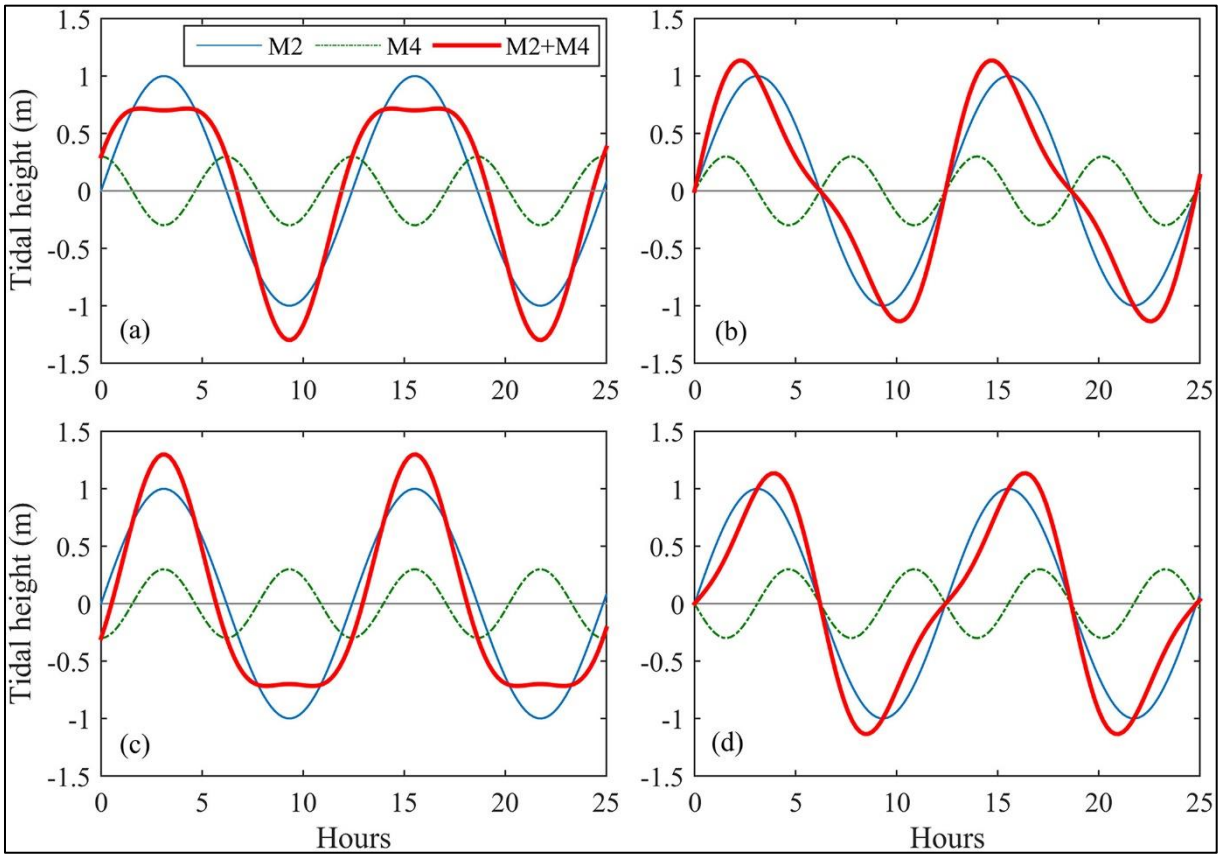

***Figure 3: Superposition of the M2 and M4 tide with multiple phase shifts* (Guo et al., 2019).**

Figure 3 shows that the phase difference between the two tidal constituents results in a different outcome of the tidal signal. In Figure 3.a and Figure 3.c, the superposition of the two tidal constituents results in a longer flood- and ebb slack water, respectively. This results in longer periods where the flow velocities are relatively low. In Figure 3.b and Figure 3.d, the superposition of the two tidal constituents results in a shorter duration of the rising and falling tide, respectively. This results in higher peak current velocities for the respective tides. Tidal asymmetry can thus heavily influence the slack water period and the resulting flow velocities in flood and ebb direction. In tidal environments such as estuaries, tidal asymmetry is therefore recognized as one of the most important factors in determining the residual sediment transport (e.g. Guo et al., 2019; Postma, 1967). In addition to the tidal asymmetry of the external tidal forcing, the tidal wave entering an estuary can get deformed as well. Factors such as the friction, the basin topography and river discharge can affect the tidal constituents and their overtides, thus resulting in a changing tidal signal over the extent of the estuary (Dronkers, 1964; Gallo & Vinzon, 2005).

1.1.2 Estuarine dunes

Bed forms are often found in estuaries. Subaqueous bed forms are spatially rhythmic patterns that exist on the bed of many water systems such as oceans, rivers and estuaries (Ashley, 1990). These bed forms can vary significantly in size, ranging in height from centimetres to several meters. Sand dunes, which are a subcategory of bed forms, are especially of interest since they can limit the depth of navigation channels (Pope, 2000) and affect the hydrodynamics such as the hydraulic roughness (Hulscher & Dohmen-Janssen, 2005; Lefebvre & Winter, 2016). Therefore, there is a need to better understand the behaviour of estuarine sand dunes.

The flow transverse bed forms in the marine environment with a height in the order of 1-10 meters and a length in the order 100-1000 meters are often termed sand waves. In this study the terminology of Ashley (1990) is adopted for the estuarine and riverine bed forms where the subaqueous flow transverse bed forms with a height in the order of 1 meter and a length in the order of 10-100 meters are termed dunes. The distinction between the dunes in estuaries and rivers is made with the term estuarine dunes and river dunes, respectively. Estuarine dunes are the subject of this thesis. However, since estuarine dunes, river dunes and sand waves have similar characteristics, they are all shortly introduced. The main similarity between these different type of bed forms, is that they are all formed and shaped by a positive morphodynamic feedback loop (Hulscher & Dohmen-Janssen, 2005) displayed in Figure 4. Where the bed topography affects the flow structure, which determines the sediment transport and consequently causes the bed level to change.

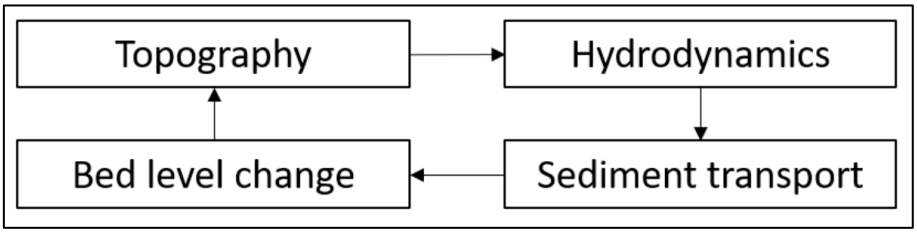

Figure 4: Schematisation of the morphodynamic feedback loop.

Sand waves

Sand waves generally exist in tidal environments where the water depth is approximately 15-50 meters (Damen et al., 2018; Hulscher & Brink, 2001). Therefore, sand waves can often be found in shelf seas such as the North Sea. Furthermore, sand waves nearly exclusively form in regions where the bed material is for the most part composed of sand with median grain sizes exceeding 255 μm (Damen et al., 2018; Hulscher & Brink, 2001; van Santen et al., 2011). Sand waves have a symmetric profile unless they are affected by either a residual current or an asymmetric tidal wave (Besio et al., 2004; Hulscher & Dohmen-Janssen, 2005; Németh et al., 2002). In such a case, the sand waves migrate in the direction orthogonal to their crest with observed migration rates of up to tens of meters per year (Van Dijk & Kleinhans, 2005). Modelling studies show that the migration of sand waves can be in the direction of the residual current (Németh et al., 2002) or against it as a result of an asymmetric tidal wave (Besio et al., 2004).

An extensive attempt has been made to obtain empirical relationships between the sand wave characteristics and the environmental parameters by Damen et al. (2018). They did not find empirical relations, but they did find correlations. Sand wave height positively correlates with the water depth and the sand wavelength negatively correlates with the tidal amplitude. Lastly, the effect of surface

waves is observed to enhance sediment stirring, resulting in longer and flatter sand waves (Van Dijk & Kleinhans, 2005).

River dunes

River dunes are important features in fluvial systems. They can alter the flow structure which in turn affects the sediment transport and water levels (Hulscher & Dohmen-Janssen, 2005). A dissimilarity with sand waves is that river dunes form in a unidirectional flow environment and therefore standardly have an asymmetric profile. Generally, river dunes are also smaller and more dynamic than sand waves. A similarity between river dunes and sand waves is that river dunes also scale with the flow depth. The height (H) and length (L) of river dunes are observed to scale with the flow depth (h) by $H = 0.13h$ and $L = 5.9h$ (Bradley & Venditti, 2017).

Dunes are commonly divided between low angle dunes (LADs) and high angle dunes (HADs) (e.g. Best & Kostaschuk, 2002; Cisneros et al., 2020; Hendershot et al., 2016). HADs are characterised by long and gentle stoss sides combined with short and steep lee sides and therefore have a very asymmetrical profile. LADs have a more symmetrical profile due to their gentler slopes. HADs are commonly created in flume experiments whereas in large rivers and estuaries, LADs are the predominant bedform (Best, 2005; Cisneros et al., 2020; Hendershot et al., 2016). A schematical representation of HADs and LADs is given in Figure 5.

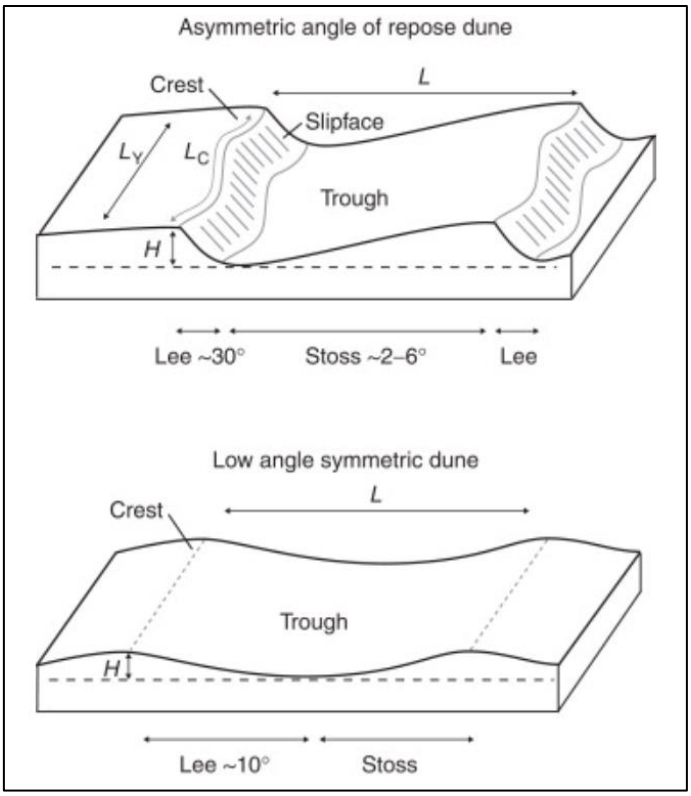

Figure 5: Schematic representation of very asymmetric high angle dunes (top) and moderately asymmetric low angle dunes (bottom) **(Venditti, 2013).**

River dunes scale with the flow conditions. High discharge events lead to greater water depths and flow velocities, resulting in longer and higher dunes (Hulscher & Dohmen-Janssen, 2005; Julien et al., 2002; Wilbers & Ten Brinke, 2003). However, the dunes do not adapt to the flow conditions instantaneously. The adaptation of river dune characteristics is observed to lag the changes in

discharge for example during a flood wave (e.g. Julien et al., 2002; Wilbers & Ten Brinke, 2003). This lag between the change in flow conditions and the adaption of the dune height and length is called hysteresis. During a flood wave in a river, the discharge increases and decreases. Due to hysteresis, dunes can have greater dimensions during the falling limb of the flood wave than during the rising limb of the flood wave, even though they are subjected to the same amount of discharge (e.g. Julien et al., 2002; Wilbers & Ten Brinke, 2003). Additionally, Warmink (2014) observed that dune height adapts to abrupt changes in flow conditions more quickly compared to the dune length.

Estuarine dunes

Estuarine dunes form in complicated hydrodynamic regions where both riverine forcing, marine forcing and estuarine specific processes play a role. They can vary in size, reaching significant dimensions such as in the Bahía Blanca estuary where heights of 5 meters and lengths of 170 meters are observed (Gómez et al., 2010; Salvatierra et al., 2015). In this estuary, the estuarine dunes were observed to migrate with 20 to 230 meters per year which was found to be in line with migration rates in other estuaries (Salvatierra et al., 2015). As with river dunes, estuarine dunes are also observed to affect the flow structure (Hu et al., 2021). Where smaller superimposed dunes are thought to affect the near bed section of the velocity and the larger bedforms themselves are thought to affect the upper section of the velocity profile.

Francken et al. (2004) and Salvatierra et al. (2015) observed postitive correlation of the estuarine dunes with the water depth in the Scheldt and Bahia Blanca estuary, respectively. These studies however still show a large spread of the data around the correlation, indicating that water depth is important in determining the size of estuarine dunes, but it is not the only determining factor.

1.2 Research goals

Estuaries thus are valuable both from an economical viewpoint as well as an ecological perspective. Estuarine dunes are often found in estuaries which can affect the hydrodynamic conditions and sediment transport. They have similar characteristics as their marine and fluvial counterparts but are less extensively studies. The correlation of estuarine dunes with environmental parameters is mostly studied in case studies such as in the Scheldt estuary (Francken et al., 2003) or the Bahia Blanca estuary (Salvatierra et al., 2015), where the focus mainly lies on the relationship between the dune height and the water depth. In these studies, a correlation was established between these two parameters. However, a large spread of the data remained that was not explained. Large scale studies, analysing multiple estuaries to investigate the correlation between estuarine dune characteristics and the relevant environmental parameters have not yet been conducted. Therefore, the goal of this study is to gain more insight in the dune characteristics by analysing the correlation of these characteristics with the environmental parameters using data of the Scheldt and Elbe estuary. The research questions to achieve the specified goal of this study are set up as follows:

1. How are the water depth, tidal asymmetry, river discharge, and sediment characteristics related to the length, height, and asymmetry of estuarine dunes in the Scheldt and Elbe estuary?
2. How do the length, height, and asymmetry of estuarine dunes compare in the Scheldt and Elbe estuary and how can this be related to differences in environmental conditions between those estuaries?

1.3 Methodology

To answer the research questions, a data analysis is conducted. This data analysis focuses on three study locations in the Western Scheldt of which bed level data is available. These study locations are used to investigate the spatial variability of the estuarine dunes. One study location is selected in the Elbe estuary for which multiple bed level measurements are available over time. This study location is used to gain more insight in the temporal variability of estuarine dunes. The bed level data of both estuaries is analysed with the developed bedform tracking tool of van der Mark et al. (2008). This tool is used to extract the dune length, height, and asymmetry from the bed level data in the selected study sites.

Environmental data is obtained from two data portals. This data contains the flow velocity and discharge data of the Elbe, and the water level and sediment characteristics of both the Elbe and Western Scheldt study locations. Furthermore, the results of a hydrodynamic model of the Western Scheldt are used. These datasets are all analysed to characterise the study locations in space (Scheldt) and in time (Elbe). The environmental characteristics are then correlated with the obtained dune characteristics to better understand the interdependency of these variables.

1.4 Reading guide

In the next chapter, an overview is given of the Scheldt and the Elbe estuary. This chapter also describes the available data and the selection of the study locations. In chapter 3, the methodology is described of how the bed level data and the environmental data are analysed. In chapter 4, the result of this analysis is presented after which in chapter 5 the results and methodology are discussed. Finally, in chapter 6, a conclusion is provided, and the research questions are answered. In chapter 7, recommendations for further research are given.

2. Estuaries under consideration: Western Scheldt and the Elbe

In this chapter, the Scheldt estuary and the Elbe estuary are introduced. Then, the available bed level data and environmental data is described.

2.1 Scheldt and Elbe estuary

2.1.1 Scheldt estuary

The Scheldt river is a 350 km long river that has its origin in the north of France and flows through Belgium and the Netherlands. In the southwest of the Netherlands, the river mouth of the Scheldt connects with the North Sea at Vlissingen. The tidal wave of the North Sea can travel land inward up to Ghent where sluices mark the upper bound of the estuary, forming an estuary of approximately 160 kilometres (Meire et al., 2005). The parts of the Scheldt estuary that are located within Belgium and the Netherlands are termed the Sea Scheldt and the Western Scheldt, respectively. An overview of the entire Scheldt estuary and the domain termed the Western Scheldt is given in Figure 6.

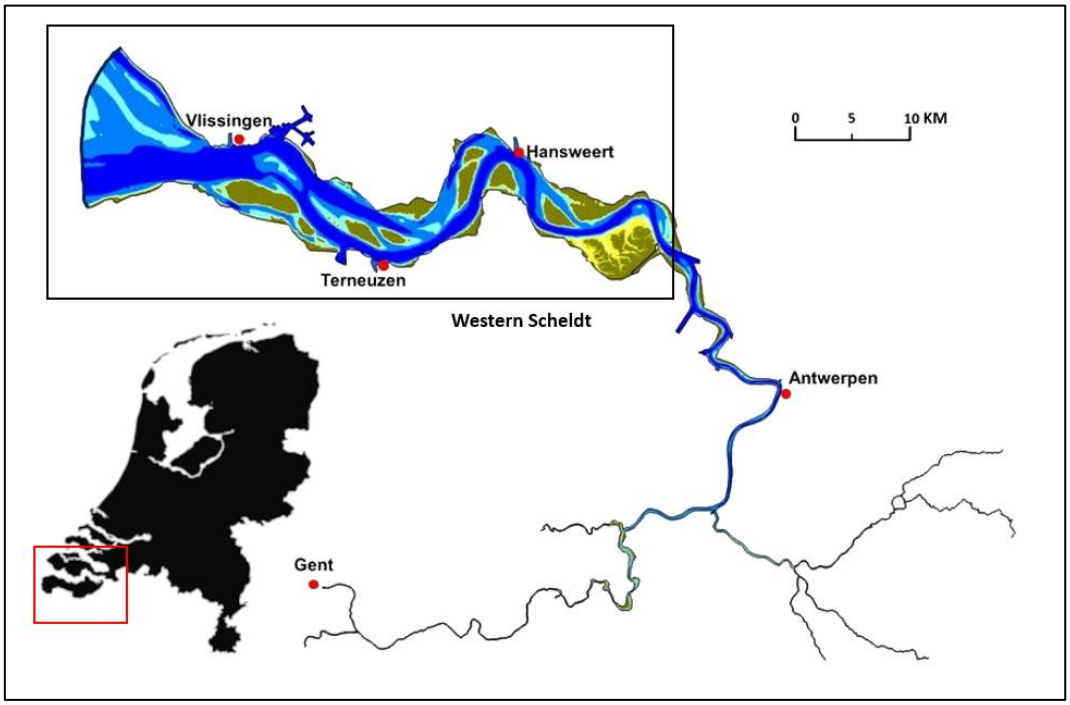

Figure 6: Scheldt estuary (adapted from* Stark, 2016*).

The Scheldt estuary has a funnel shape geometry where the width varies from 6 km near Vlissingen, 2-3 km at the transition from the Western Scheldt to the Sea Scheldt, and less than 100 m at Ghent (Wang et al., 2002). The marine driving force is a semi-diurnal tide where the mean tidal range increases from 3.8 m at the mouth near Vlissingen up to 5.2 m just upstream of Antwerp, after which it decreases again to 2 m at Ghent (Meire et al., 2005). Therefore, the Scheldt estuary falls within the meso-/macrotidal range and is hypersynchronous. The riverine forcing is the discharge of the Scheldt river which is on average 120 m^3/s with a minimum and maximum between 20 and 600 m^3/s (Wang et al., 2002). With a tidal prism of $2x10^9$ m^3, aggregating the mean and maximum discharge over the duration of the semi-diurnal tide, the river discharge amounts to 0.27% and 1.3% of the total tidal prism of the Scheldt estuary, respectively (Wang et al., 2002). The ratio of these driving forces causes the Scheldt estuary to be tide-dominated where the majority of the morphological development is caused by the tidal flow (Wang et al., 2002).

In the Scheldt estuary, there is a distinct difference between the morphology of the Western Scheldt and Sea Scheldt. As can be seen in Figure 6, the Western Scheldt displays a braided pattern of ebb and flood channels combined with intertidal flats (Winterwerp et al., 2001). More upstream, near the transition of the Western Scheldt into the Sea Scheldt, the braided pattern transitions into a single channel system. The multichannel system in the Scheldt estuary can be divided into macro-cells where each of these macro-cells are characterised by an ebb- and flood dominated channel (Winterwerp et al., 2001). In flood dominated channels, more water and sediment is transported during flood compared to ebb. The contrary holds for ebb channels. A schematisation of the configuration of these channels in the Western Scheldt is provided in Figure 7.

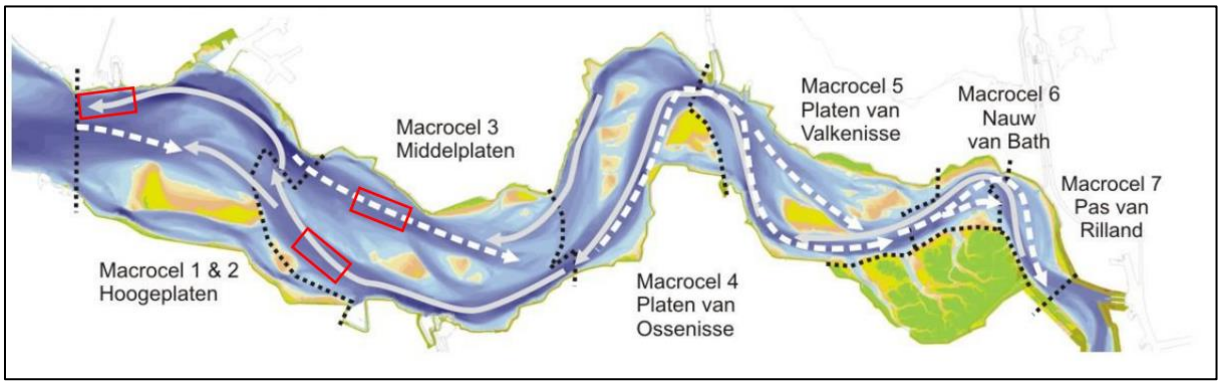

***Figure 7: Multichannel system of the Western Scheldt where the arrows indicate an ebb- or flood dominance and the locations of the study areas are already indicated by the red rectangles* (adapted from Laan et al., 2014).**

2.1.2 Elbe estuary

The Elbe river is a 1100 km long river that has its origin in the Czech Republic and flows through a large part of Germany where it connects to the North Sea (Amann et al., 2012). The tidal influence of the North Sea reaches from the estuary mouth at Cuxhaven up until the weir at Geesthacht (Figure 8). In total, this leads to an estuary of approximately 150 km (Amann et al., 2012). As can be seen in Figure 8, the Elbe estuary is divided into two sections based on the salinity: an upper limnic (i.e. freshwater) section and a lower transitional area where the water is brackish (Carstens et al., 2004).

The catchment area of the Elbe with a surface area of 148.300 km^2 is approximately 7 times larger than that of the Scheldt river. This results in the average discharge of the Elbe to be 700 m^3/s, which is also 7 times greater than the average discharge of the Scheldt (Amann et al., 2012). The discharge in the Elbe has a seasonal cycle which is influenced by the melting snow from the Czech Republic. This causes an increase of the discharge in January-April and falling discharge values in June-September (Li et al., 2014). In spring, discharge values can reach up to 3900 m^3/s (Streif, 2004). Geerts et al. (2017) compare the cross-sectional area of the Scheldt and the Elbe and conclude that they roughly follow the same shape. Due to the general greater values and seasonal effect of the discharge in the Elbe, combined with approximately equal cross-sections in the Scheldt, makes the riverine forcing more of influence in the Elbe estuary.

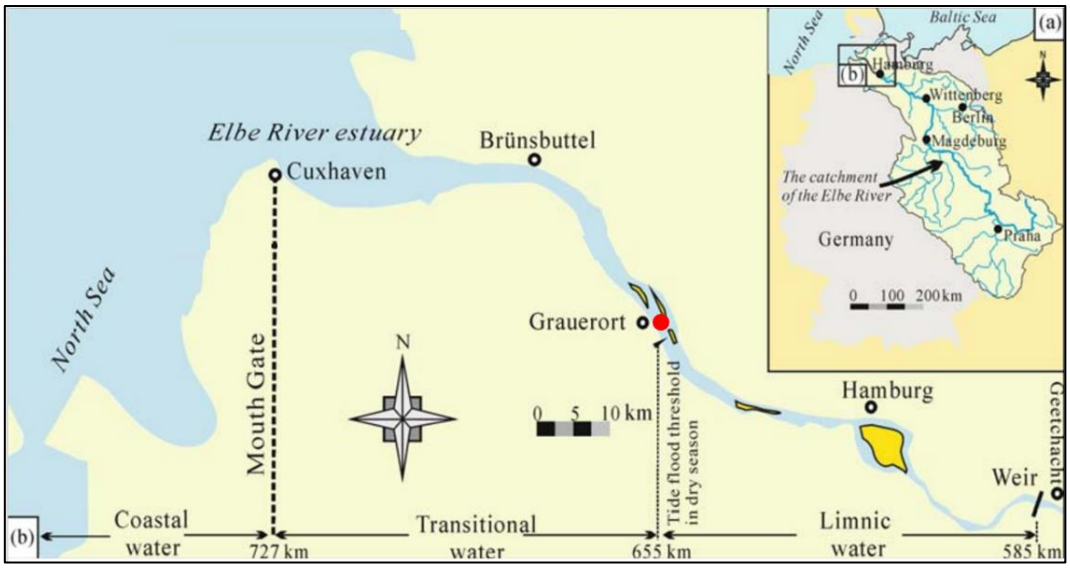

***Figure 8: The Elbe estuary where the location of the study site is already indicated by the red circle* (adapted from Li et al., 2014).**

The Elbe estuary is furthermore influenced by the semi-diurnal tidal forcing. At the mouth of the estuary at Cuxhaven, the tidal range is 3.03 m (Streif, 2004). The tidal range increases slightly up until Hamburg, with a tidal range of 3.35 m, after which is reduces again until the upstream boundary at Geesthacht with a tidal range of 1.43 m. On average, the tidal forcing causes 650x10^6 m^3 of sea water to enter the estuary (Streif, 2004). Over a semi-diurnal cycle, the average discharge amounts to approximately 4.8% of the tidal prism.

Where the Scheldt estuary displays a gradual funnel shape, the widening in the Elbe is much more prismatic. Showing a significant widening between Brünsbuttal and Cuxhaven (Figure 8) where the single channel shortly splits up in two channels (Li et al., 2014). Furthermore, the Elbe estuary upstream of Brünsbuttel is characterised by a single channel system.

2.2 Available data

2.2.1 Bed level data

Of the Western Scheldt, topographic data is obtained from the Dutch Department of Waterways and Public Works. This data contains 2DH bed elevation maps of the area between Hansweert and Vlissingen (Figure 6) in the period between 2017 and 2019 where the bed level is measured relative to the Amsterdam Ordnance Datum (NAP). In the data, the Western Scheldt is subdivided in smaller areas where the bed is mapped with a multibeam echosounder (MBES) attached to a vessel. In the period between 2017 to 2019, in total 313 measurements were conducted over a collection of 68 unique locations. In most of the areas, the MBES data is aggregated to a resolution of 1x1 meters, fewer areas are aggregated with a resolution of 2x2 meters, and some areas are measured with a singlebeam echosounder. These locations are measured in transects where the distance between points on a transect are 1 meter but the distance between transects can be up to 200 meters. An example of a MBES dataset located at Vlissingen with a resolution of 1x1 m is given in Figure 9.

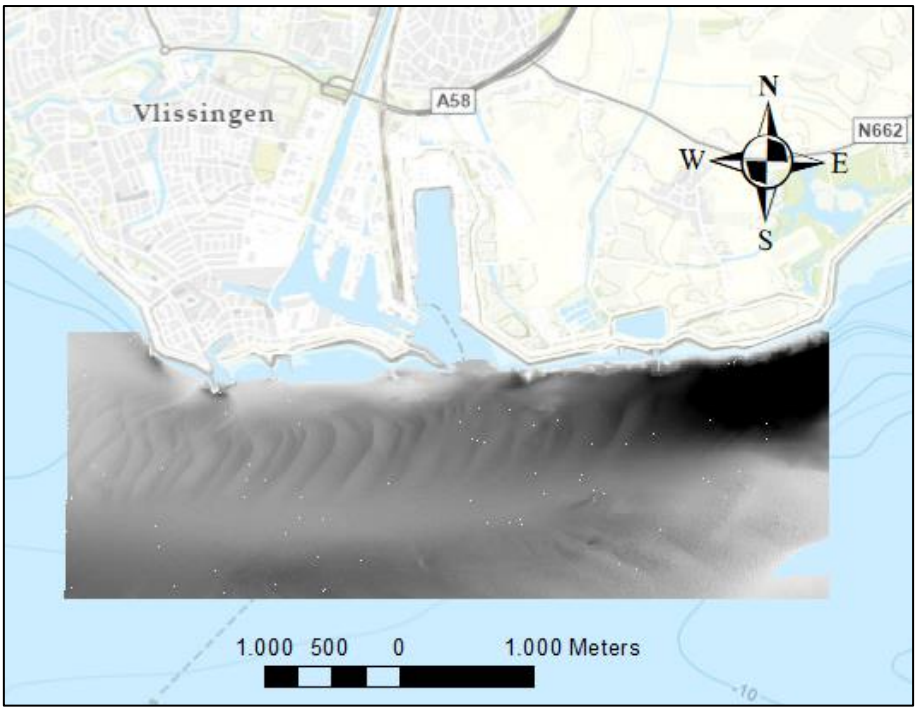

Figure 9: Multibeam echosounder data at Vlissingen.

In the Elbe, bed elevation data is available for the period 2012-2014. In this period, the bed level is measured 74 times for a section of approximately 2.5 kilometres long near Grauerort (Figure 8). The bed is mapped with multibeam echosounders resulting in a 2DH elevation map. In this map, the datapoints are aggregated to a resolution of 2x2 meters where the bed level is provided with respect to the German vertical datum DHNN92. Most of the measurements contain the main channel axis with a resolution of 2x2 meters. Some of the data samples also contain the main channel axis but are measured in single transects while other samples are obtained with multibeam echosounders from the sides of the channel. In the period of 2012-2014, the main channel axis of the Elbe estuary in the region of Grauerort is mapped 60 times with a resolution of 2x2 meters. The distribution of these bed elevation measurements in the Elbe is visualised in Figure 10.

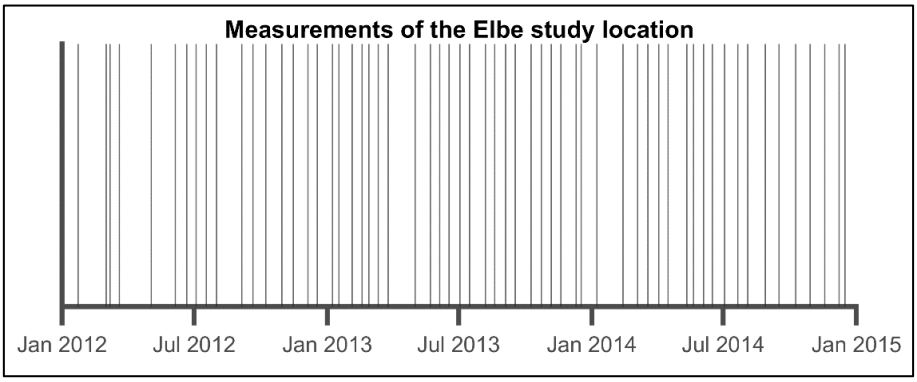

Figure 10: Measurements of the Elbe bed level data.

2.2.2 Environmental data

Multiple sets of environmental data were used in this study. This data covers the flow velocity, water level, sediment characteristics of both the Elbe and Scheldt estuary while the river discharge is only obtained for the Elbe estuary.

In the Western Scheldt multiple measurement stations are situated. The data of these measurement stations can be accessed through the waterinfo.rws.nl data portal. From this data portal, the water level is obtained for the Vlissingen, Borssele and Terneuzen Westsluis measurement stations in the period of January 2017 until December 2019. The location of these measurement stations is indicated in Figure 11. This data contains the water level at these stations with respect to the Amsterdam Ordnance Datum (NAP) measured in 10-minute intervals.

In-situ measurements of flow velocity in the Western Scheldt are scarce. Therefore, a different source is used to obtain flow characteristics. The results of a fully calibrated and validated Delft3D-NeVla model of the Scheldt estuary have been made available for the use of this study. This model simulates the depth-averaged water flow for a complete year as a result of the tide, surface waves, wind, river discharge, salinity gradients and secondary flow based on input data of 2013. The full description and validation of the model is given by Vroom et al. (2015). The results of this model are composed of two files. One of these files, further referred to as the map file, has data stored for the entire model domain. From this map file, the bed level is obtained which is used for the model calculations. Furthermore, the map file contains hydrodynamic data for every grid cell. However, since the hydrodynamic data in this map file is stored in 24-hour intervals, the subtidal variations are lost. Therefore, hydrodynamic data from the map file is not included in this research. The second file, further referred to as the monitoring file, contains hydrodynamic data on specified monitoring locations. These monitoring locations are of two categories: observation locations and cross-sections. Observation locations contain the data of the hydrodynamics such as the water level or flow velocity for a single grid cell. Cross-sections contain data such as the discharge crossing multiple cells. Both these types of monitoring locations have the model data stored in 10-minute intervals.

In-situ measurements of the Elbe are readily available. A range of hydrodynamic data in the period 2012-2014 can be acquired from the data portal kuestendaten.de. Flow velocity and flow direction data in 5-minute intervals are obtained from the monitoring stations “D3 – Pagensand-Nord” and “D4 - Rhinplate-Nord”. Both these measurement stations contain the velocity and direction of the flow at 1 meter above the bed and 1.5 meter below the surface and are in the same area as where the bed level data of the Elbe is available (Figure 12). In this report, the “D3 – Pagensand-Nord” measurement station is further referred to as the upstream measurement station while the “D4 - Rhinplate-Nord” is further referred to as the downstream measurement station. Furthermore, the kuestendaten data portal is also used to obtain water level and discharge data. The water level is acquired from the Kollmar measurement station which is situated along the bank of the Elbe estuary where the bed level data is also available (Figure 12). This station monitors the water level every minute where the water level is registered with respect to the German elevation system DHHN92. Discharge data is obtained from the Teufelsbrück flow station. This station is situated at the seaward end of Hamburg and deduces the total discharge through the channel in cubic meters per second for every 5 minutes, based on the water level using a rating curve. This data series does however contain a lot of missing values. Another discharge station is situated more upstream in the Neu Darchau harbour. This flow station also deduces the daily average discharge values in cubic meters per second based on the water level and contains no missing data in the period 2012-2014.

Sediment data for both estuaries is available as well. For the Western Scheldt, the results of the field measurement conducted by McLaren (1993) are acquired. This data contains the median grain diameter (D50) of the bed on a 500-meter grid. This sampling frequency is denser on the intertidal flats

with an intermediary distance of 250 meters. The bed composition of the Elbe estuary is obtained from the data portal kuestendaten.de. Among multiple sieve results and ecological parameters, this dataset also includes the median grain size. The sediment data in the Elbe estuary is a composition of multiple field measurements in the period 1993-2018.

2.3 Study sites

As mentioned in paragraph 2.2.2, multiple sets of bed level data are available. However, not all data samples are usable in this study due to a variety of reasons. In order to select suitable study locations to analyse the natural response of estuarine dunes to the environmental conditions, several criteria have been set up. These criteria are the following:

1. Upon visual inspection, the bed level data needs to display a dune pattern.
2. The grid resolution of the study location needs to be at minimum 2x2 m.
3. The study location needs to be measured at least twice in the period of which bed level data is available.
4. The study locations need to be in a proximity to stations measuring the environmental conditions.

These criteria assure that the selected study sites contain dunes (1) that can be quantified (2) for at least two separate measurements (3) and can be correlated to environmental conditions (4). Furthermore, the bed level data of the Western Scheldt contains MBES data dispersed over a vast spatial range while there are often only yearly or bi-yearly measurements taken. The contrary holds for the Elbe where the spatial extent of the bed level data is more limited, but the same extent has many temporal observations. In the Scheldt, the influence of the river discharge is limited, and the morphology shows a braided pattern with ebb- and flood dominated channels. Therefore, in the Western Scheldt, the focus is more on the spatial variation. In the Elbe, the influence of the discharge is more significant with a seasonal cycle. Therefore, in the Elbe, the temporal variation of the estuarine dunes is studied.

Figure 11: Locations of the selected study sites in the Western Scheldt with their abbreviation. The triangles indicate the water level measuring stations.

Based on these selection criteria and the available bed level data, three study sites were selected in the Western Scheldt and one study site was selected in the Elbe estuary. The three study sites in the Western Scheldt are depicted in Figure 11. These study sites are named after the nearby cities Vlissingen (Vlis), Borssele (Bors) and Terneuzen (Tern). It appears as if the Terneuzen and Borssele study sites are close together, but it should be noted that Borssele is located in a flood dominated channel while the Terneuzen site is located in an ebb-dominated channel (Figure 7). These differences likely also result in differences in the characteristics of estuarine dunes. All three of these study locations are measured twice in the period 2017-2019. The date on which these bed level measurements were taken is given in Table 1. As can be seen, all three locations are measured in 2019. In the available dataset, Vlissingen is first measured in 2018 and Borssele and Terneuzen are first measured in 2017.

Table 1: Bed level data collection for the three study sites in the Western Scheldt.

	Measurement 1	**Measurement 2**
Vlissingen	19-03-2018	11-02-2019
Borssele	22-07-2017	01-07-2019
Terneuzen	08-11-2017	01-10-2019

In the Elbe estuary one study location is chosen to analyse over time. The location of this study site can be found in Figure 12. This study location is chosen because it is the furthest away from any tributaries, the bed level data shows the least amount of rapid trend variation which could influence the flow structure and affect the dunes, and the dunes in this study location show a relatively homogeneous field.

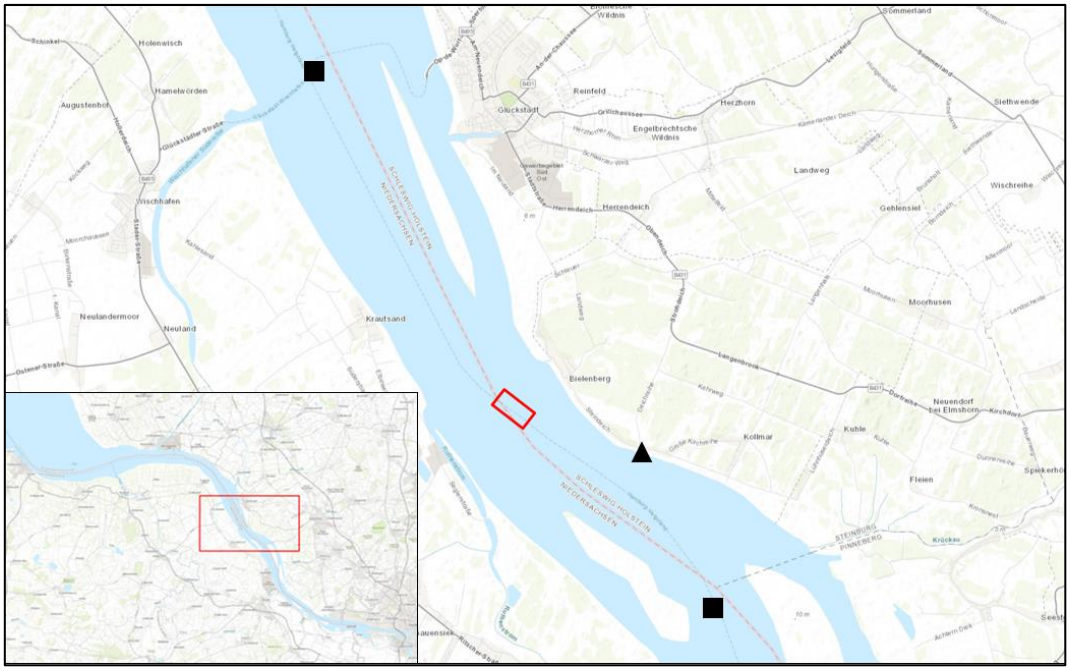

Figure 12: Study location in the Elbe estuary. The triangle indicates the water level measuring station, and the squares provide the locations of the flow velocity measurements.

3. Methodology

In this chapter, the methodology is elucidated which is used to obtain the results. First a description is given how the available data is prepared such that it can be analysed. Then, the further processing of the data is explained which can be used to obtain correlations between the environmental data and the estuarine dune characteristics.

3.1 Data preparation

3.1.1 Spatial interpolation

A well-established bedform tracking tool of Van der Mark et al (2008) is developed in Matlab in order to quantify the dune characteristics. This tool processes bed elevation profiles and identifies the crests and the troughs of the dunes by the means of a zero-crossings method. To analyse the topographical data with the developed bedform tracking tool, one-dimensional bed elevation profiles (BEPs) of the dunes are required. For these profiles to not contain missing data, the missing data in the topographical data needs to be interpolated. This is done using the ArcGIS software and is in detail described in Appendix A.

3.1.2 Transects

With the missing data interpolated, the bed elevation profiles are extracted. An important decision is the orientation of the bed elevation profiles. When studying sand wave fields, it is common to choose the orientation of analysis based on the orientation of the sand waves themselves. This can for example be done using a 2-D Fourier transform as is described by Van Dijk et al. (2008) and applied by Damen et al. (2018) and van Santen et al. (2011). In riverine studies, it is more common to define the orientation of the bed elevation profiles based on the river axis, and with that, based on the general streamwise direction. This approach is for example applied by van der Mark et al. (2008) and de Ruijsscher et al. (2020). The study locations in the Western Scheldt are located within the ebb- and flood channels. In the Elbe estuary, the study location is located in the main channel. The bathymetries of these study locations show a greater resemblance with the bathymetry of rivers than with the bathymetry of a general marine environment. Therefore, the approach of the riverine studies is also applied in this study, setting the direction of the bed elevation profiles in line with the channel axis. In the Elbe, the direction of the main channel is easily obtained since the borders of the topographical data also indicate the borders of the main channel. The direction of the main channel axis for the Elbe study location is depicted in Figure 13. In the Scheldt, the main channel direction of the study locations is not as easily obtained since the topographical data is not limited to the channels as can be seen in Figure 9. In order to get the main channel axis of the Scheldt study locations, a modelling study of Deltares is used (Rijn, 2011). In this study, a hydrodynamic model of the Western Scheldt estuary was created in Delft3D. In their report, the depth-averaged flow direction at maximum flood and ebb flow over the entire Western Scheldt are depicted. The vectors in these figures are used to approximate the channel axis in the Western Scheldt study locations. An example of one of these figures is given in Figure 14. The figures used and the resulting orientation of the study locations can be found in Appendix B.

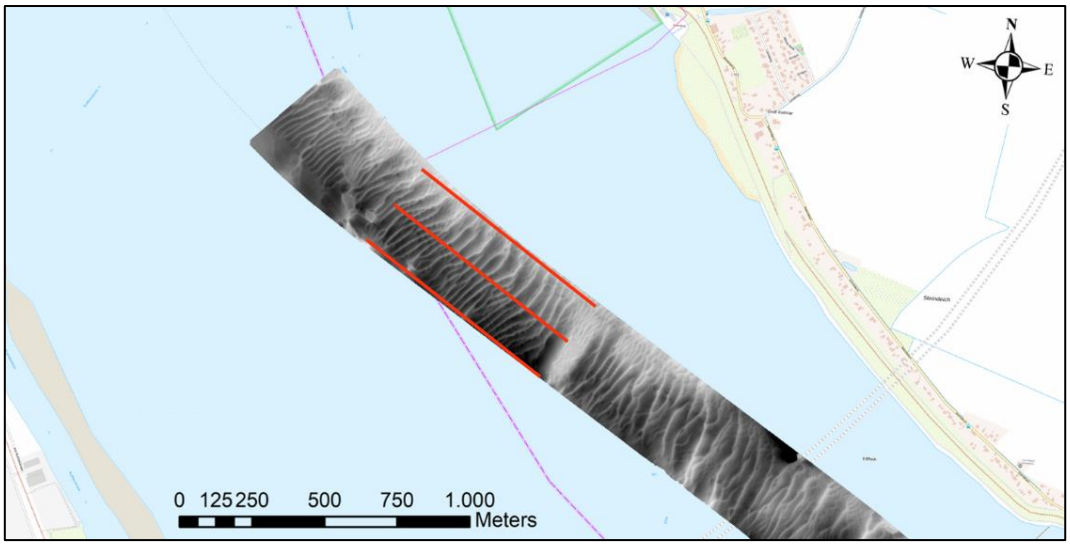

Figure 13: Topographic data of the main channel in the Elbe study location. The red lines are drawn to indicate the direction of the main channel axis.

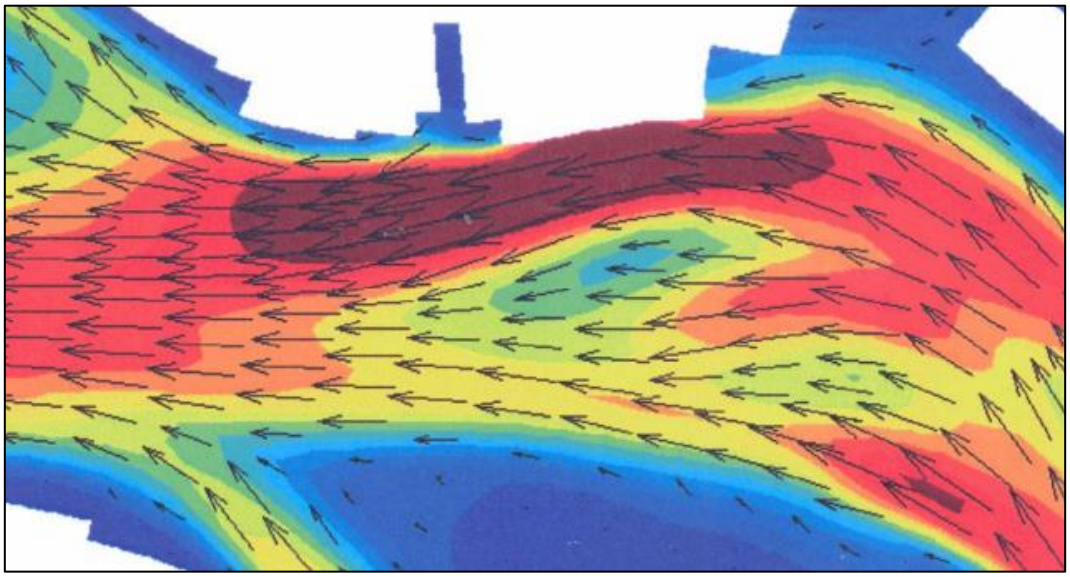

Figure 14: Vectors indicating the flow direction during peak ebb flow at the Vlissingen study area (Rijn, 2011).

With the direction of the transects determined in ArcGIS, the bed elevation profiles are extracted. In the Elbe the focus lies with the temporal variation. Therefore, a transect is selected in the middle of the main channel and this transect is kept constant throughout time. The location of this transect is depicted in Figure 15. On this transect, equidistant points are created using the "Points along line" feature with an intermediary distance of 2 meters since this is also the resolution of the MBES data. On these points, the bed level is extracted from all 60 raster files using the "Extract multi-values to points" toolbox. This generates a table where every column contains the bed elevation profile of a bed level measurement. This table is exported to Excel using the "Table to Excel" toolbox such that the bed elevation profiles can be further processed in Matlab.

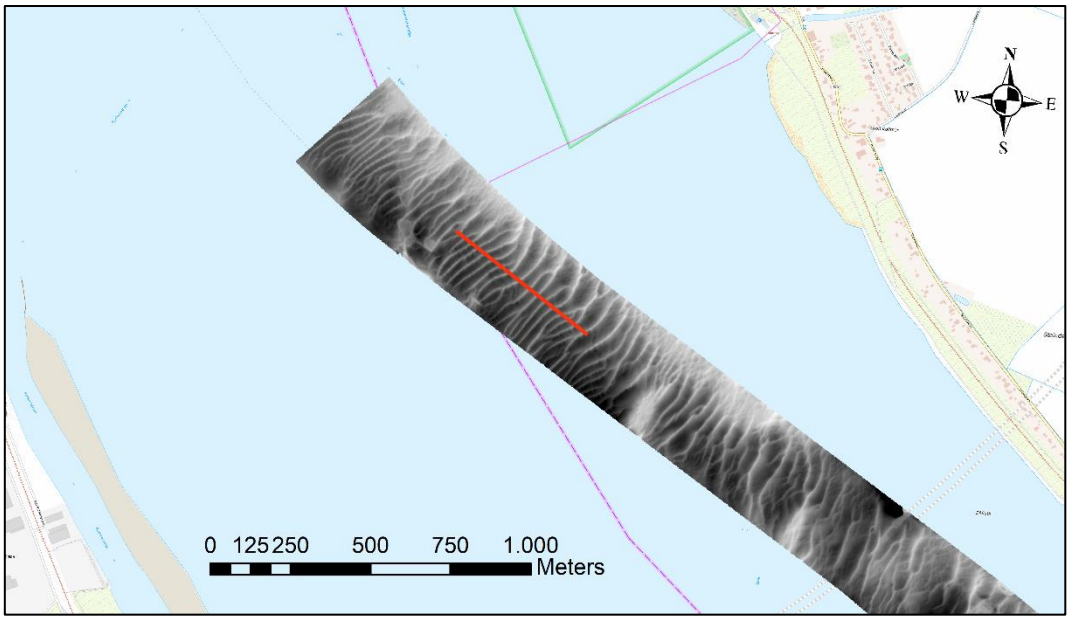

Figure 15: Transect over which the bed elevation profiles are extracted for the Elbe study location.

In the Western Scheldt, the focus lies on the spatial variation of estuarine dunes. Therefore, in the Scheldt study locations, the dune fields are addressed in their entirety by extracting transects over the entire width of the dune fields. This is done using a custom toolbox in ArcGIS developed in Python which is in detail described in Appendix C. This tool results in an Excel file where the BEPs, with an intermediary distance equal to the grid size of the underlying topography, are stored in the rows. The BEPs are always oriented in such a way that the first point is the most upstream part of the BEP.

3.1.3 Velocity data

The velocity data of the Western Scheldt study locations and the Elbe study location have a different origin. Due to a scarcity of in-situ measurements in the Western Scheldt, the results of a Delft3D flow model are used to represent the flow velocity in these study locations. In the Elbe, flow velocity measurements are available. Therefore, for the study location in the Elbe, in-situ measurements are used to quantify flow velocities.

As described in paragraph 2.2.2, the Delft3D model results consist of a 2DV map where the attributes are stored every 24 hours, and of monitoring locations where the attributes are stored every 10 minutes. Since the tidal signal in the Scheldt estuary is semi-diurnal, a 24-hour sampling interval is too coarse to obtain velocity data over the course of the semi-diurnal tide. Therefore, the specified observations in the model are used to identify the flow velocities in the areas of interest. The observations in the model consist of two types: observation locations covering one grid cell and cross-sections covering multiple grid cells. Since the model is not set-up with this study in mind, the observation locations of the model do not coincide with the areas of interest as specified in this study. Since the velocity can vary quite rigorously depending on whether you are located in the centre of the channel or for example a nearby harbour, these observation locations are not fit to quantify the velocity of the study locations in the Western Scheldt. Three of the cross-sections do however correspond with the channels where the study locations are located. Therefore, these cross-sections, measuring the instantaneous discharge, are used to quantify the velocity in the study locations. The locations of these three cross-sectional observations in the Western Scheldt which are used in this study are depicted in Figure 16. For the cross-sections, the same term is used as the study locations.

In other words, the cross-section covering the channel in which the Borssele study location is located, is termed the Borssele cross-section. The same holds for the other two cross sections.

Figure 16: Locations of the cross-sectional observations in the Delft3D flow model of the Scheldt estuary (blue) and the locations of the study sites (red).

From the cross-sectional observations in Figure 16, the instantaneous discharge can be obtained from the Delft3D model results in total cubic meters per second crossing the cross-section in 10-minute intervals. In order to convert this discharge into the velocity, the following equation is used:

$$v = Q/A \qquad \text{Eq.1}$$

Where v denotes the channel average depth-averaged flow velocity in m/s, Q represents the instantaneous discharge through the channel in m^3/s and A is the cross-sectional area in m^2 which is dependent on the water level. Hence, to obtain the cross-sectionally averaged flow velocity, the cross-sectional area over time is required.

The area of the cross-sections depicted in Figure 16 are obtained by first identifying the depth profile over these cross-sections. These depth profiles are acquired from the bed level input in the Delft3D model and are visualized in Figure 17. In Figure 17, the depth profiles are depicted with the reference system again looking downstream. This means that at a distance of zero in Figure 17, the location is equal to the very south end of the cross-sections in Figure 16. The cross-sectional depth profile is combined with the model water level observation locations in the Vlissingen and Terneuzen harbour entrances. The integral is calculated to obtain the area of the cross-sectional channel which is below the water level. Then, the cross-sectionally averaged flow velocity is calculated by dividing the instantaneous discharge by the cross-sectional area as described by Eq.1. For consistency, again the reference system is set in downstream direction. Therefore, in this analysis, a positive velocity is in downstream/ebb direction while a negative velocity is in upstream/flood direction. The result of this

data preparation are three vectors containing the cross-sectionally averaged flow velocity in ebb direction (positive) and flood direction (negative) for each of the cross-sections.

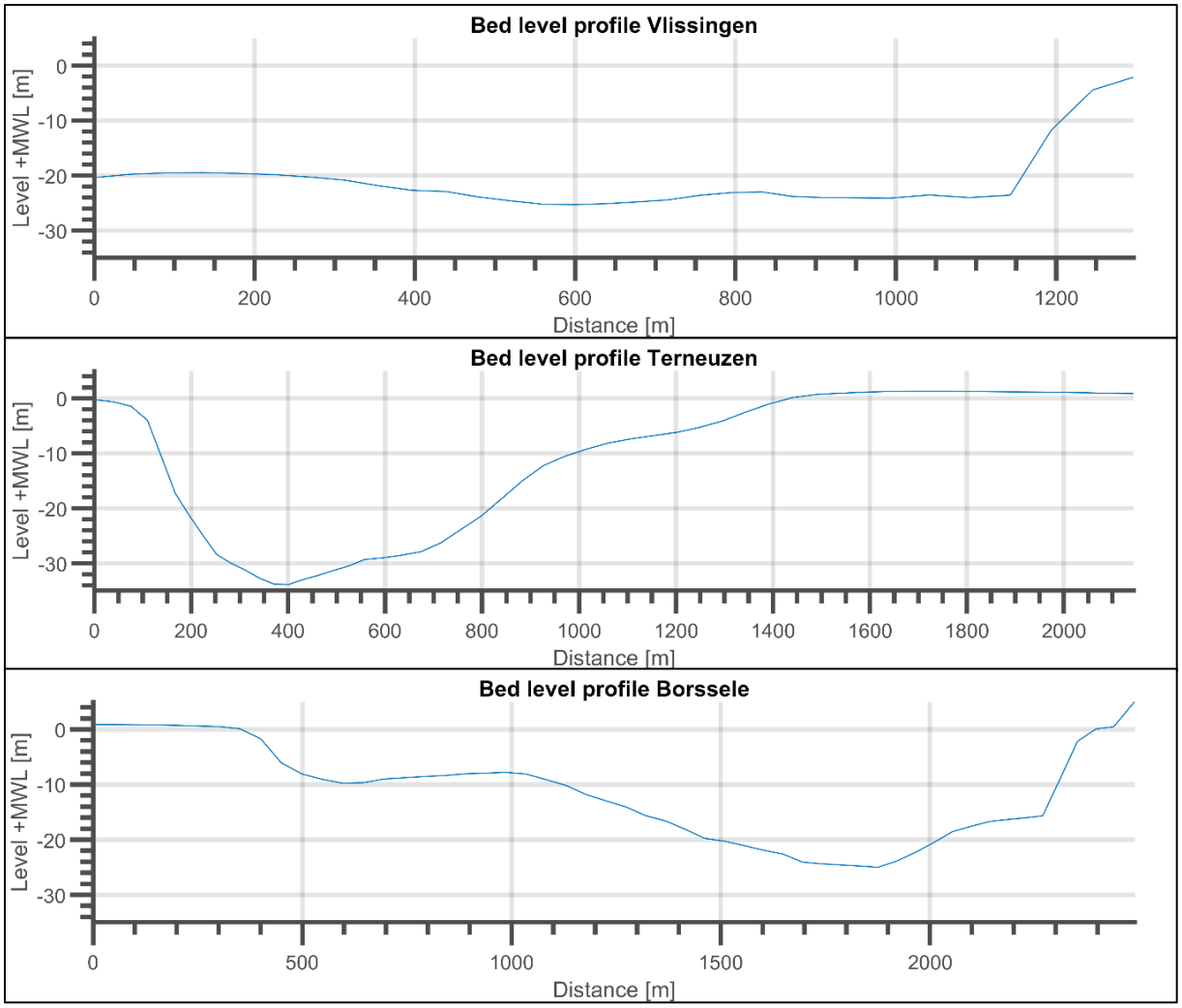

Figure 17: Bed level profiles of the cross-sections with respect to the mean water level in the Delft3D model.

In the Elbe estuary, flow velocity measurements are less scarce. Therefore, to identify the flow velocity for the study location in the Elbe estuary over time, in-situ measurements were used. These measurements, described in paragraph 2.2.2, contain the velocity magnitude and the direction in the period 2012-2014 in 5-minute intervals at two measurement stations. In this analysis, the velocity data of both the upstream and downstream measurements are processed. Of both these measurement stations, only the near bed velocity is used since the flow near the bed is more related to the dunes than the flow at the surface. For further analysis, the flow velocity magnitudes (only positive values) of both measuring stations are converted into the flow velocity in ebb- and flood direction (positive and negative values). This is achieved by first decomposing the velocity magnitude into the x- and y-vector component using the direction of the flow. Then, a Principal Component Analysis is conducted on the x- and y velocity vector to acquire the principal tidal axis. In this Principal Component Analysis, the data is not de-meaned such that the centre of the principal axes align with the centre of the x- and y-axes. Using the results of the Principal Component Analysis, for both measuring stations the velocity in the direction of the first principal axis is determined and used further in this study. The collection of velocity vectors in the Elbe dataset of the upstream measurement station is depicted in Figure 18. For

consistency, again the reference system is set in downstream direction. Therefore, in this analysis, a positive velocity is in downstream/ebb direction while a negative velocity is in upstream/flood direction. The results of this data preparation are two vectors containing the axial velocity magnitude (positive and negative) for every 5 minutes in the period of 01-01-2012 until 31-12-2014 for the upstream and downstream measurement station.

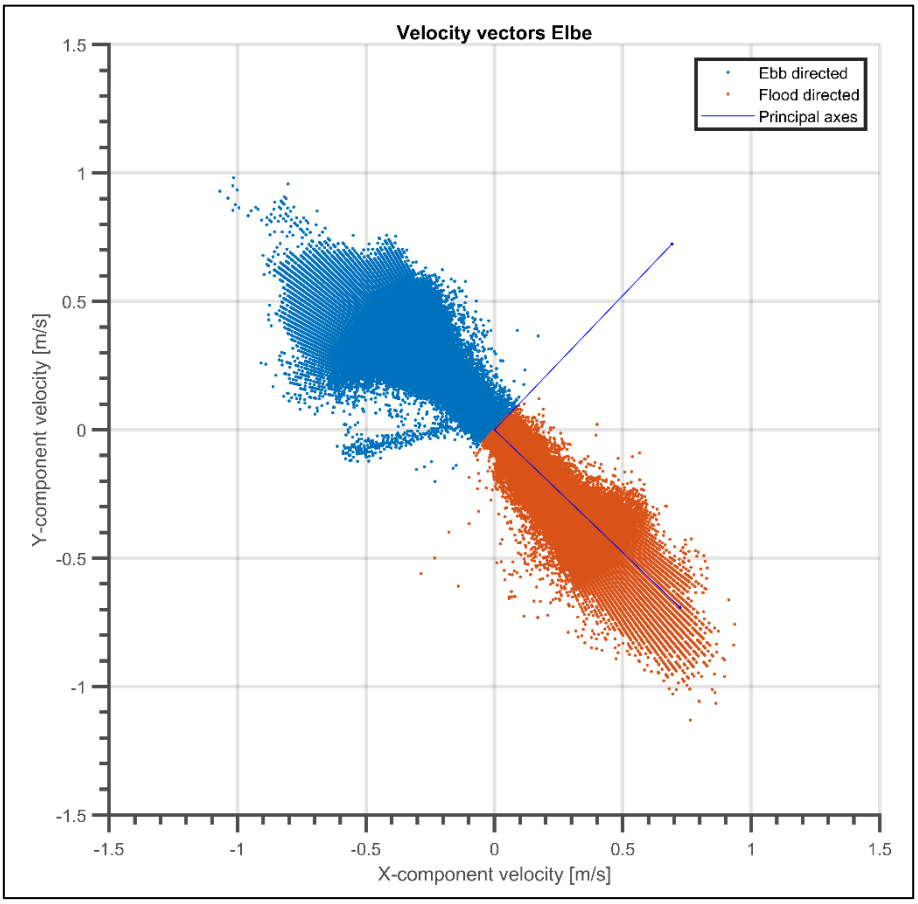

Figure 18: Velocity vectors of Elbe upstream near-bed velocity data, where a Principal Component Analysis is conducted to determine ebb and flood direction.

3.1.4 Discharge Elbe

As stated in Chapter 2, the discharge in the Scheldt estuary is relatively small. Combined with the fact that the Western Scheldt study locations are located near the mouth where the hydrodynamics are mainly tide dominated, the discharge for the Scheldt estuary is not taken into account. For the Elbe estuary on the other hand, the discharge is considered.

As described in paragraph 2.2.2, the discharge for the Elbe estuary is obtained at two locations. The dataset obtained from the Neu Darchau flow station contains daily average discharge values and is not further pre-processed. The dataset obtained from the Hamburg flow station contains the discharge measured in 10-minute intervals. Since this flow station is located in the tidally influenced region, the dataset contains both negative and positive discharges. In this dataset, the lower low ebb occurrences are determined. This way, the daily average discharge can be determined from the fluctuating discharge such that it can be compared with the Neu Darchau dataset and used in characterising the discharge at the study location. These lower low ebb occurrences are defined as the moments in time where the discharge crosses 0 m^3/s after which the discharge is directed in flood direction again. The

daily average discharge is the mean of the discharge in two cycles of the semi-diurnal tide. Thus, in between three lower low ebb occurrences of approximately 24 hours and 50 minutes. This results in a vector containing the average daily discharge obtained from the 10-minute measurements.

3.1.5 Water level

The origin of the sets of water level data is described in paragraph 2.2.2 and contains the water level of both the Elbe and Scheldt study locations. For each of these datasets, a similar approach is applied as described in the discharge section above. The moments of lower ebb are identified in the signal using a local minima function in Matlab. Then, the average water level is defined as the mean water level in a semi-diurnal tidal cycle which is in between two lower ebb conditions. Per measurement station, this results in the average water level in each semi-diurnal tidal cycle. This data can further be used to determine the water depth of the dunes and is described in paragraph 3.2.5.

3.2 Data processing

3.2.1 Bedform tracking tool

The bed elevation profiles (BEPs) as described in paragraph 3.1.2 can be processed in the bedform tracking tool developed in Matlab. The bedform tracking tool consists of 8 steps (van der Mark et al., 2008):

1. Outliers. The average absolute distance between consecutive points is determined. A point is considered an outlier when both the vertical distance with the previous point and the consecutive point is greater than 5 times the average absolute distance. If an outlier is identified, it is replaced by linear interpolation.
2. Trendline. The trendline is determined by applying a weighted moving average filter to the BEP. The weighted moving average filter applies a Hann window to smoothen the BEP. This Hann window requires a so-called filter span of an odd integer so that a symmetrical Hann window can be created. The filter span that is used determines the degree in which the trendline follows the original BEP. To determine the suitable filter span, all possible filter spans are considered, which are all odd integers within the range of the amount of datapoints of the signal. The BEP is detrended using all the possible filter spans iteratively. Each iteration, a Fourier transform is applied on the resulting detrended BEP. The outcome of this Fourier transform is used to determine the wavenumber for which the spectral power density is greatest. This way, a filter span is coupled with a wavelength which is dominant after detrending. To illustrate this step, a synthetic signal is created with three sinusoidal functions superimposed on a linear trend. These sinusoidal functions have a period of 25, 100 and 300 meters and an amplitude of 0.5, 1 and 3 meters, respectively. The resulting signal can be seen in Figure 19.

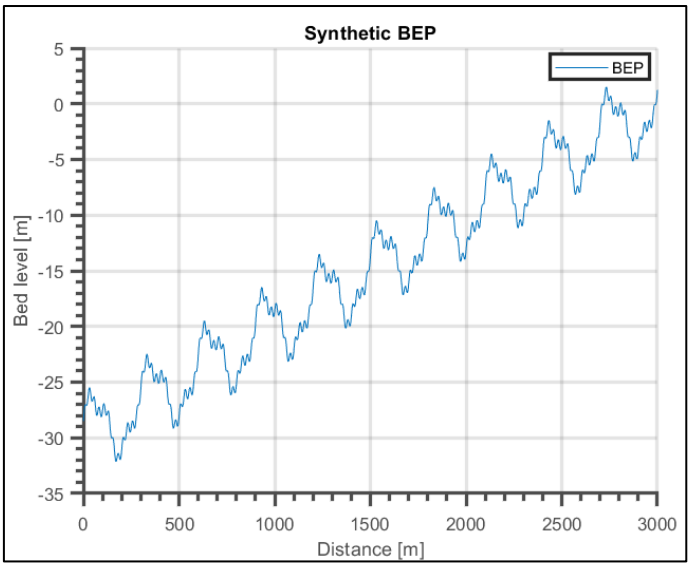

Figure 19: A synthetic bed elevation profile.

As stated, applying this step as described results in multiple filter spans with the accompanying dominant wavelength left in the BEP after detrending. This is depicted in Figure 20. In Figure 20, the different wavelengths of which the synthetic signal is composed can be clearly seen by the different sills. It is up to the user to determine which wavelength is of most relevance for the study. Depending on the choice which wavelength is most relevant, the trendline can differ. This is illustrated in Figure 21 for the choices where a wavelength of 100 or 300 meter are the focus of the study. The final span that will be applied to detrend the BEP is the span which is at 0.4 the length of the sill in Figure 20. Van der Mark et al. (2008) described that it is up to the user to give input and decide which bedform length is relevant to the study. Since in this study several thousands of BEPs are processed, this decision is automated and will be further elaborated later in this chapter.

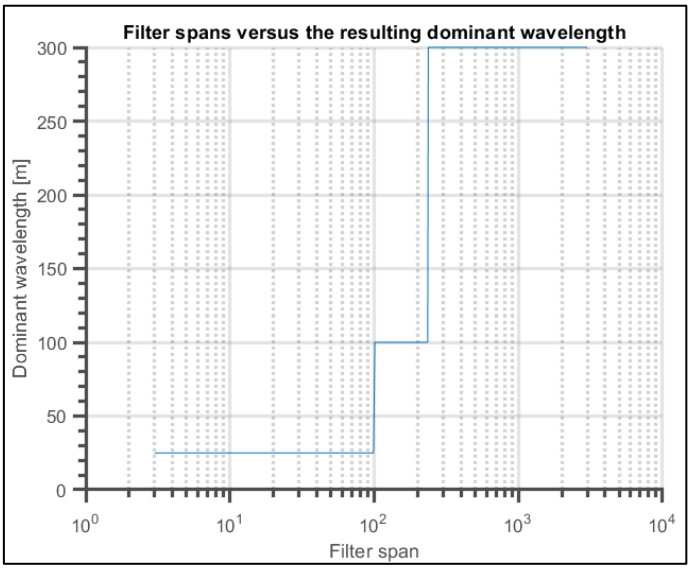

Figure 20: Dominant wavelength remaining in the BEP after detrending using a filter span.

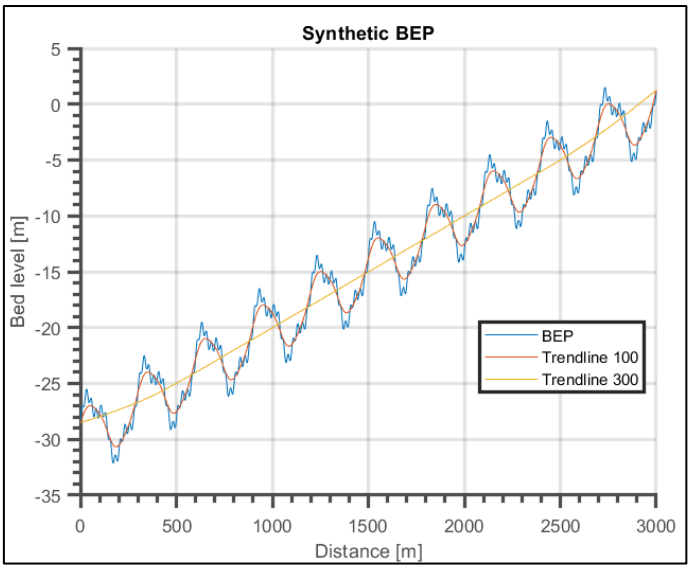

Figure 21: Resulting detrending trendlines based on which dominant wavelength in the BEP is most interesting for the study.

3. Detrending. The BEPs can be detrended by subtracting the determined trendline.
4. Weighted filter. Dunes will be identified by so-called zero-crossings in the next step. To prevent all fluctuations crossing the zero line to be identified as an individual crest or through, a weighted moving average is again determined with a Hann window and a corresponding span window. The span window is based on the average length of the dunes in the detrended BEP. To obtain the average dune length in the BEP, a Fourier transform is conducted on the detrended BEP. With the results of this Fourier transform, the spectral centroid is determined. The spectral centroid in a sense describes the average wavelength by a weighted averaging of the powers at the frequencies. The spectral centroid (average wavelength) is defined as follows:

$$\frac{1}{L_{av}} = \frac{\sum_{i=1}^{K} P_i * f_i}{\sum_{i=1}^{K} P_i}$$

Where L_{av} is the average wavelength in the detrended BEP $[m]$, K is the number of frequencies resulting from the Fourier transform, f represents the frequency bins resulting from the Fourier transform $[m^{-1}]$ and P is the power in the frequency bins $[m^2]$.
With the average wavelength, the average amount of datapoints per dune can be calculated:

$$A = L_{av}/d + 1$$

Where A is the average amount of datapoints per dune, L_{av} is the average dune length in the detrended BEP and d is the horizontal distance between two datapoints $[m]$.
The filter span used to define the filtered BEP in order to determine the zero-crossings is then computed as follows:

$$P = AC$$

Where P is the filter span to be used to filter the detrended BEP, A is the average amount of datapoints per dune and C is a filter span constant. Van der Mark and Blom (2007) defined the filter span constant as $1/6$. However, in this analysis a filter span of $1/3$ is more suitable and will be further elaborated later in this chapter.
5. Zero crossings. The downcrossings and upcrossings are the locations where the moving weighted average, as determined in step 4, crosses the zero line in downward and upward direction, respectively. The upcrossing and downcrossings combined are the zero crossings.
6. Crests and Throughs. A dune crest is located in between an upcrossings followed by a dowcrossings whereas a through is located after a downcrossing and before the consecutive upcrossing. It should be prevented that the crest is located at the highest fluctuation in the BEP instead of at the actual crest. To accomplish this, first the maximum of the weighted

average from step 4 is determined in between an upcrossing and a downcrossing (for convenience the location of this peak is termed maxwa). Then, a range is set using maxwa plus and minus half the filter span of step 4. The actual crest is the maximum of the detrended BEP within this range. The same procedure is performed in finding the throughs

7. Boundary crests and throughs. At the boundaries, throughs or crests may be located which are not bordered by both an upcrossing and downcrossing. In this analysis, the troughs at the boundary which are not bordered by both an upcrossing and a downcrossing are included if there are enough datapoints preceding or following the trough for a trough at the start or the end of the BEP, respectively. "Enough datapoints" is defined as $0.5P$ which is half of the filter span as defined in step 4. Crests at the boundary of the signal which are not bordered by both an upcrossing and a downcrossing are not included since they do not add extra information based on the definition of the dune characteristics which will be defined later.
8. Dune characteristics. Based on the obtained locations of the crests and throughs, the dune characteristics are determined. In this analysis the dune length is defined as the distance between two troughs, the height is defined as $H = z_c - \frac{z_1 L_2 + z_2 L_1}{L}$, and the asymmetry is defined as $A = \frac{L_1 - L_2}{L}$. A visualization of these dune characteristics is provided in Figure 22. The depth associated with a dune is determined by adding the water depth above the crest and the height of the dune after the method of Zhou et al. (2020).

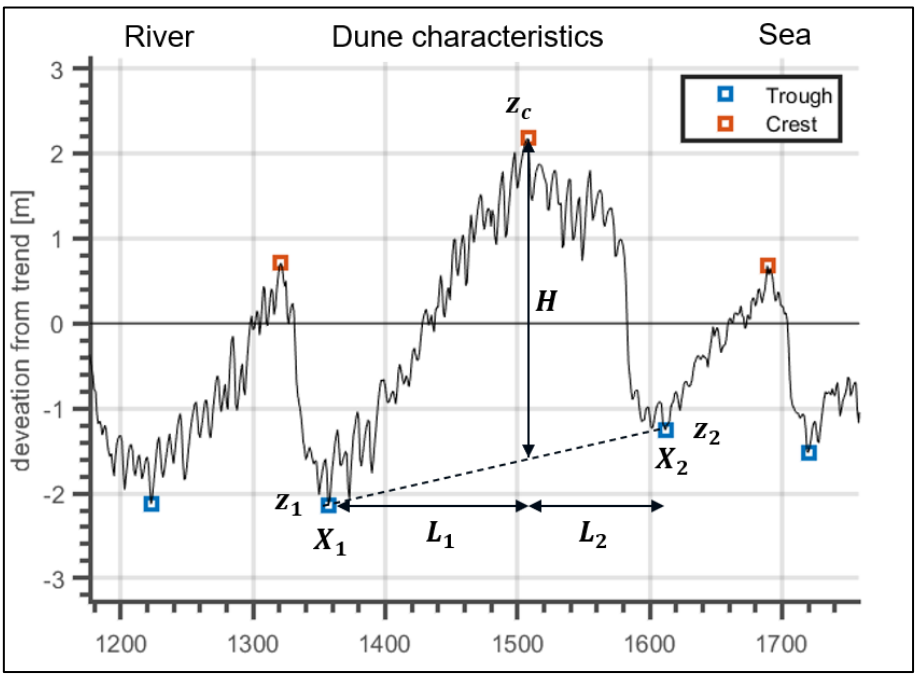

Figure 22: Dune characteristics derived from the troughs and crest positions.

In step 4, the bedform tool as described by van der Mark and Blom (2007) asks the user to define the bedform length he/she is interested in. Since in this study several thousands of BEPs are analysed, this approach is automated. In addition to saving the dominant wavelength in the signal after detrending with the corresponding filter span, also the power of this wavelength is saved with the filter span. When plotting the filter span versus the maximum occurring wave energy in the detrended BEP, a repetitive pattern can be seen. There is a local maximum in spectral power corresponding with the different wavelengths in the BEP. An example of this pattern is given in Figure 23 where the described methodology is applied to the synthetic signal of Figure 19. In this study, the focus lies on the dunes. Therefore, the interest lies with the bedforms that have the highest spectral energy. Based on Figure 23, the filter span with the highest spectral density is selected. With this filter span, the wavelength of

interest is selected from the data plotted in Figure 20. With the wavelength of interest determined, the bedform tracking tool resumes as described in the steps above. In order to prevent the underlying trend to become the wavelength of interest, a conditional statement is set that requires the wavelength of interest to be smaller than a fourth of the length of the BEP. This ensures that the bedforms identified by this procedure occur in the BEP at least four times.

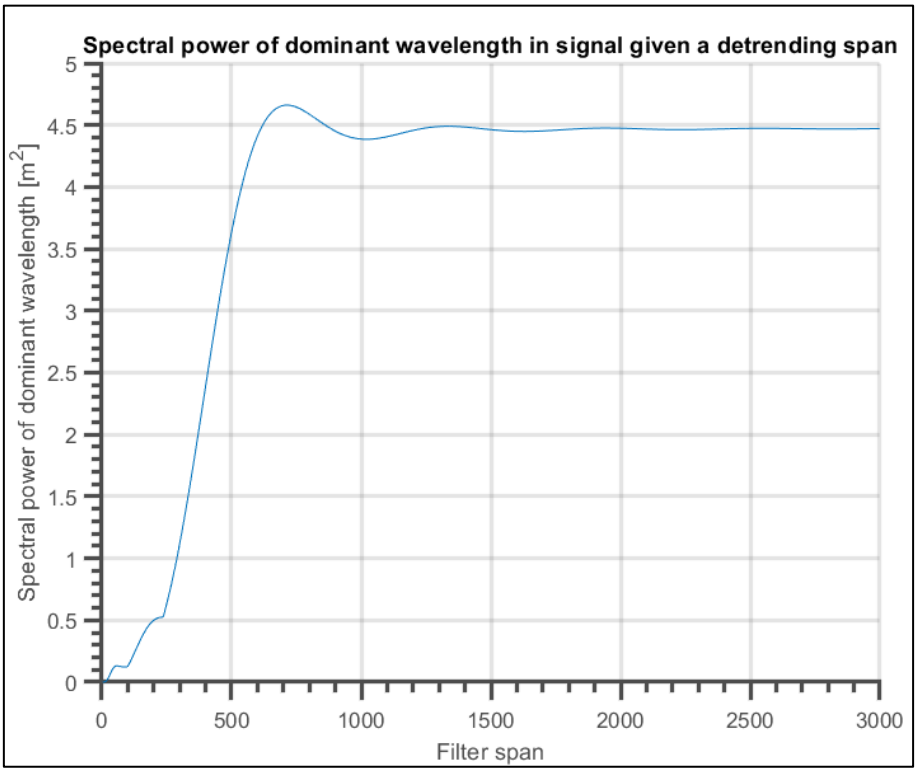

Figure 23: Spectral power of the dominant wavelength in the BEP after detrending using the different detrending spans.

A second adaption to the bedform tracking tool as described by van der Mark and Blom (2007) is the filter span constant. They used a sensitivity analysis on riverine data to come to a value of $1/6$ (see step 4). In this analysis, the bedform tracking tool is applied to estuarine data. In order to obtain a suitable filter span constant for this study, a similar sensitivity analysis is conducted. For this sensitivity analysis in the Western Scheldt, the middle transects of the study locations in 2019 are used to obtain the bed elevation profiles. For the Elbe, multiple bed elevation profiles are extracted throughout time. These bed elevation profiles are extracted from the transect as defined in Figure 15. These bed elevation profiles are processed using the bedform tracking tool with a varying filter span constant. The resulting dune characteristics can then be plotted against the used filter span constant to see which filter span constant is suitable. For the sensitivity analysis, the filter span constant is varied from $\frac{1}{20}$ to $\frac{20}{20}$ with increments of $\frac{1}{20}$ and a refined resolution in the area of interest. This procedure results in Figure 24 for the Western Scheldt study locations and in Figure 25 for the Elbe measurements. From Figure 24, it can be seen that the dune characteristics of the Western Scheldt area are sensitive to the filter span constant. A filter span constant of $1/3$ has been chosen as a suitable constant since at this value, the dune length and height have become nearly stable. This has also been the reasoning of van der Mark and Blom (2007) but with different data and a different outcome. From Figure 24 and Figure 25can be seen that the dune characteristics of the Elbe measurements are less sensitive to the filter span constant. In this area, a filter span constant of $1/3$ also results in stable dune characteristics.

Therefore, all bed elevation profiles of both the Scheldt estuary as well as the Elbe estuary are processed using a filter span constant of 1/3.

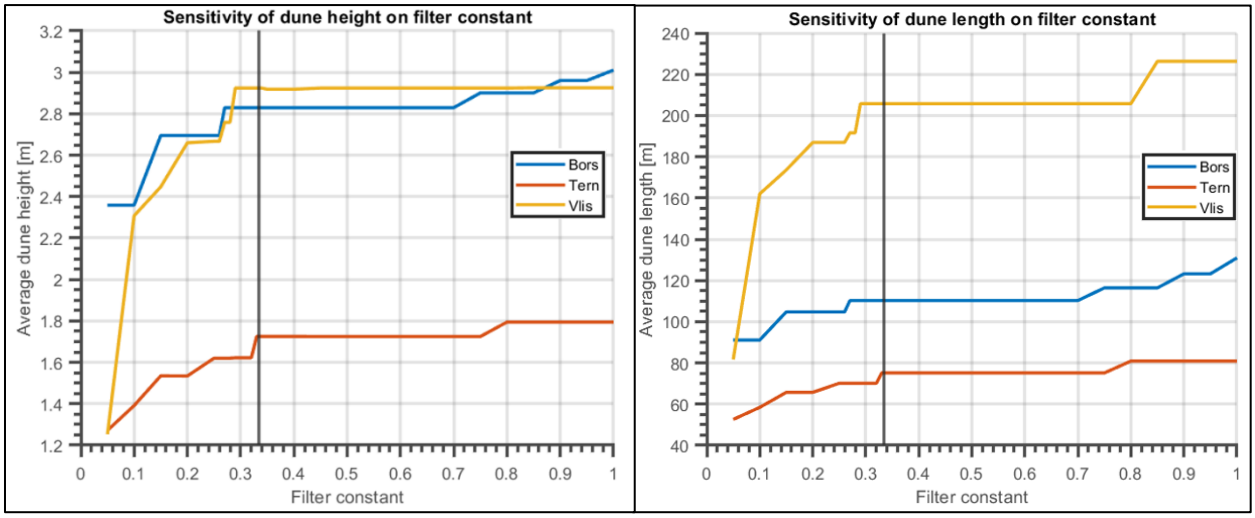

Figure 24: Sensitivity of the average dune height and dune length on the filter span constant for different areas in the Western Scheldt.

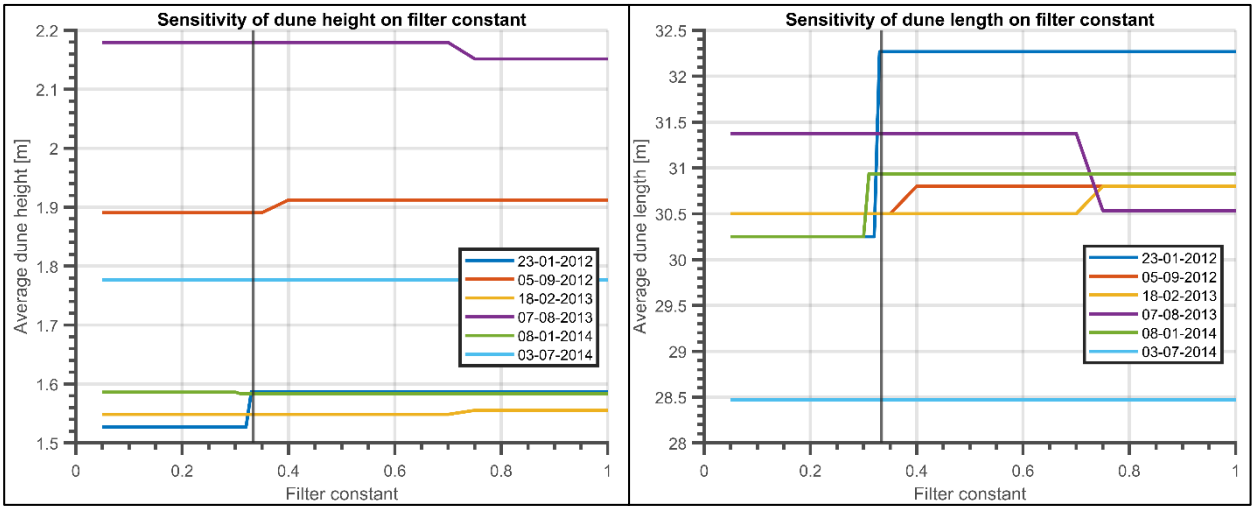

Figure 25: Sensitivity of the average dune height and dune length on the filter span constant for the Elbe study location for multiple bed level measurements.

3.2.2 Representative transect Western Scheldt

In order to relate the characteristics of a dune field with environmental conditions that are only available on a larger scale, the characteristics of the Western Scheldt dune fields need to be represented in single values. This can for example be done with the mean value of the dune lengths and the standard deviation of the dune lengths. In paragraph 3.1.2, it is described that the transects are drawn parallel with a resolution that is equal to the underlying grid. When all transects drawn over the study location are taken into account to represent the dune field, the same dunes are measured every meter resulting in statistically homogeneous measurements. It is therefore chosen to select a single transect over the dune field which represents the dune field. In the Elbe study location, a single transect is already selected. Therefore, the approach described here only applies for the study locations in the Western Scheldt.

As a first step to obtain a representative transect for the Western Scheldt study locations, all parallel transects are processed using the bedform tracking tool as described in paragraph 3.2.1. Then, for each transect the average height and length is determined. From this data, the average height and length for the entire dune field is determined as is depicted in Figure 26. For every transect it is determined how the mean dune height and length of the transect deviate from the mean dune height and length of the entire field. This difference is normalized with the mean dune height and length of the field. For a transect, the normalized deviation of the mean dune height of the transect from the mean dune height of the field is summed with the normalized deviation of the mean dune length of the transect from the mean dune length of the field. Based on this result, a transect can be selected which contains dunes that have characteristics that are closest to the average characteristics of the dune field. This is visualized in Figure 27, where the representative transect is indicated by the red cross. This representative transect is used to define the characteristics of the dune field. The derivation of all representative transects of the Western Scheldt study locations is visualized in Appendix D.

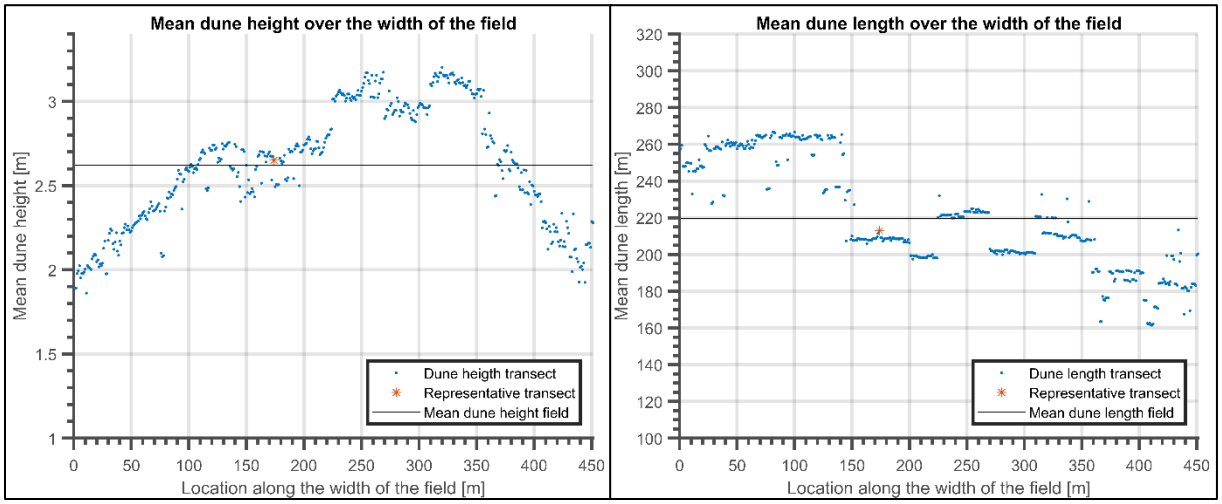

Figure 26: Mean dune height and length of transects plotted over the width of the field for the Vlissingen study area in 2019.

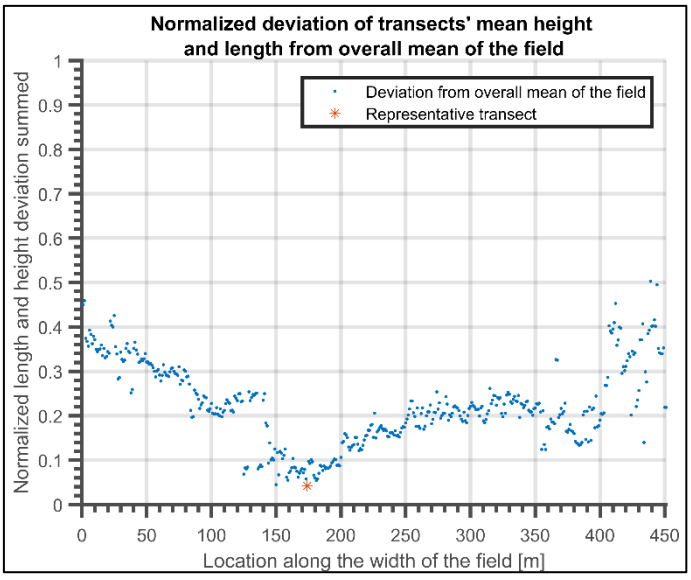

Figure 27: Normalized deviation of the dune height and length from the total mean over the width of the field for the Vlissingen study area in 2019.

3.2.3 Velocity asymmetry

In paragraph 3.1.3, it is described how the representative flow velocity is derived for the study sites. In the Western Scheldt, the flow velocities for the study sites are cross-sectionally averaged velocities from the Delft3D flow model results. In the Elbe, the flow velocities are obtained from in-situ measurement stations in the same period as the bed level measurements. These measurements of flow velocity vectors are decomposed into a magnitude of the velocity along the first principal axis as described in paragraph 3.1.3. The flow velocity in estuaries in ebb and flood direction can be asymmetric in nature as described in paragraph 1.1.1. Here, it is described how the obtained velocity datasets are analysed for velocity asymmetry.

The asymmetry of the prepared velocity data is quantified using a statistical skewness measure. This method follows the procedure as implemented by Gong et al. (2016), Guo et al. (2019) and Nidzieko & Ralston (2012). In this statistical measure, the skewness of a signal is quantified by normalizing the third moment about zero with the second moment about zero to the power 2/3 (Nidzieko & Ralston, 2012). The skewness of a signal can be defined as follows:

$$\gamma_0 = \frac{\mu_3}{{\mu_2}^{3/2}} \qquad \text{Eq.2}$$

In Eq.2, the mth moment about zero can be expressed as follows:

$$\mu_m = \frac{1}{N-1}\sum_{i=1}^{N}(n_i)^m \qquad \text{Eq.3}$$

Where N is the number of data samples and n_i denotes the i^{th} data sample.

The peak current asymmetry (PCA) is obtained when using the velocity signal as input for Eq.2 and Eq.3. The PCA is mostly associated with the residual flux of the coarser sediment (bed load transport) due to differences in magnitude and duration of the peak ebb and flood flow velocity (Guo et al., 2018; Nidzieko & Ralston, 2012). The slack water asymmetry (SWA) can be calculated when the derivative of the flow velocity is used as input in Eq.2 and Eq.3. The SWA is mostly associated with the residual transport of suspended load (Guo et al., 2018; Nidzieko & Ralston, 2012). Since in this study focusses on the dune characteristics, which is mostly affected by the bed load (e.g. Naqshband et al., 2014), only the PCA is computed. Furthermore, the PCA as described is the third moment about zero normalized with the second moment about zero to the power 3/2. This normalization results in a ratio describing the velocity asymmetry in a relative manner. However, in order to correlate the dune characteristics to the velocity asymmetry, the velocity asymmetry is also expressed in its absolute value. This way, the velocity asymmetry is not dampened by the normalization. Therefore, in addition to the peak current asymmetry as described, the PCA is also computed without normalizing with the second moment about zero. This metric is further termed the non-normalized PCA and is computed by only the third moment about zero using Eq.3. Since bedload transport generally scales with the flow velocity cubed (e.g. Allen, 1982), taking the third moment of the near bed flow velocity is seen as a good indication of the residual bed load transport and thus a relevant metric to correlate with the dune characteristics.

In order to capture the subtidal variations of the velocity asymmetry (both PCA and non-normalized PCA), the skewness is determined for each discrete lunar day as is done by Nidzieko & Ralston (2012) and Gong et al. (2016), where a lunar day is defined by three moments of lower-low water (LLW) since both estuaries are influenced by a semi-diurnal tide. Furthermore, a threshold of 0.15 m/s is

implemented as is done by Guo et al. (2018). This threshold serves as a lower limit for the (non-normalized) PCA. This threshold states that the (non-normalized) PCA is calculated using the velocity signal u where $\mathrm{abs}(u) > 0.15\ \mathrm{m/s}$. This threshold ensures that the velocities during slack water tide are not used to calculate the (non-normalized) PCA. As stated, the orientation is chosen such that the downstream direction is the positive direction. Therefore, the positive velocities indicate flow in the ebb direction which means that a positive velocity skewness is also ebb directed.

As described in paragraph 1.1.2, dunes do not adapt to the changes in environmental conditions instantaneously. To take this lag into account when testing the correlating between the dune asymmetry and the velocity asymmetry, a cross-correlation is first conducted to analyse the lag of these dune characteristics. In this cross-correlation, the dune asymmetry is first correlated with the non-normalized PCA of the same day the topographic measurements were taken. The resulting R-squared and p-value of this correlation are registered. Then, the dune asymmetry is correlated with the mean non-normalized PCA of the day the topographic measurements were taken and its preceding day. Again, the resulting R-squared and p-value of this correlation are registered. This is process is repeated for the preceding 2 to 28 days. The result is a plot with the R-squared and p-value of the correlation between the dune asymmetry and velocity asymmetry when a lag between 0 and 28 days is applied. It should be noted that this cross-correlation is only possible for the Elbe study location since for this location both the velocity asymmetry and the topographic data are available for the same period. For the Scheldt study locations, the dune asymmetry is correlated with the average non-normalized PCA of the model output, without cross-correlating.

3.2.4 Discharge Elbe

In paragraph 3.1.4, the preparation of the discharge data of the Elbe estuary is described. This discharge data is used to correlate with the extracted dune characteristics of the Elbe measurements. First, the lag of the dune characteristics to the discharge is investigated using the same cross-correlation technique as described in paragraph 3.2.3 but using the discharge of the Elbe and the dune characteristics. Then, the dune characteristics are correlated with the river discharge using the lag that is obtained from the cross-correlation.

3.2.5 Water depth

The same approach as described for the discharge is applied to the water level. This holds both for the water level of the Elbe measuring station as well as for the water level of the Western Scheldt measuring stations. The water depth obtained from the data preparation contains tidally averaged water levels. A distinction between the water depth and discharge dataset is that the discharge is equal for the entire Elbe dune field. Therefore, the discharge data is correlated with the average characteristics of the observed dunes. The water depth can be determined for each dune individually. As described in paragraph 3.2.1, following the method of Zhou et al. (2020), the water depth is defined as the distance between the surface level and the dune crest combined with the dune height. The bedform tracking tool has extracted the dune heights and distance from the dune crests to the reference level. In the Western Scheldt, this reference level is the Amsterdam Ordnance Datum (NAP) while in the Elbe the reference level is the German vertical datum DHNN92.

To determine the lag of the dune characteristics on the water level, again a cross-correlation is conducted as is described in paragraph 3.2.3 but using the water depth and dune characteristics. Then the dune characteristics are correlated with the water depth based on the lag resulting from the cross-

correlation. This cross-correlation is again only conducted for the Elbe study site since for this location 60 bed level measurements are available. For the Scheldt, only two bed level measurements are available per study site making a cross-correlation not as reliable. Therefore, the Scheldt dune characteristics are correlated with the average water level of the preceding 14 days since this is in the same order as is obtained from the Elbe cross-correlations.

3.2.6 Velocity magnitude

It is difficult to compare the occurring flow velocities in the two estuaries since they are both obtained in different methods. The flow velocity representing the Scheldt study location is expressed in the cross-sectionally averaged flow velocity. The flow velocities representing the Elbe study location are obtained from point measurements near the bed and near the surface. In order to be able to compare these datasets, the velocity amplitudes are computed. The velocity datasets that are already addressed are the cross-sectionally averaged velocities of the Borssele, Terneuzen and Vlissingen study area and the flow velocities near the bed at the upstream and downstream measurement station of the Elbe study site. The velocities near the surface at these measurement stations of the Elbe study site are yet unaddressed but are included in this analysis. For all these datasets, the maximum ebb and flood flow velocity per tidal cycle are identified to quantify the flow velocity range. As a next step, the average velocity amplitude is calculated for the entire modelling period in case of the Scheldt study areas. For the Elbe velocity measurements (upstream and downstream, near the bed and near the surface), the average velocity amplitude is calculated for the entire surveying period of 2012-2014. Even though these amplitudes represent a different velocity (cross-sectionally averaged or point measurements), they can be used to obtain a general idea of the occurring velocities and conduct basic comparisons.

3.2.7 Sediment

Thus far, the preparation of the sediment sampling data has not been discussed. The sediment data both in the Elbe and Scheldt estuary show a high variability depending on the location. Generally, the main channels contain sediment with larger grain sizes compared with the areas outside the main channels. Therefore, there is a higher spatial correlation of sediment size in the direction of the main channels compared to the cross-sectional direction. This makes it difficult to create accurate and valid spatial interpolation maps of the sediment grain sizes. Therefore, a simpler approach is applied. For each study location, the sediment samples which are in the proximity of the study area are selected. Only these samples, containing the median grain size (D_{50}) of the measurements, are used to characterise the grain sizes of the study locations. The sediment sample dataset of McLaren which is used in the Scheldt estuary does not cover the Vlissingen study area. For the Elbe, Borssele and Terneuzen study area, the sediment samples which are used to characterise these areas are depicted in Figure 28, Figure 29, and Figure 30, respectively.

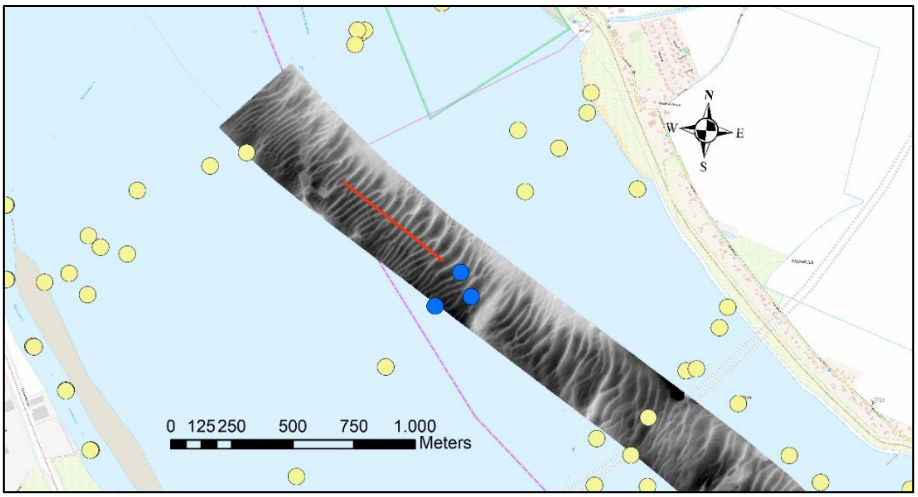

Figure 28: Sediment samples of the Elbe estuary where the blue-marked samples are included to characterise the study area.

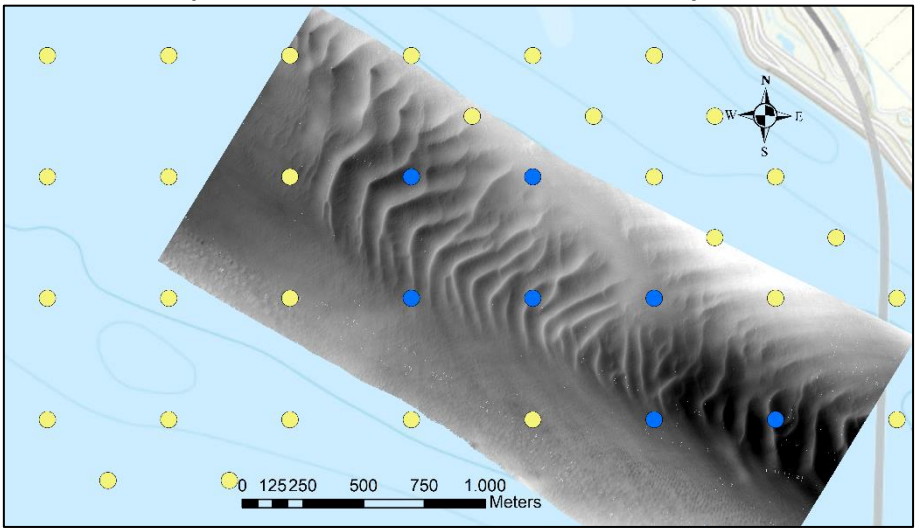

Figure 29: Sediment samples of the McLaren dataset where the blue-marked samples are included to characterise the Borssele study area.

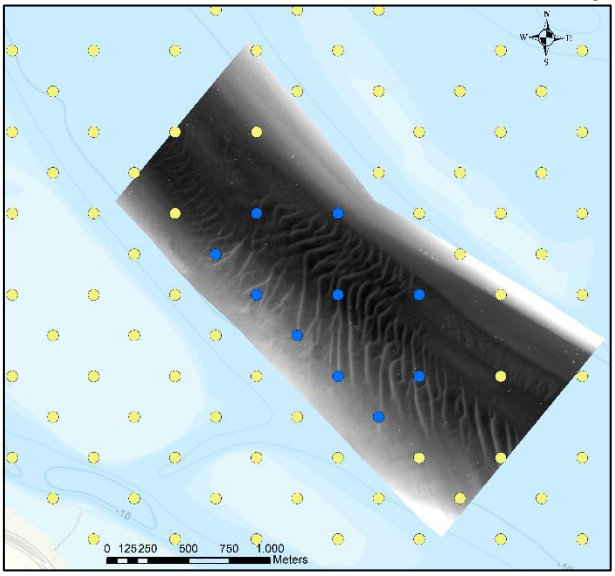

Figure 30: Sediment samples of the McLaren dataset where the blue-marked samples are included to characterise the Terneuzen study area.

4. Results

In this chapter, the results of the conducted data analysis are described. First, the dune characteristics, environmental parameters, and correlations of the Western Scheldt study locations are shown. Then, the results of the Elbe study location are presented. The first set of results for both the Scheldt and Elbe study locations are provided in Figure 31. This figure depicts the average dune height and length of the study fields combined with the variability of the characteristics within the dune fields.

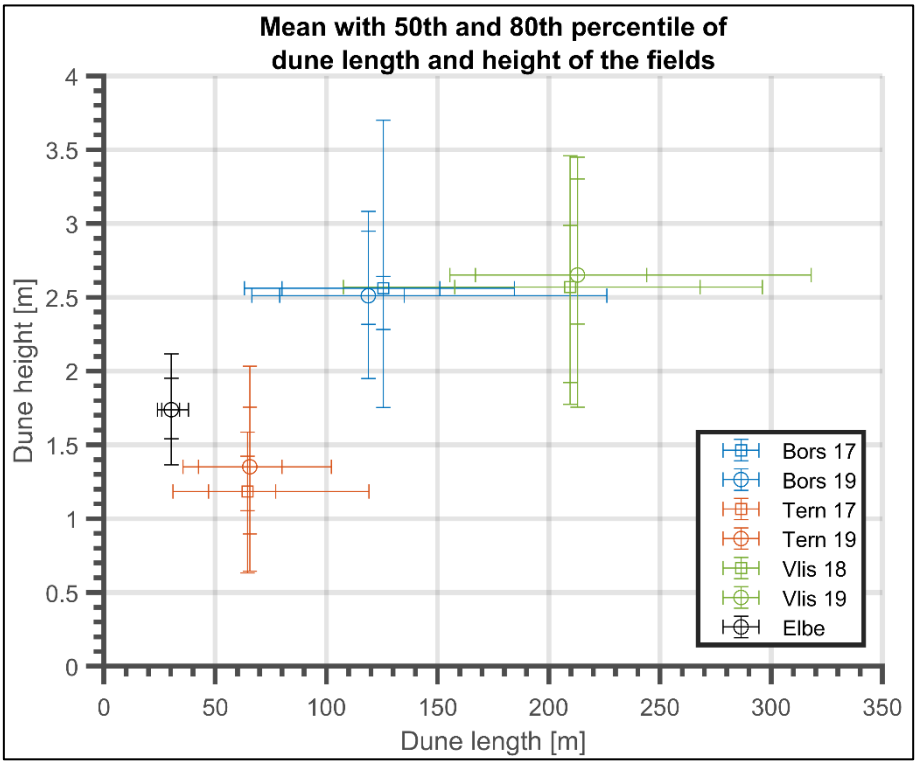

Figure 31: Length and height of three dune fields in the Western Scheldt for two measurements and for the complete measurements of the Elbe study site. The number in the legend indicates in what year the measurement was taken.

4.1 Spatial variability: Western Scheldt

The orientation of the transects and the derivation of the representative transects for the Scheldt study locations can be found in Appendix B and Appendix D, respectively. The dune characteristics presented here are obtained from these representative profiles. The dune length and height of the three dune fields for the two measurements in the period 2017-2019 can be seen in Figure 31. This figure also displays the variation of the lengths and height of the dunes in the representative transects. Figure 31 shows the situation that is expected. In the Western Scheldt, the height and length of the dunes vary over the spatial extent but are relatively constant over time. The height of the dunes observed in the Borssele study location are similar to the height of the dunes observed in the Vlissingen study area. The lengths of the dunes in these two areas do differ, where the lengths of the dunes in the Vlissingen study area are much longer compared to those in the Borssele area. Both the height and length of the dunes in the Terneuzen study site are significantly smaller compared to the Vlissingen and Borssele area.

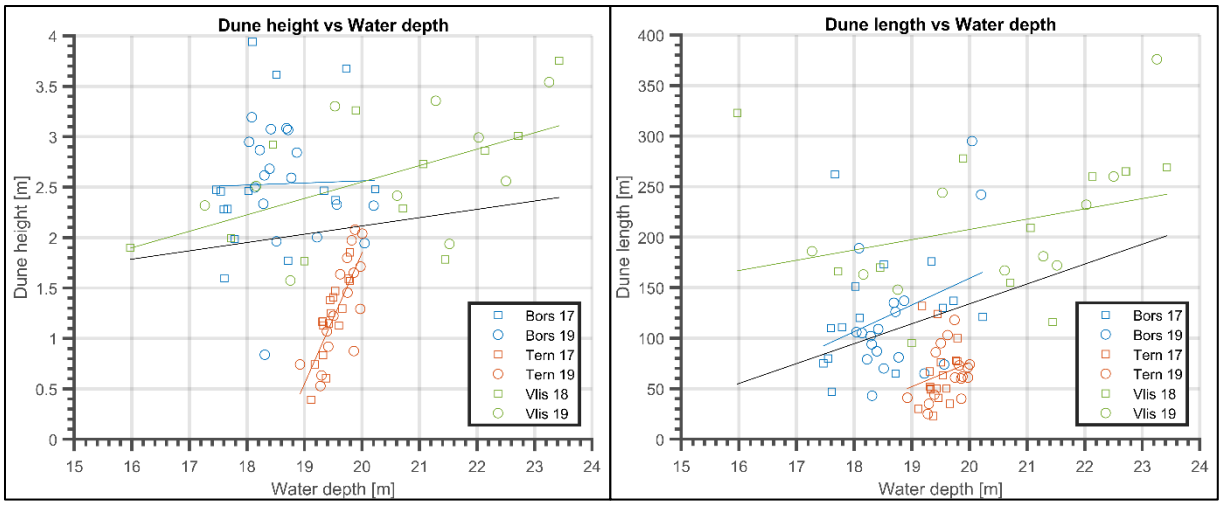

Figure 32: Dune height (left) and dune length (right) correlated with the mean water depth of the preceding 14 days in the Scheldt study locations. Linear models are fitted per location (same colour) and for all locations combined (black).

The dune height and length are plotted and correlated with the water depth in Figure 32. The corresponding R-squared and p-value metrics of the correlations displayed in Figure 32 are given in Table 2 and Table 3. A striking correlation is found in the dune height correlation with the water depth in the Terneuzen study location. With a p-value of $1.5 * 10^{-7}$, this correlation is the most convincing in the dataset. It is however questionable whether this correlation can be extrapolated to smaller and larger depths since the depth range of the Terneuzen area is quite limited. The Vlissingen study area, with the largest variability in water depth, also shows a significant correlation between dune height and water depth. With a p-value of $1.3 * 10^{-2}$, indicating that approximately once every 75 tests this correlation is a false outcome, the correlation explains 28% of the variation in dune height. However, when combining all observations and setting the alpha level to 0.05, no significant correlation is found between the dune height and water depth. Considering the same alpha level in the correlation between water depth and dune length, a significant correlation is found when combining all datapoints. Even though individually only the Borssele study area shows a significant correlation.

Table 2: Regression metrics for the water depth vs dune height relation in the Scheldt study locations.

	R-squared	P-value
Borssele	$7.0 * 10^{-4}$	$8.8 * 10^{-1}$
Terneuzen	$5.9 * 10^{-1}$	$1.5 * 10^{-7}$
Vlissingen	$2.8 * 10^{-1}$	$1.3 * 10^{-2}$
Total	$2.7 * 10^{-2}$	$1.3 * 10^{-1}$

Table 3: Regression metrics for the water depth vs dune length relation in the Scheldt study locations.

	R-squared	P-value
Borssele	$1.2 * 10^{-1}$	$5.0 * 10^{-2}$
Terneuzen	$5.6 * 10^{-2}$	$1.8 * 10^{-1}$
Vlissingen	$9.3 * 10^{-2}$	$1.8 * 10^{-1}$
Total	$1.4 * 10^{-1}$	$5.0 * 10^{-4}$

The asymmetry of the dunes of the three study locations is provided in Figure 33. In this figure, the central red mark indicates the median value. The lower and upper edge of the box indicate the 25th and 75th percentiles, respectively. The dotted line extends to the extreme datapoints which are not considered outliers and the red crosses indicate the outliers. Figure 33 shows a clear distinction between the Borssele study area compared to the Terneuzen and Vlissingen area. In both measurements of the Borssele area, the dunes are predominantly asymmetric in landward/upstream direction. Both the dunes in the Terneuzen and Vlissingen area show an asymmetry in seaward/downstream direction. Of these two locations, the dunes in the Vlissingen area are more asymmetric than the dunes in the Terneuzen area.

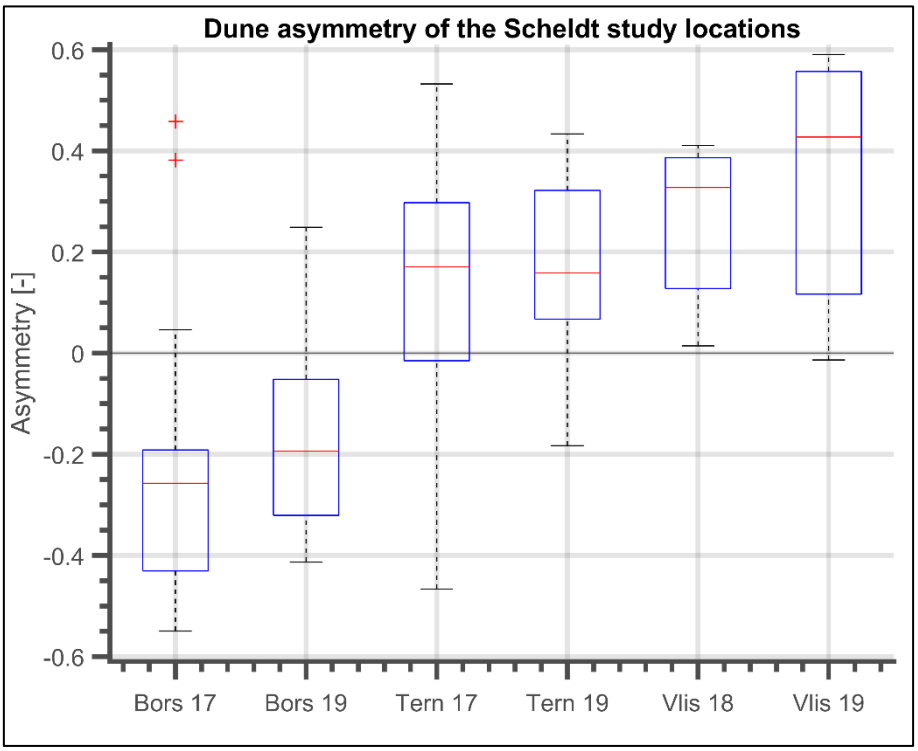

Figure 33: Asymmetry of three dune fields in the Western Scheldt for two measurements. The number in the labels indicates the year the measurement was taken.

The results of the velocity analysis of the data obtained from the Delft3D flow model can be observed in the following figures. Figure 34 displays the peak current asymmetry (PCA), and Figure 35 shows the non-normalized peak current asymmetry of the three study locations. Since the orientation is chosen such that the velocity in seaward/downstream direction is considered positive and the velocity in landward/upstream direction is considered negative, the skewness measure follows this orientation. Meaning that a negative skewness indicates flow velocity asymmetry in landward/upstream direction while a positive skewness indicates an asymmetry in seaward/downstream direction. In Figure 34, the differences in PCA can be seen. The skewness of the Terneuzen and Vlissingen area are both in seaward/downstream direction for the complete year that the model simulates. Where the Vlissingen area is more skewed compared to the Terneuzen area. It can also be seen that in the Borssele area the PCA is skewed in the landward/upstream direction. In Figure 35, the same statements hold for the non-normalized PCA, where Vlissingen and Terneuzen show a velocity asymmetry in seaward/downstream direction and Borssele displays a velocity asymmetry in landward/upstream direction. These observations neatly align with the observations of the dune asymmetry previously made. Due to not normalizing, the asymmetry skewness indicator is, especially for the Terneuzen and

Borssele study area, closer to zero compared to the normalized PCA. Also, in Figure 35 the effect of the neap-spring cycle on the velocity asymmetry can be better observed.

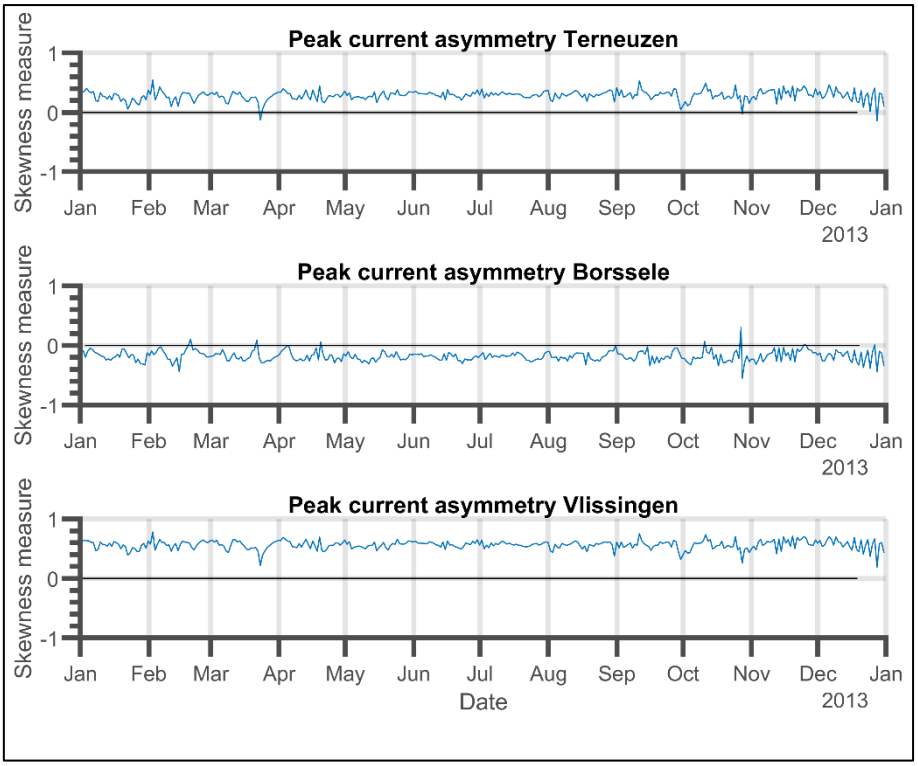

Figure 34: Peak current asymmetry for the three study locations in the Scheldt. Obtained from analysing the Delft3D cross-sectional discharge data.

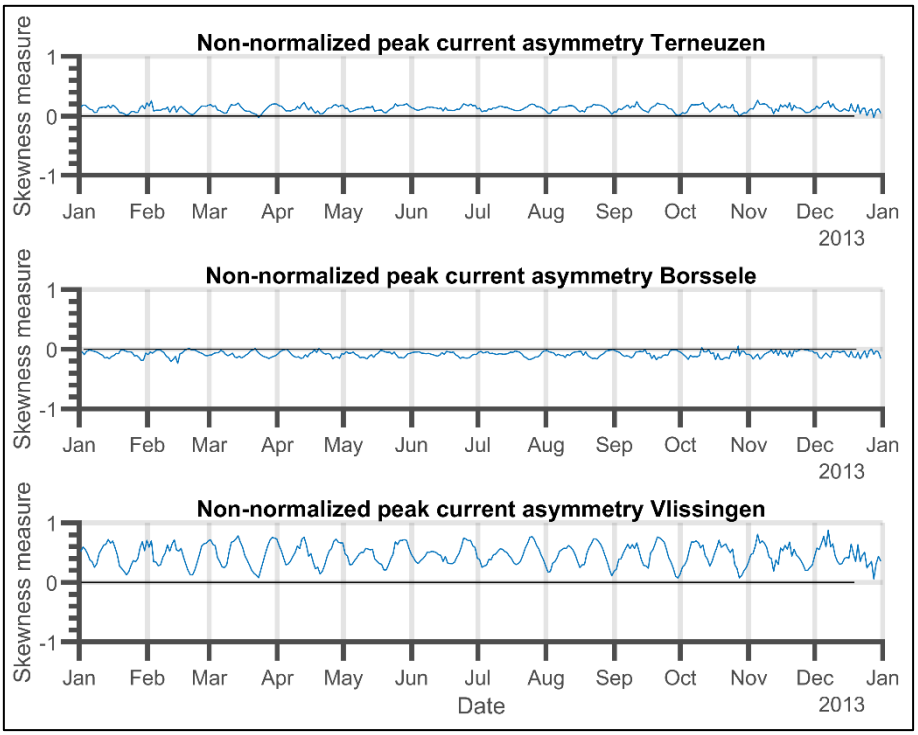

Figure 35: Non-normalized peak current asymmetry for the three study locations in the Scheldt. Obtained from analysing the Delft3D cross-sectional discharge data.

In Figure 36, the average non-normalized velocity asymmetry of the Delft3D model results is plotted against the average observed dune asymmetry of the study sites. With a P-value lower than 0.05 and a R-squared of 0.86, this correlation confirms the observations made that the velocity asymmetry aligns with the observed dune asymmetry.

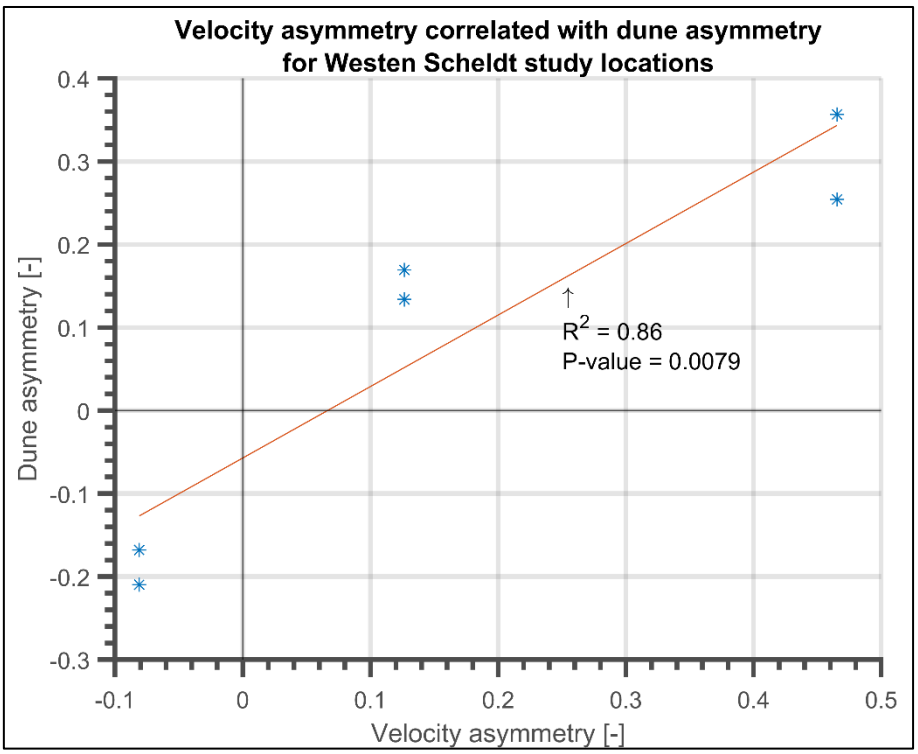

Figure 36: Average non-normalized velocity asymmetry plotted against the average dune asymmetry of the Western Scheldt study locations.

For a complete neap-spring tidal cycle, the cross-sectionally averaged flow velocities of the cross-sections from the Delft3D model are depicted in Figure 37. In this figure, the flow velocity at the Vlissingen study area shows significantly larger peaks in the seaward/downstream direction which is also expected with the considerable seaward/downstream peak current asymmetry (Figure 34 & Figure 35). For the Borssele and Terneuzen study areas, the differences in flow velocity peaks are also observable but less significant.

The flow velocity amplitude for the three cross-sections is given in Table 4. This velocity amplitude is the mean of all the velocity amplitudes occurring in the modelled year. The Vlissingen cross-section shows the greatest velocity amplitude which can also be seen in Figure 37. Remarkably, the Borssele and Terneuzen cross-section show the exact same velocity amplitude.

Table 4: Mean of the cross-sectionally averaged flow velocity amplitudes for the entire modelled year.

Study site	Velocity amplitude
Vlissingen	1.30 m/s
Borssele	1.05 m/s
Terneuzen	1.05 m/s

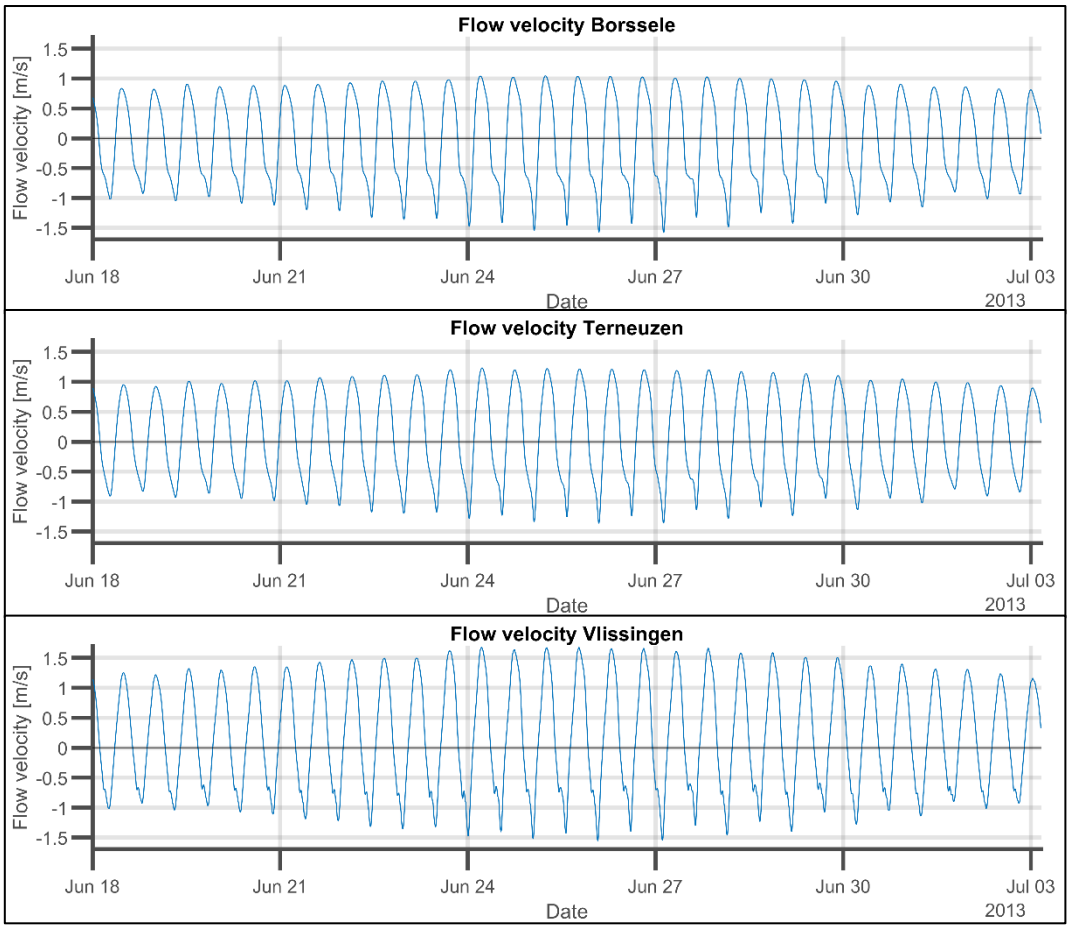

Figure 37: Cross-sectionally averaged flow velocities obtained from the cross-sections of the Delft3D model for a complete neap-spring cycle.

The median grain sizes of the sediment samples characterising the Terneuzen and Borssele study area are given in Table 5. The locations of these sediment samples are defined in Figure 29 and Figure 30. From this result can be obtained that the Terneuzen and Borssele study area have a very similar sediment composition.

Table 5: Median grain sizes of the sediment samples characterising the Terneuzen and Borssele study locations.

Terneuzen	Borssele
406 µm	280 µm
243 µm	306 µm
328 µm	241 µm
359 µm	286 µm
237 µm	263 µm
288 µm	318 µm
375 µm	328 µm
243 µm	-
265 µm	-
245 µm	-
Mean: 299 µm	Mean: 289 µm

4.2 Temporal variability: Elbe estuary

This paragraph describes the results obtained from the data analysis for the Elbe study area. The mean and the variation of the dune characteristics of the Elbe estuary are depicted in comparison with the Scheldt study locations in Figure 31. It can be observed that the dune length of the dunes in the Elbe study location is significantly smaller compared to the length of the dunes in the Scheldt study locations. The dune height of the dunes in the Elbe study site is smaller than the height of the dunes of the Borssele and Vlissingen study area while they are larger than dune height in the Terneuzen area. In Figure 38, the mean and the variation of the Elbe dune characteristics are plotted over time. Here, the variation of the dune characteristics is depicted by the 50th and 80th percentile bands. It can be seen that the dune length remains nearly constant over time and is therefore not further considered in the correlation analysis. The dune height and asymmetry do show a fluctuation. It appears as if the asymmetry of the dunes is mostly directed in landward/upstream direction only to be asymmetric in seaward/downstream direction in the start of 2012 and spring and early summer of 2013.

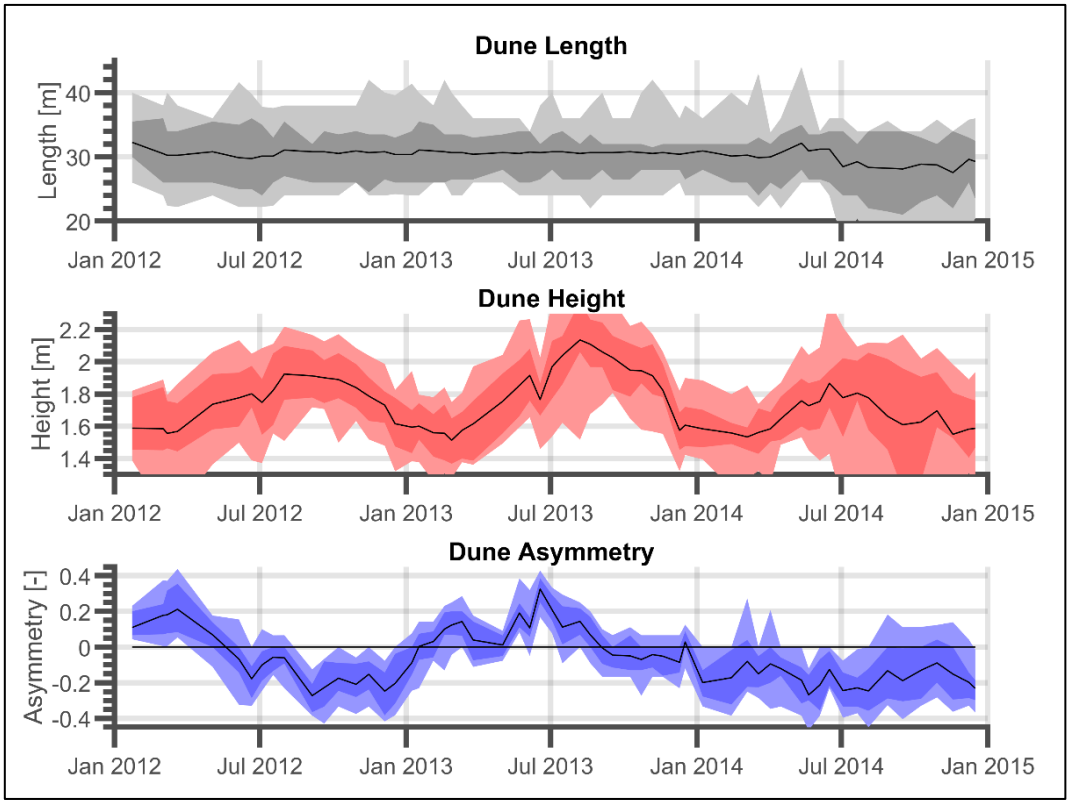

Figure 38: Characteristics of the dunes in the Elbe study site over time where the bands represent the 50th and 80th percentile.

The daily average discharge of the Elbe is depicted in Figure 39. This daily average discharge is derived in two ways as described in paragraph 3.2.4. The daily discharge determined from the data of Hamburg using the average discharge in two semi-diurnal cycles is very similar to the daily average discharge measured at Neu Darchau. Since the discharge obtained from the Hamburg flow station contains missing data (e.g., see Feb-Apr 2012), and the Neu Darchau data does not, the discharge obtained from the Neu Darchau measuring station is used for further analysis. In Figure 39, a clear discharge peak is observed in the summer of 2013. Furthermore, a high discharge is also observed in the start of 2012 and 2013. These observations already show similarities with the observed variation in dune asymmetry.

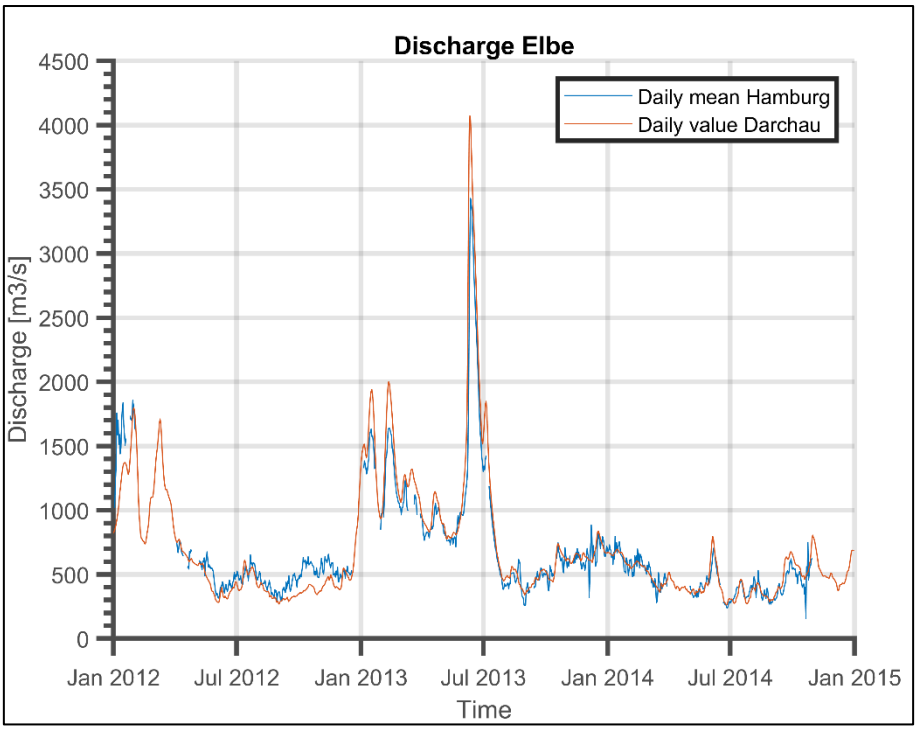

Figure 39: Discharge in the Elbe in 2012-2014 determined using two methods.

The result of the cross-correlation between the environmental parameters and the dune characteristics is depicted in Figure 40 and Figure 41. From Figure 40 (left) can be observed that the R-squared gradually increases when the dune height is correlated with the mean water depth of a larger number of preceding days. The dune height cross-correlated with the average preceding river discharge does not show an improvement of the R-squared (Figure 40 right). This means that there is no increase of similarity between the dune height and average discharge when the average preceding river discharge is determined using an increasing number of days. The p-value makes no difference when the lag is altered. It is very small in the depth cross-correlation, indicating a statistically significant correlation throughout. In case of the correlation with the dune height, the p-value is above 0.05 for all evaluated lags.

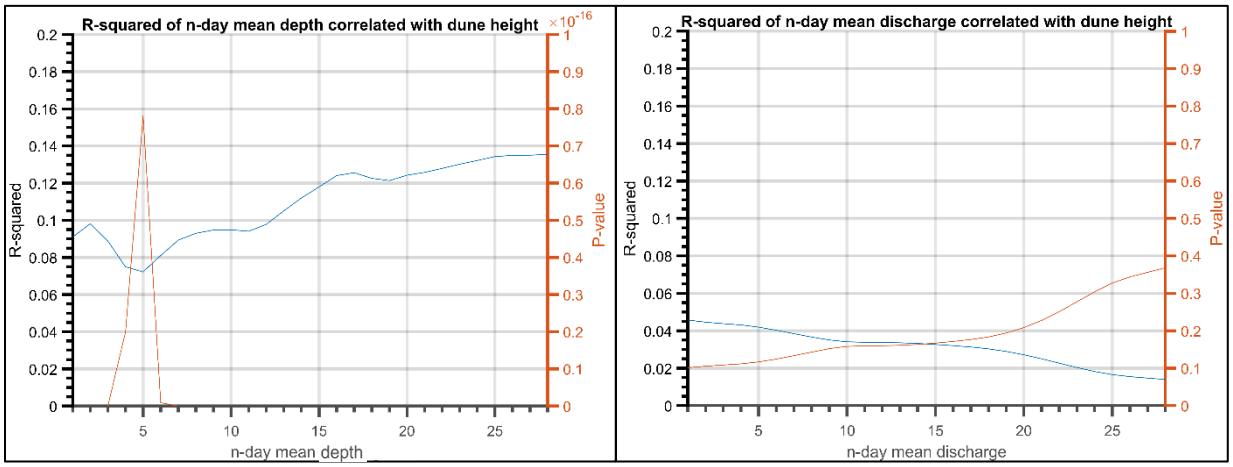

Figure 40: Cross-correlation between the depth (left) and discharge (right) and the dune height indicated by R-squared (blue) and P-value (red). Where the n-day mean depth and discharge denote the number of preceding days of which the mean depth and discharge are taken to correlate with the dune characteristics.

The cross-correlation between the dune asymmetry and the mean preceding discharge does show a clear local optimum in Figure 41. When the dune asymmetry is correlated with the average discharge of the preceding 19 days, the dune height and discharge show the greatest similarity. Again, the p-value is far below 0.05 for all considered lags. Since no significant local optima are observed in Figure 40, the dune height and asymmetry are correlated with the mean discharge and water depth of the preceding 19 days.

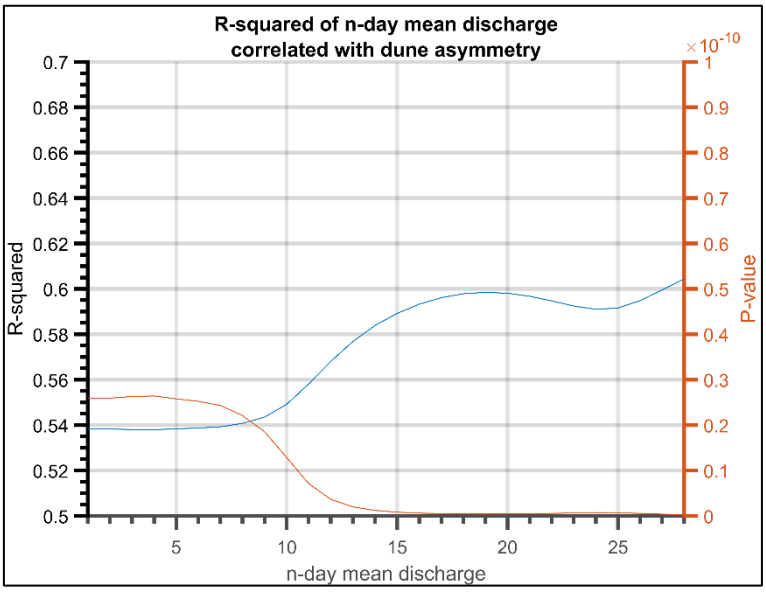

Figure 41: Cross-correlation between the discharge and the dune asymmetry indicated by R-squared (blue) and P-value (red). Where the n-day mean discharge denotes the number of preceding days of which the mean discharge is taken to correlate with the dune asymmetry.

The dune height and asymmetry of the Elbe study area are plotted and correlated with the mean discharge of the 19 preceding days in Figure 42. In this figure, also the R-squared and p-value metrics of the correlations are given. Surprisingly, the dune height does not show a significant correlation with the discharge. The dune asymmetry on the other hand does provide a convincing correlation where 60% of the variance is explained by the linear regression.

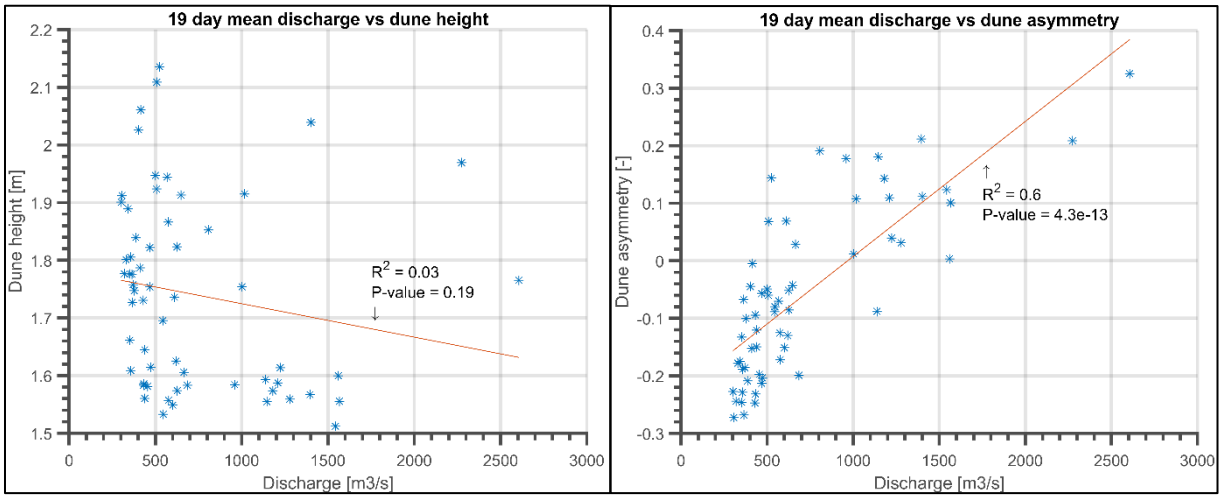

Figure 42: Dune height (left) and asymmetry (right) correlated with the average discharge of the preceding 19 days.

In contrast with the discharge, the dune height does show a striking correlation with the water depth in Figure 43. The linear regression in Figure 43 shows a convincing p-value but only explains 11% of the variance. The obtained correlation is also compared with the relation found by Bradley & Venditti (2017). The dunes in the Elbe estuary are smaller compared to what is expected by the empirical relation derived by Bradley and Venditti.

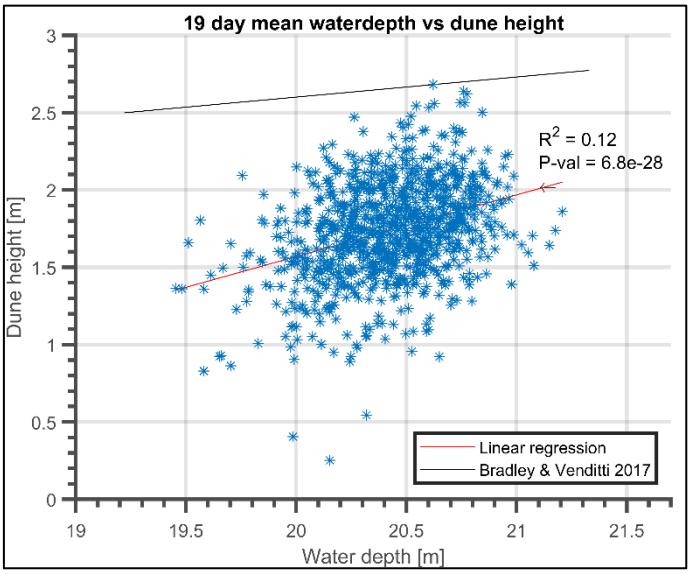

Figure 43: Dune height correlated with the mean water depth of the preceding 19 days.

The resulting asymmetry of the Elbe velocity data is depicted in Figure 44 for the downstream measurement station and in Figure 45 for the upstream measurement station. The gaps in these graphs are caused by missing data in the measurements. Looking at Figure 44, the peak current asymmetry and non-normalized peak current asymmetry are very similar and only differ in the magnitude (settings of the axes). For this downstream measurement station, the velocity asymmetry fluctuates both in landward/upstream and seaward/downstream direction. This fluctuation of velocity asymmetry can be observed to show similarities with the fluctuation of the dune asymmetry in Figure 38 and the river discharge in Figure 39. Looking at the velocity asymmetry of the upstream measurement station in Figure 45, the PCA and non-normalized PCA are again very similar and only differ in the magnitude. For this upstream measurement station however, the velocity asymmetry is dominantly landward/upstream directed with very little fluctuations towards the seaward/downstream direction. This is not what is expected since the velocity asymmetry is anticipated to show similar fluctuations as the dune asymmetry. This subject is further discussed in the discussion section.

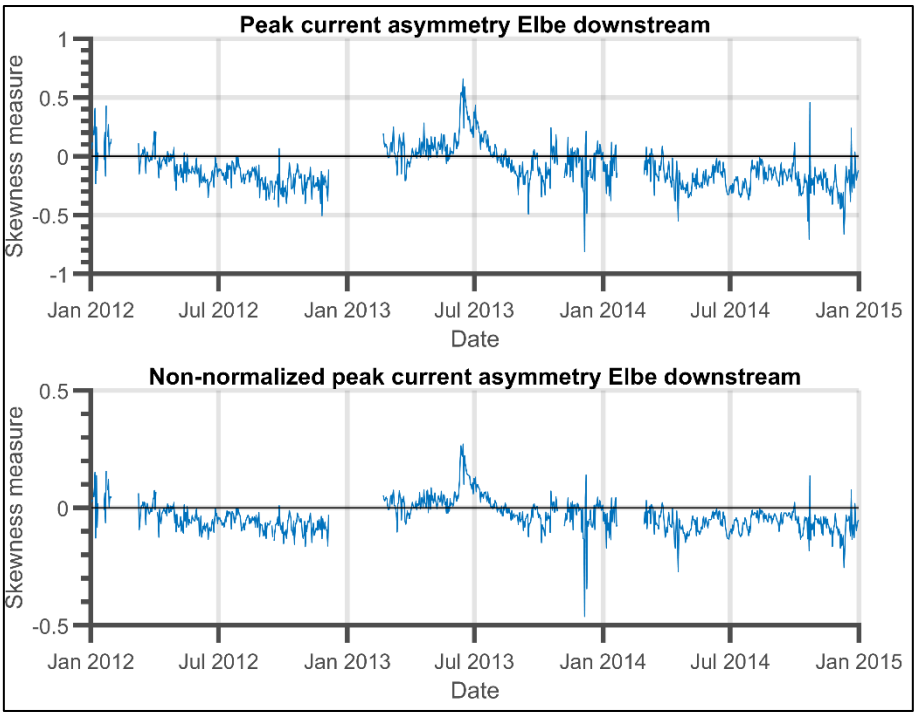

Figure 44: Normalized and non-normalized PCA of the velocity data of the downstream measurement station in the Elbe estuary.

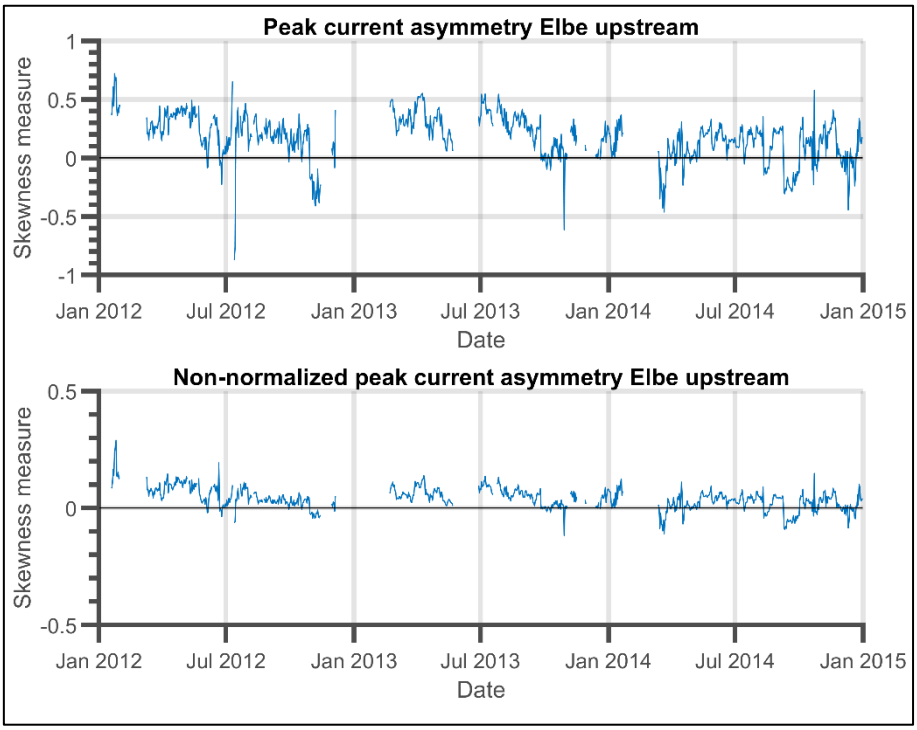

Figure 45: Normalized and non-normalized PCA of the velocity data of the upstream measurement station in the Elbe estuary.

In order to investigate the sensitivity of the lag between the dune asymmetry and the preceding velocity asymmetry, a cross-correlation is conducted. In this cross-correlation, the dune asymmetry is correlated with the average velocity asymmetry of the preceding day and the R-squared is recorded as the measure of similarity. The resulting cross-correlation is depicted in Figure 46. The cross-correlation between the dune asymmetry and the velocity asymmetry of the upstream velocity measurement station (Figure 46 right) shows a gradual increase of the R-squared with no local optimum. The cross-correlation between the dune asymmetry and the velocity asymmetry of the downstream velocity measurement station (Figure 46 left) does shows a local optimum. At 10 days, the steep increase transitions into a gradual increase. In both cross-correlations, the p-value remains far below 0.05 throughout the entire cross-correlation. Therefore, the dune asymmetry is correlated with the mean velocity asymmetry of the preceding 10 days.

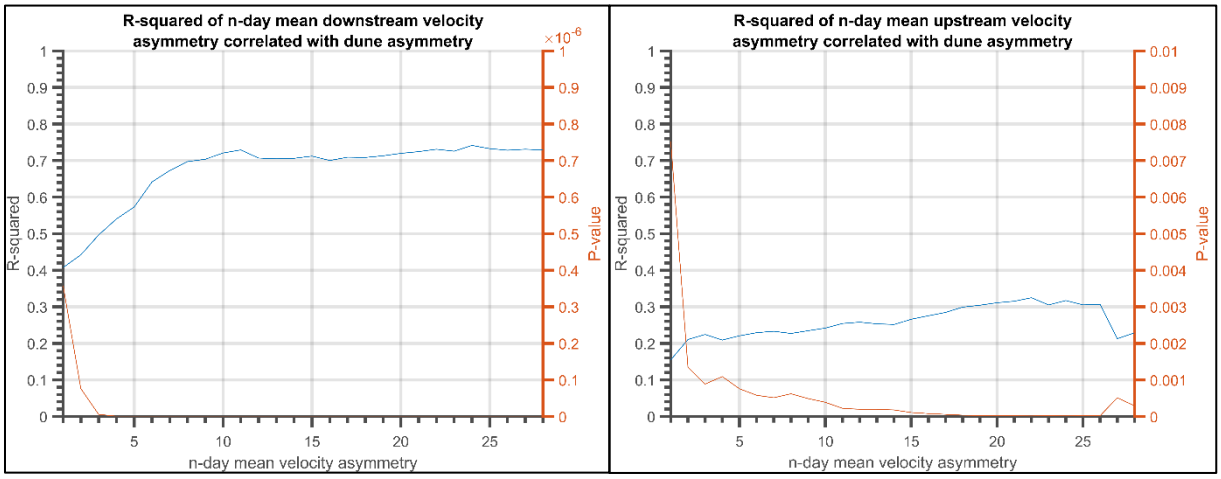

Figure 46: Cross-correlation between the velocity asymmetry of the downstream (left) and upstream (right) velocity measurement stations with the dune asymmetry indicated by R-squared (blue) and P-value (red). Where the n-day mean velocity asymmetry denotes the number of preceding days of which the mean velocity asymmetry is taken to correlate with the dune asymmetry.

The correlation of the dune asymmetry and the velocity asymmetry is depicted in Figure 47 for the downstream (left) and upstream (right) measurement stations. It can be seen that the velocity asymmetry of both measurement stations is positively and statistically significantly correlated with the dune asymmetry with a p-value smaller than 0.05. The dune asymmetry correlation with the downstream measurement station shows a much greater R-squared compared to the upstream measurement station (R-squared 0.73 vs 0.24). Furthermore, it can be observed that the linear regression in Figure 47 on the left nearly crosses the origin. This is also what is expected. If the velocity asymmetry swaps between landward/upstream directed to seaward/downstream directed, it is expected that the dune asymmetry swaps as well. The linear regression of the upstream measurement station does not show the same crossing through the origin. This subject of the differences between asymmetry of the upstream and downstream measurement station is, as mentioned, further discussed in the discussion section.

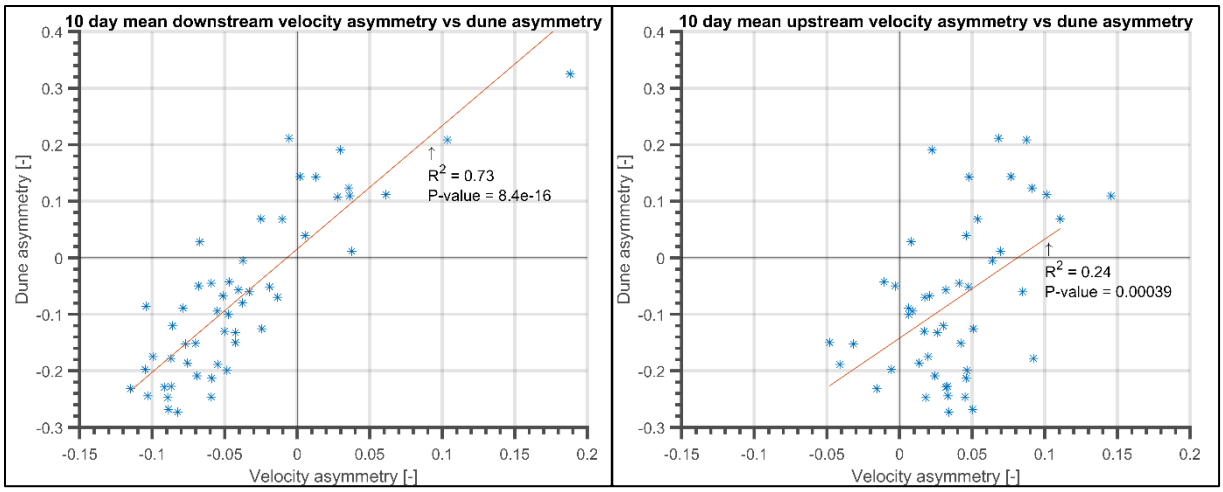

Figure 47: Correlation between the dune asymmetry and the mean velocity asymmetry of the preceding 10 days for the downstream (left) and upstream (right) velocity measurement stations.

The flow velocities of the downstream measurement station are plotted in Figure 48 for the same period as the neap- spring cycle of the Scheldt in Figure 37. For this measurement station and the upstream measurement station, both the flow velocity at the bed as well as the velocity at the surface are processed to obtain the average velocity amplitude over the monitoring period of 2012-2014. These resulting average velocity amplitudes are given in Table 6.

Table 6: Average velocity amplitudes for the upstream and downstream measurement station near the bed and at the surface over the period of 2012-2014.

	Bed	Surface
Downstream	0.96 m/s	1.28 m/s
Upstream	0.83 m/s	1.25 m/s

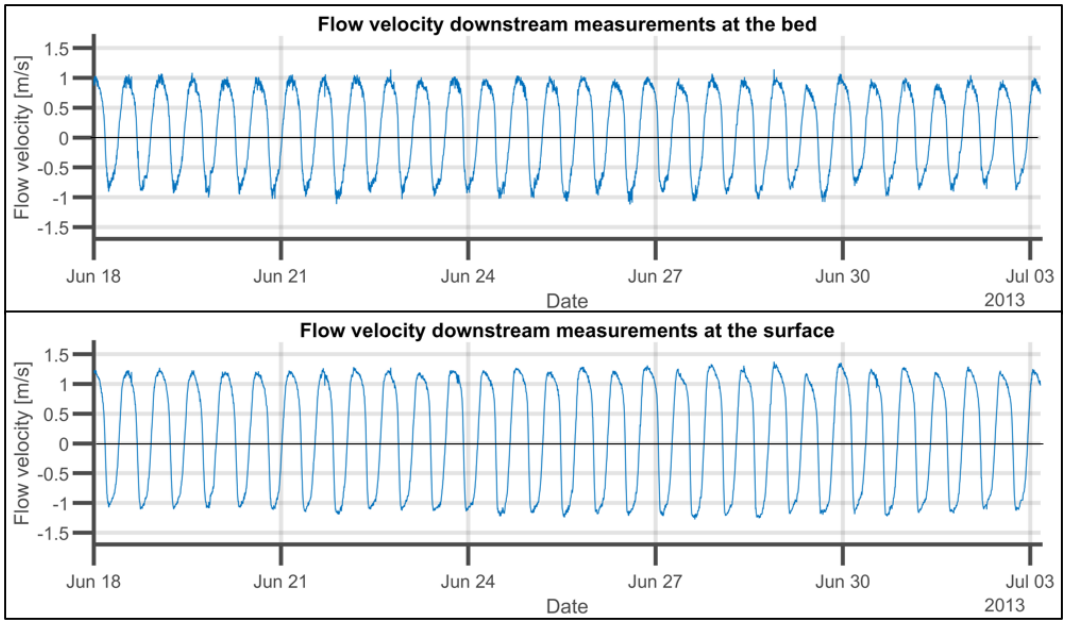

Figure 48: Flow velocities at the downstream measurement station near the bed (top) and at the surface (bottom).

The median grain size of the sediment samples characterising the Elbe study area are given in Table 7. The locations of these sediment samples are defined in Figure 28. There is quite some variability between the measured median grain sizes. This can possibly be explained by the significantly varying river discharge in the Elbe since greater discharges and flow strengths can transport greater sediment sediment particles (e.g. Powell et al., 2001). However, all three samples show a greater grain size compared to the average median grain sizes of the Scheldt study locations.

Table 7: Median grain sizes of the sediment samples in the Elbe study location.

Date of measurement	Median grain size [μm]
24-10-1994	478
01-01-2002	343
10-06-2005	401
	Mean: 407

5. Discussion

This section discusses the conducted study. First some points of attention regarding the methodology are examined. Then, a discussion of the obtained results is provided.

5.1 Methodology

5.1.1 Study sites

The first point of discussion, regarding the methodology, is the selection of study sites. A criterion was stated that, upon visual inspection, the bed level needs to display a repetitive dune pattern. This is not necessarily a wrong criterion to state since the goal of this study is to analyse the dunes that are present. However, this method does lead to the selection of study areas where dunes are relatively large since these are more distinguishable. For example, under the same environmental circumstances such as the water depth, the dunes may vary in height and length. Due to the visual based selection of study sites, there is a bias to the larger occurring dunes in this environmental parameter range.

5.1.2 Transects

Secondly, the orientation of the transect is chosen to align with the main channel axis. The crests of the observed dunes are however not always perpendicular to this channel axis. When measuring dunes with a transect that is not perpendicular to the crests of the dunes, the measured dune length will increase. This is mostly the case for the southern side of the Vlissingen and Terneuzen study area as can be seen in Appendix B. Moreover, in this study, the dune fields are described using representative transects. It is necessary to capture the characteristics of the dune fields in single values since the environmental parameters such as the flow velocity and discharge are available on the same scale as the dune field and not for individual dunes. The method to obtain representative transects is set up as objective as possible. However, a representative transect does not capture all variations over the width of the dune field. Therefore, by applying this methodology, the dune fields are simplified, and information is lost.

5.1.3 Velocity asymmetry

Lastly, the velocity asymmetry is calculated with the cross-sectionally averaged flow velocity in the Western Scheldt study locations. The cross-sections used for this analysis are relatively close to the study areas in case of the Vlissingen and Borssele area. In comparison, the cross-section representing the Terneuzen area is located relatively further away from the Terneuzen study location. This may result in the obtained velocity being less representative in case of the Terneuzen area compared to the Vlissingen and Borssele study cases. The in-situ velocity measuring stations representing the Elbe study area are located approximately 5 km upstream and downstream of the study location (Figure 12). The upstream flow station is located in the main channel, but this main channel has two smaller side channels. The downstream measurement station is also located in the main channel where the estuary is split up into a main channel and a side channel. On the contrary, the study location is located in a section where there is only a main channel and no side channels. It may be that the side channels alongside the flow stations affect the incoming flood wave differently than the outgoing ebb wave. This could generate a different tidal asymmetry observed at the flow station compared with the study location without the side channels.

5.2 Results

5.2.1 Scheldt

The first point of discussion regarding the results is the correlation of the estuarine dune height with the water depth. In the Elbe, a significant but weak (R^2 = 0.12) positive correlation is found between the water depth and the dune height. This is also as expected since both river dunes (e.g. Bradley & Venditti, 2017) and sand waves (e.g. Damen et al., 2018) are (weakly) correlated with the water depth. It is therefore remarkable that, when combining the data of the estuarine dunes in the Scheldt estuary, such a correlation is not found. It is suspected that this is caused by the data obtained from the Terneuzen area. These dunes exist in the same range of depth as the Vlissingen and Borssele study sites, but they are considerably smaller and shorter. In Appendix B, the depth average flow direction is presented and used to determine the orientation of the dune fields. These figures also indicate the magnitude of the flow velocity at maximum ebb and flood flow using a colour scheme. A possible explanation of the smaller and shorter dunes in the Terneuzen area is that they are exposed to smaller flow velocities compared to the other two study sites. This hypothesis is supported by the figures presented in Appendix B. The obtained velocity amplitudes in Table 4 do however not comply with this hypothesis. It was obtained that indeed the Vlissingen study area has the greatest occurring velocities with an average cross-sectionally averaged velocity amplitude over the entire year of 1.30 $\mathrm{m/s}$. However, the Borssele and Terneuzen cross-section show the exact same yearly average velocity amplitude of 1.05 $\mathrm{m/s}$. In Figure 49, the channel topography of the Western Scheldt is provided with the locations of the study areas and cross-sections. It can be argued that at the Terneuzen cross-section, the channel is much narrower compared to the Terneuzen study area. This would lead to greater flow velocities at the cross-section compared to the study site. This way it can be argued that the flow velocities at the Borssele study site are greater than the flow velocities at the Terneuzen study site. However, to be sure, further measurements need to be conducted.

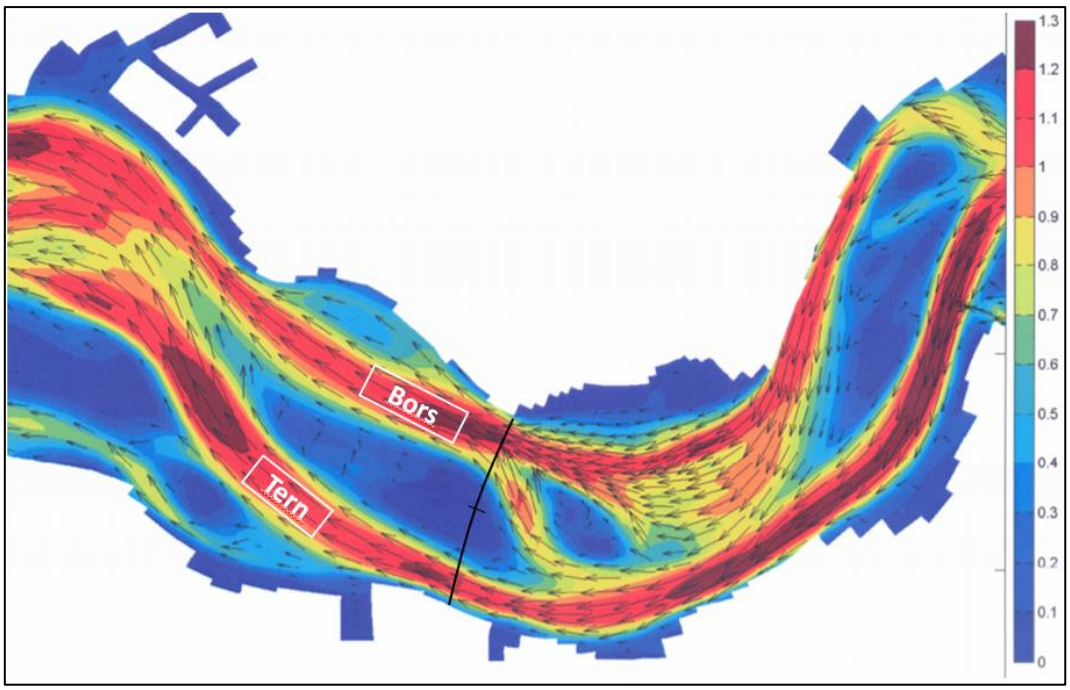

Figure 49: Location of the Terneuzen and Borssele study area and the accompanying cross-sections with the underlying channel topography (adapted from* Rijn, 2011*).

Another plausible cause of the shorter and smaller dunes in Terneuzen is investigated by the sediment availability. The thickness of the erodible layer is mapped by G. Dam (2013) and is depicted in Figure 50. This thickness of the erodible layer is taken as an indication of the sediment availability. It can be seen that in comparison, at the Terneuzen study area, less sediment is available. Le Bot & Trentesaux (2004) investigated two dune fields in the Dover strait which had, compared to each other, similar environmental conditions, only differing in the sediment availability. They observed that the dunes in the sediment scarce environment had a three-dimensional geometry and larger intermediary distance compared to the two-dimensional dunes in the sediment rich environment. The effect of sediment scarcity is also investigated by Porcile et al. (2017) using an idealized model. This idealized model supported the observations that in a sediment scarce setting, the bedforms display a greater wavelength compared to a sediment rich environment. Currently, further research is conducted on this subject by Damveld et al. (2021), using a fully numerical model. Their preliminary results agree with the find that in sediment scarce environments, sand wave lengths increase. Furthermore, they found that, next to an increase in wavelength, the wave height tends to decrease. Looking at the dunes in the Terneuzen study area, the dune height is indeed smaller compared to the two other study areas. However, the dune length is smaller as well. It is therefore suspected that sediment scarcity is not the explaining factor for the different dune characteristics of the Terneuzen study area compared to the other two study areas in the Western Scheldt.

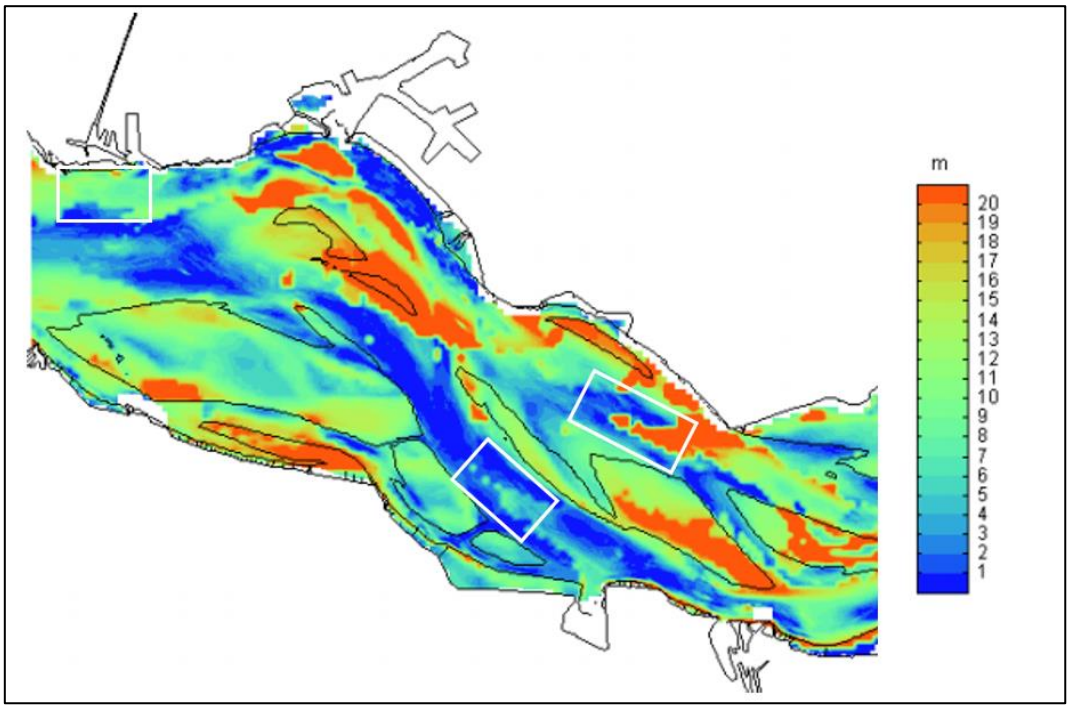

***Figure 50: Thickness of the erodible above the non-erodable layer as of 2011 where the study areas are indicated by the white rectangles* (adapted from G. Dam, 2013).**

Using only the heights and depths of the dunes in the Vlissingen and Borssele area does lead to a weakly significant positive correlation with an R-squared of 0.09 and a p-value of 0.03 (Figure 51).

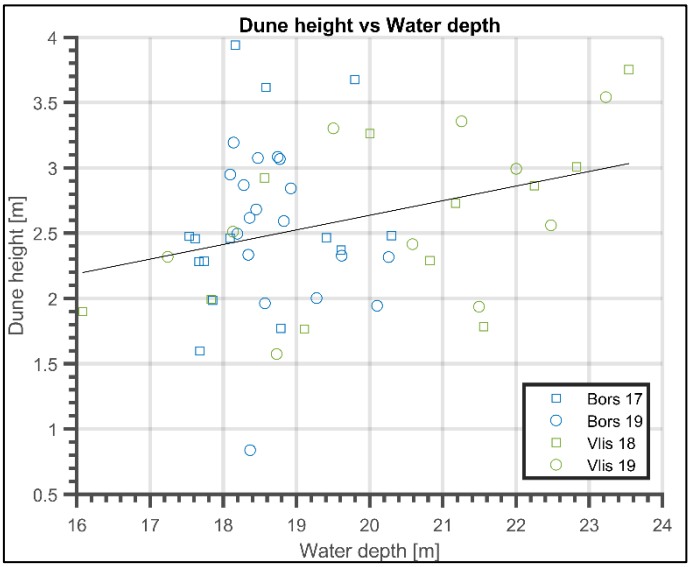

Figure 51: Dune height correlated with the water depth of only the Borssele and Vlissingen study area

The second point of discussion concerns the dune length of the Vlissingen study area. Even though the dunes in the Borssele and Vlissingen area both display a mean dune height of approximately 2.6 meters, the dunes in the Borssele study location have a length of 120 m compared to a length of 210 m of the dunes in the Vlissingen area. This can partly be explained by the difference in water depth. The Vlissingen study area has a greater range of water depth, reaching greater water depths. Since there is a positive correlation in water depth and dune length, this explains that there are longer dunes in the Vlissingen area. However, dunes in the Vlissingen area that exist in the same range of water depth as the dunes in the Borssele area are slightly longer as well. A possible explanation for this observation is the orientation of the transects. In the Borssele study area, the dunes are nearly perfectly perpendicular to the determined main axis while in the Vlissingen study area, the dunes are slightly oriented with respect to the determined main axis. A different arguable explanation is the effect of surface waves, which is not researched in this study. Van Dijk & Kleinhans (2005) showed through an approximation that sand waves at a depth of 25 meters, consisting of sediment with grain size up to 300 μm could be affected by surface waves of 3 meters. The model results reported by Vroom et al. (2015) (using the same model of which the results are also used in this study for flow velocity), do show a difference in surface wave height between the Vlissingen and Borssele study area (Figure 52). This is also expected since the Vlissingen area is located in the very mouth of the estuary where the Borssele site is more sheltered. However, the significant surface waves in the Vlissingen area, in a period of substantial waves, reach only a height of approximately 1 meter. It is therefore suspected that the effect of surface waves does not influence the dune length in the Vlissingen area.

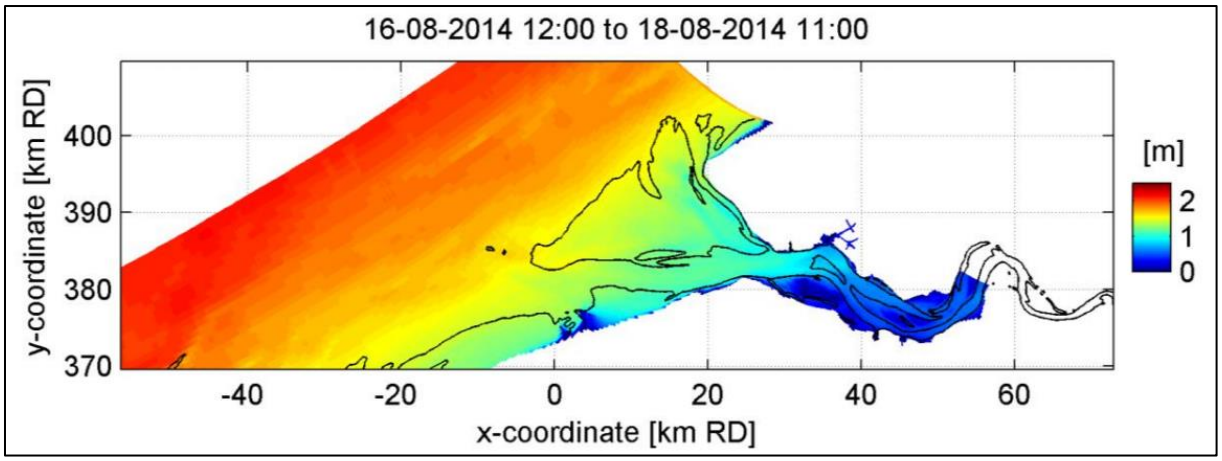

***Figure 52: Average significant surface wave height in a period of substantial surface waves* (Vroom et al., 2015).**

5.2.2 Elbe

In the Elbe, a significant and strong correlation is found between the 19-day average discharge and the dune asymmetry. When correlating the dune height with the 19-day average discharge, no significant correlation was found. It was however expected that these parameters would correlate since dunes generally scale with the flow conditions (e.g. Hulscher & Dohmen-Janssen, 2005; Julien et al., 2002; Wilbers & Ten Brinke, 2003). Looking at Figure 39, a trend is identified in the dune height. This trend is however different from the trend observed in the dune asymmetry and the river discharge. The latter is also tested using a cross-correlation. This leads to believe that there is a different environmental trend affecting the dune height which is not investigated in this study. No further explanation of the lack of correlation between the dune height and river discharge is found.

In the Scheldt, a statistically significant and strong correlation is observed between the non-normalized peak current asymmetry (PCA) and the resulting asymmetry of the dunes. In the Elbe, the asymmetry of the dunes also shows a statistically significant correlation with the non-normalized peak current asymmetry. However, this correlation is much stronger with the downstream velocity measurements compared to the upstream velocity measurements. Furthermore, the PCA of the upstream velocity measurement station is predominantly asymmetric in ebb direction even though the dunes are both asymmetric in flood and ebb direction. On the contrary, the downstream velocity measurements do display this fluctuating ebb/flood dominance. This leads to the correlation of the dune asymmetry with the downstream non-normalized PCA to nearly cross the origin, indicating that an ebb directed PCA leads to ebb directed dune asymmetry and vice versa. The correlation of the dune asymmetry with the upstream non-normalized PCA does not display this crossing through the origin. This correlation therefore does not display the same dependency of the dune asymmetry direction on the PCA direction.

Two possible explanations can be provided for this observation. As described in paragraph 5.1.3, the flow measurement stations used to represent the Elbe study area are located in sections where the bathymetry differs from the section where the study location is situated. The study location is located in the main channel without side channels while the measurement stations do have side channels. It may be that these side channels affect the flow velocity of ebb and flood flow differently, resulting in these different correlations. A second explanation is that of a longitudinal salinity gradient. In paragraph 1.1.1 is described that salinity gradients can cause a gravitational circulation. Gravitational

circulation is the process of landward moving water near the bed and seaward moving water near the surface. Stanev et al. (2019) used a model to better understand the dynamics of the Elbe estuary. They plotted the resulting gravitational circulation in the period of 08/01/2012-09/03/2012 (Figure 53). It can be seen that the gravitational circulation is greatest between the 740 and 710 km mark which is in the area of Cuxhaven which is the estuarine mouth. However, it can be observed that the gravitational circulation is, to a lesser extent, also present at the 680 km mark. Using the same kilometrage, the study location of the Elbe considered in this report is located at 670 km. In the period 08/01/2012-09/03/2012 the discharge is relatively high. Stanev et al. (2019) state that during periods of lower discharge, the salinity front can penetrate further land inward causing gravitational circulation more upstream. It is therefore plausible that the asymmetric dunes in flood direction observed in periods of low discharge are caused by the gravitational circulation.

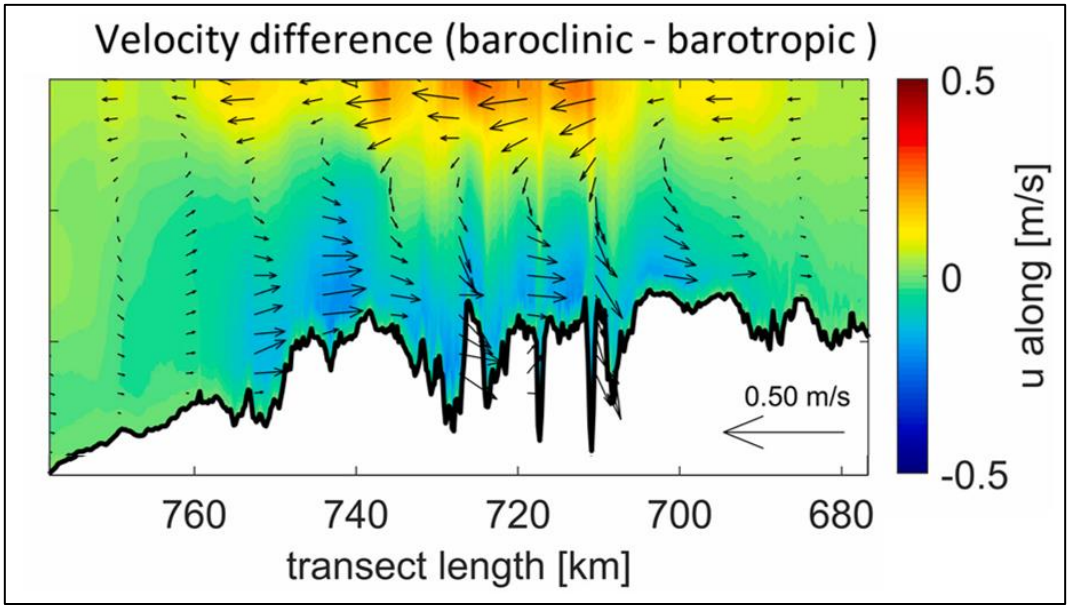

Figure 53: Gravitational circulation in the Elbe estuary **(Stanev et al., 2019).**

The asymmetry reversal of large dunes has also been observed in the Gironde estuary. Berne et al. (1993) conducted two surveys in 1987 and 1989 in an area with large dunes. The asymmetry of these dunes swapped from being flood directed in 1987 to ebb directed in 1989. Van Der Sande et al. (2021) investigated the theory that this turning of asymmetry can be attributed to the change in salinity gradient caused by the river discharge. A greater river discharge preceding the survey in 1987 causes a steeper salinity gradient and accompanying gravitational circulation in comparison with the lower river discharge preceding the 1989 survey. Van Der Sande et al. developed an idealised process-based model to test the influence of gravitational circulation as an effect of a longitudinal salinity gradient. They concluded that in the Gironde estuary, indeed the dune migration (associated with the asymmetry orientation) can be explained by the longitudinal salinity gradient differences in both survey periods.

The idealised process-based model of Van Der Sande et al. (2021) is used to investigate the effect of the longitudinal salinity gradient in the Elbe. For this model run, the default parameter settings are kept except for those given in Table 8. The dune length and water depth of the Elbe are obtained from Figure 38 and Figure 43, respectively. The salinity gradient in the Elbe is obtained from (Vandenbruwaene et al., 2013). The depth-averaged river flow velocity is estimated by dividing the discharge in a period of low river discharge ($400 \mathrm{m}^3/\mathrm{s}$) by the cross-section of 25.000 m^2 in the region

of the study area (Geerts et al., 2017). A period of low discharge is chosen since for these moments in time, the dunes tend to be asymmetric in flood directon. The tidal amplitude is estimated by applying a fourier analysis to the velocity data at the surface and extracting the amplitude at the M2 tidal frequency. This resulted in an M2 tidal amplitude of $1\ \mathrm{m}$ at the surface. The depth-averaged M2 tidal amplitude is estimated to be $0.7\ \mathrm{m}$.

Table 8: Parameter settings Elbe.

Parameter	Value
Dune length	$30\ \mathrm{m}$
Depth	$20\ \mathrm{m}$
Salinity gradient	$0.38\ \mathrm{psu/km}$
Depth-averaged river flow velocity	$0.0016\ \mathrm{m/s}$
Tidal amplitude M2	$0.7\ \mathrm{m/s}$

With the parameter setting as described, Figure 54 is the result. This figure displays the sensitivity of the migration rate of the Elbe dunes with a length of 30 meters to the salinity gradient. It can be seen that, with the specified parameter settings, the dune migration rate is positive for a salinity gradient of $0.38\ \mathrm{psu/km}$. This means that, according to the model, it is expected that the dunes are oriented in the ebb direction given the estimated Elbe environmental conditions. The results of the idealised model therefore do not align with the theory that gravitational circulation induced by the longitudinal salinity gradient explains the differences in the correlations between the dune asymmetry and the velocity asymmetry upstream and downstream. It should however be noted that this model is idealised. In this model for example, the tide is symmetrical, and the eddy viscosity is taken to be constant. The latter means that strain-induced periodic stratification (SIPS), which enhances gravitational circulation (Burchard & Hetland, 2010), is not taken into account. Furthermore, the parameters used to represent the Elbe are estimations. For further clarification on the effect of gravitational circulation on the asymmetry of the dunes in the Elbe, further measurements and research is required.

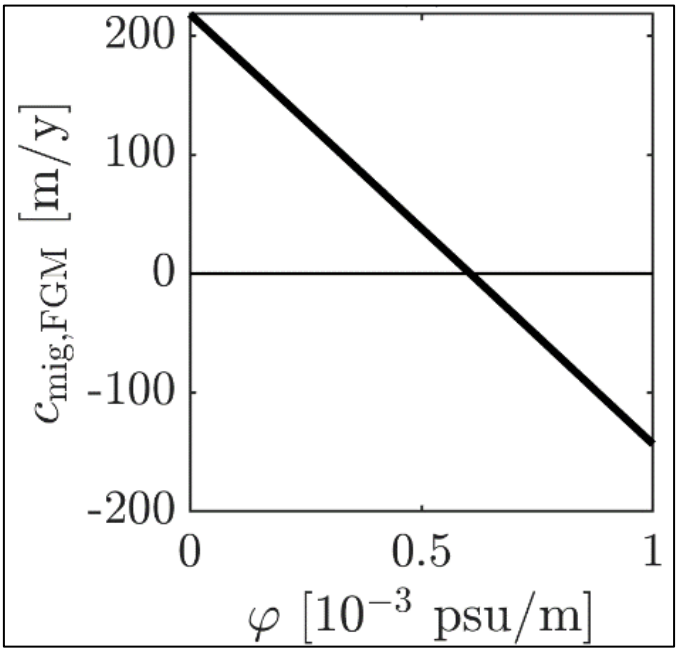

Figure 54: Sensitivity of the dune migration rate to the salinity gradient, given the Elbe parameter settings.

5.2.3 Comparison

The dunes examined in the Western Scheldt have average lengths of 60, 120, and 210 meters combined with heights of 1.4, 2.5, and 2.6 meters for the Terneuzen, Borssele, and Vlissingen study area respectively. In the Elbe study location, the dunes have a steady length of approximately 30 meters where the height fluctuates between 1.5 and 2.1 meters (Figure 31 & Figure 38). In the Elbe, the dunes thus have length significantly smaller compared to the Western Scheldt. The height of the dunes in the Elbe is smaller than those of the Borssele and Vlissingen study area but they are slightly larger than the dunes observed in the Terneuzen area.

In the Scheldt estuary, dune length shows a statistically significant correlation with the water depth while the dune height does not. Only when the dunes of the Terneuzen area are excluded from the correlation, the water depth shows a significant but weak correlation with the dune height. In the Elbe, the dune height shows a convincing but weak correlation with the water depth. In this area, no correlation is tested for the dune length since it remains relatively constant throughout time. Combining the correlations of water depth with dune height of the Elbe and water depth with dune length in the Western Scheldt, one would be able to explain longer and larger dunes in greater water depths and vice versa. However, the dunes in the Western Scheldt and the Elbe exist in the same range of water depth. The dunes in the Western Scheldt are formed in a water depth ranging from 17 to 23 meters. The dunes in the Elbe exist in a water depth of 19.5 to 21 meters. Therefore, the difference observed in dune height and length cannot be explained by the water depth.

An environmental difference between the study locations of the Western Scheldt and the Elbe study location is the composition of the bed. In the Borssele and Terneuzen study area, the sediment is characterised by a median grain diameter of 299 and 289 μm, respectively. The bed in the Elbe study area is characterised by a median grain diameter of 407 μm. This is quite a significant difference. This larger sediment grain size in the Elbe study area does not explain the difference in dune height. The dunes in the Elbe study location have a height in between the height of the dunes in the Terneuzen and Borssele site. Having a greater sediment size than both of these study locations, one would expect the Elbe study site to also show either a greater or smaller dune height than both these Western Scheldt locations, which is not the case. The dune length of the Elbe site is smaller than both the dune lengths of the Borssele and Terneuzen location. Based on this, one could say that the grain size is negatively correlated with the dune length. This does however contradict existing findings where sand wave lengths tend to increase with increasing sediment sizes (e.g. Flemming, 2000).

It is difficult to compare the flow velocities between the different study areas and different estuaries. This is because the flow velocities in the Scheldt are characterised by cross-sectionally averaged flow velocities using the results of a Delft3D model. The flow velocities in the Elbe are characterised by in-situ measurements at the bed and at the surface. However, some level of comparison is possible. In the Western Scheldt, average flow velocity amplitudes of the cross-sectionally averaged flow velocity are calculated being 1.05, 1.05 and 1.30 m/s for the Terneuzen, Borssele and Vlissingen study area respectively. Average flow velocity amplitudes in the Elbe are calculated near the bed and at the surface. Near the bed, velocity amplitudes of 0.96 and 0.83 m/s are calculated for the downstream and upstream measurement stations, respectively. At the surface, velocity amplitudes of 1.28 and 1.25 m/s are calculated for the downstream and upstream measurement stations, respectively. The Vlissingen cross-section is relatively rectangular (Figure 17). Therefore, the cross-sectionally averaged flow velocity can also be taken as an estimate for the depth-averaged flow velocity. Since then, the

depth-averaged flow velocity of 1.30 $\mathrm{m/s}$ is greater than the velocity at the surface for both measurement stations in the Elbe, it can be said with certainty that the Vlissingen study area is subjected to greater flow velocities than the Elbe study location. The Terneuzen and Borssele cross-sections have a more complicated bed profile (Figure 17). In general, greater flow velocities occur in the centre of the channel than at the sides of the channel due to the bed friction effects and water depth. Therefore, the depth-averaged flow velocity in the main channel will be greater than the cross-sectionally averaged flow velocity of 1.05 $\mathrm{m/s}$ for both the Terneuzen and Borssele cross-section. However, to what extent the depth-averaged velocity is greater cannot be foreseen. Furthermore, in paragraph 5.2.1, it is already discussed that even though the cross-sections representing the Borssele and Terneuzen study area have the same cross-sectionally averaged flow velocity amplitudes, different flow velocities may occur at the study locations themselves. Therefore, to accurately investigate the effect of the flow velocity on the dunes for the different study areas and estuaries, further measurements and research is required.

6. Conclusion

In this section, the research questions are answered. First the research questions are stated again after which an answer is provided.

How are the water depth, tidal asymmetry, river discharge, and sediment characteristics related to the length, height, and asymmetry of estuarine dunes in the Scheldt, Elbe estuary?

For the Western Scheldt, the dependency of the dune characteristics was only investigated based on the water depth, tidal asymmetry, and sediment characteristics. The river discharge was not taken into account since this is argued to be negligible. The bed level sediment data was available for two of the three selected study sites. These study sites however, showed very similar median grain sizes and could therefore not explain differences in the observed dune characteristics. The water depth showed a significant but weak positive correlation with the dune length, indicating that in greater water depths, the dunes tend to grow longer. Combining all obtained dune heights in the Western Scheldt with the water depth, no significant correlation was found. This is most likely due to the dune observations of the Terneuzen area which are outliers compared to the dunes of the Vlissingen and Borssele study sites. Combining only the dune heights of the Borssele and Vlissingen study sites with the water depths (excluding the dunes of the Terneuzen area), a significant but weak positive correlation was found. The most convincing correlation was that of the dune asymmetry and the non-normalized peak current asymmetry. This result showed that dunes which are subjected to a tidal signal with a flood-dominant peak current asymmetry, were also flood asymmetric themselves and vice versa.

In the Elbe, all environmental parameters were obtained. Only one study site is selected to observe over time. Since the temporal resolution of the sediment data was not dense enough to follow the temporal observations of the Elbe study site, the effect of sediment characteristics could not be used to explain variations in dune characteristics. In the Elbe, the dune length was nearly constant over time and was therefore not correlated with environmental parameters. Therefore, the focus in the Elbe was on the correlation of the dune height and asymmetry with the water depth, river discharge and tidal asymmetry. The dune height was observed to weakly, positively correlate with the water depth. When correlating the dune height with the mean preceding river discharge, no significant correlation was found. The asymmetry of the dunes in the Elbe estuary showed a significant and a very strong correlation with the non-normalized peak current asymmetry at the downstream measurement station. The upstream measurement station also displayed a significant but weaker correlation between the dune asymmetry and velocity asymmetry. It is hypothesised that this difference in the correlation between the measurement stations can be attributed to the gravitational circulation. Furthermore, the dune asymmetry also showed a significant and strong positive correlation with the river discharge.

How do the length, height, and asymmetry of estuarine dunes compare in the Scheldt and Elbe estuary and how can this be related to differences in environmental conditions between those estuaries?

The dunes in the Western Scheldt were (much) longer than those observed in the Elbe estuary. Only the mean dune height of the dunes observed in the Terneuzen area was smaller than those observed in the Elbe study location. The mean dune height of both the Borssele and Vlissingen study site was greater than observed in the Elbe study location. These absolute differences in mean dune length and height could not be explained based on the observed environmental characteristics.

A difference between the dunes in the Western Scheldt and Elbe is the steadiness over time. In the Western Scheldt, the height, length, and asymmetry were nearly identical in the observation period. The lengths of the dunes in the Elbe estuary were also steady, but the height and asymmetry of these dunes did fluctuate. This can partly be explained by the water depth. The water depth fluctuated, causing higher dunes. The asymmetry of the dunes in the Elbe also showed a fluctuating pattern. Both the asymmetry of the dunes in the Western Scheldt and the Elbe strongly correlated to the velocity asymmetry. In the Elbe however, the velocity asymmetry fluctuated over time, causing the asymmetry of the dunes to fluctuate over time as well. Furthermore, in the Elbe, the dune asymmetry was highly correlated to the river discharge. In high discharge events, the added discharge caused the Elbe velocity asymmetry and consequently the dune asymmetry to be asymmetric in seaward direction. In low discharge events, it is hypothesised that the salinity front can further penetrate land inward causing gravitational circulation effects in the Elbe study location. The gravitational circulation is then thought to cause the dunes to grow asymmetric in landward direction.

7. Recommendations

In this chapter, the first paragraph describes the relevance of the conducted study. In the second paragraph, recommendations are given for further research.

7.1 Relevance

It has been discussed that dunes increase the flow roughness (Hulscher & Dohmen-Janssen, 2005). Herrling et al. (2021) recently investigated the effect of dune asymmetry on the resulting hydrodynamics and sediment transport in estuaries using a numerical model. They concluded that the dune asymmetry orientation is a crucial parameter when modelling the estuarine and coastal tidal- and sediment dynamics. Herrling et al. (2021) therefore expresses the need to implement a time-varying bedform roughness based on whether the tide is in the same or opposing direction of the dune asymmetry. One of the main finding of this report is the significant and strong correlation between the dune asymmetry and the non-normalized peak current asymmetry. This information could be beneficial to estuarine/coastal modelers since the dune asymmetry could be deduced from the non-normalized peak current asymmetry.

7.2 Further research

In the relevance section of this chapter, the correlation between the velocity asymmetry and dune asymmetry is emphasized. As addressed in the discussion section, the hydrodynamic measurements used in this study are not ideal. The hydrodynamic data of the Scheldt results from a Delft3D model where the data could not be obtained at the same location as the study locations. The flow velocities for the Elbe did originate from the in-situ measurements. However, these measurements also are not taken at the same location as the Elbe study site. In addition, the two different velocity measurement stations in the Elbe show a difference in correlation strength between the velocity asymmetry and the dune asymmetry. For further research, it is suggested to measure the hydrodynamics at the same location as the dunes under consideration. This would strengthen the relevance of the finding in this study.

For further research extending on the correlation between dune characteristics and the environmental parameters, it is encouraged to express the environmental characteristics in the same metric, if possible. In this study, due to an absence of data in the Western Scheldt the flow velocities are expressed in cross-sectionally averaged while in the Elbe the velocities are measures near the bed and the surface. Even though the study sites are characterised based on the environmental conditions, using different metrics still makes it tough to compare these study sites. Furthermore, when extending on this research or conducting a similar study, it is recommended to include as many study sites as possible. In this case, three study sites were selected in the Scheldt estuary to investigate the spatial variability. Of these three study sites, one (Terneuzen) displayed dune characteristics different from the other two study sites. When conducting a correlation study, the strength lies in having a lot of data to correlate. This way, the effect of outliers is reduced and a general overview of the correlation between parameters can be obtained.

In this study, reasoned decisions are made to form the methodology. For example, the decision to orient the bed elevation profiles in line with the main channel, or to select a representative transect to characterise a dune field. For further research it would be interesting to analyse the effect of these decisions by for example orienting the BEPs based on a 2D-fourier analysis or to take a dune field average value to represent the dune field characteristics.

Bibliography

Allen, J. R. L. (1982). Sedimentary Structures Their Character and Physical Basis Volume II. In *Clinician's Handbook of Adult Behavioral Assessment: Vol. II*.

Amann, T., Weiss, A., & Hartmann, J. (2012). Carbon dynamics in the freshwater part of the Elbe estuary, Germany: Implications of improving water quality. *Estuarine, Coastal and Shelf Science*, *107*, 112–121. https://doi.org/10.1016/J.ECSS.2012.05.012

Ashley, G. M. (1990). Classification of large-scale subaqueous bedforms: a new look at an old problem; SEPM bedforms and bedding structures. *Journal of Sedimentary Research*, *60*(1), 160–172. https://doi.org/10.1306/212f9138-2b24-11d7-8648000102c1865d

Berne, S., Castaing, P., Le Drezen, E., & Lericolais, G. (1993). Morphology, internal structure, and reversal of asymmetry of large subtidal dunes in the entrance to Gironde Estuary (France). *Journal of Sedimentary Petrology*, *63*(5), 780–793. https://doi.org/10.1306/D4267C03-2B26-11D7-8648000102C1865D

Besio, G., Blondeaux, P., & Vittori, G. (2006). On the formation of sand waves and sand banks. *Journal of Fluid Mechanics*, *557*, 1–27. https://doi.org/10.1017/S0022112006009256

Besio, Giovanni, Blondeaux, P., Brocchini, M., & Vittori, G. (2004). On the modeling of sand wave migration. *Journal of Geophysical Research C: Oceans*, *109*(4), 4018. https://doi.org/10.1029/2002JC001622

Best, J. (2005). The fluid dynamics of river dunes: A review and some future research directions. *Journal of Geophysical Research: Earth Surface*, *110*(F4), 4–6. https://doi.org/10.1029/2004JF000218

Best, J., & Kostaschuk, R. (2002). An experimental study of turbulent flow over a low-angle dune. *Journal of Geophysical Research: Oceans*, *107*(C9), 18–1. https://doi.org/10.1029/2000JC000294

Bradley, R. W., & Venditti, J. G. (2017). Reevaluating dune scaling relations. In *Earth-Science Reviews* (Vol. 165, pp. 356–376). Elsevier B.V. https://doi.org/10.1016/j.earscirev.2016.11.004

Burchard, H., & Hetland, R. D. (2010). Quantifying the Contributions of Tidal Straining and Gravitational Circulation to Residual Circulation in Periodically Stratified Tidal Estuaries. *Journal of Physical Oceanography*, *40*(6), 1243–1262. https://doi.org/10.1175/2010JPO4270.1

Carstens, M., Claussen, U., Bergemann, M., & Gaumert, T. (2004). Transitional waters in Germany: The Elbe estuary as an example. *Aquatic Conservation: Marine and Freshwater Ecosystems*, *14*(SUPPL. 1). https://doi.org/10.1002/aqc.652

Cisneros, J., Best, J., van Dijk, T., Almeida, R. P. de, Amsler, M., Boldt, J., Freitas, B., Galeazzi, C., Huizinga, R., Ianniruberto, M., Ma, H., Nittrouer, J. A., Oberg, K., Orfeo, O., Parsons, D., Szupiany, R., Wang, P., & Zhang, Y. (2020). Dunes in the world's big rivers are characterized by low-angle lee-side slopes and a complex shape. *Nature Geoscience 2020 13:2*, *13*(2), 156–162. https://doi.org/10.1038/S41561-019-0511-7

Dalrymple, R. W., & Choi, K. (2007). Morphologic and facies trends through the fluvial-marine transition in tide-dominated depositional systems: A schematic framework for environmental and sequence-stratigraphic interpretation. *Earth-Science Reviews*, *81*(3–4), 135–174. https://doi.org/10.1016/j.earscirev.2006.10.002

Damen, J. M., van Dijk, T. A. G. P., & Hulscher, S. J. M. H. (2018). Spatially Varying Environmental Properties Controlling Observed Sand Wave Morphology. *Journal of Geophysical Research: Earth Surface*, *123*(2), 262–280. https://doi.org/10.1002/2017JF004322

Damveld, J., Porcile, G., Blondeaux, P., & Roos, P. (2021). *Nonlinear dynamics of sand waves in sediment scarce environments*. https://doi.org/10.5194/EGUSPHERE-EGU21-16019

de Ruijsscher, T. V., Naqshband, S., & Hoitink, A. J. F. (2020). Effect of non-migrating bars on dune dynamics in a lowland river. *Earth Surface Processes and Landforms*, *45*(6), 1361–1375. https://doi.org/10.1002/esp.4807

Dronkers, J. J. (1964). *Tidal computations in rivers and coastal waters*. https://www.worldcat.org/title/tidal-computations-in-rivers-and-coastal-waters/oclc/177017

Flemming, B. W. (2000). *The role of grain size, water depth and flow velocity as scaling factors controlling the size of subaqueous dunes*. Conference Paper. https://www.researchgate.net/publication/234841879_The_role_of_grain_size_water_depth_and_flow_velocity_as_scaling_factors_controlling_the_size_of_subaqueous_dunes

Flemming, B. W. (2011). Geology, Morphology, and Sedimentology of Estuaries and Coasts. In *Treatise on Estuarine and Coastal Science* (Vol. 3). Elsevier Inc. https://doi.org/10.1016/B978-0-12-374711-2.00302-8

Francken, F., Wartel, S., Parker, R., & Taverniers, E. (2004). Factors influencing subaqueous dunes in the Scheldt Estuary. *Geo-Marine Letters*, *24*(1), 14–21. https://doi.org/10.1007/s00367-003-0154-x

G. Dam. (2013). Harde lagen Westerschelde -Achtergrondrapport A-28. *Deltares Rapport*.

Gallo, M. N., & Vinzon, S. B. (2005). Generation of overtides and compound tides in Amazon estuary. *Ocean Dynamics 2005 55:5*, *55*(5), 441–448. https://doi.org/10.1007/S10236-005-0003-8

Geerts, L., Cox, T. J. S., Maris, T., Wolfstein, K., Meire, P., & Soetaert, K. (2017). Substrate origin and morphology differentially determine oxygen dynamics in two major European estuaries, the Elbe and the Schelde. *Estuarine, Coastal and Shelf Science*, *191*, 157–170. https://doi.org/10.1016/j.ecss.2017.04.009

Gómez, E. A., Cuadrado, D. G., & Pierini, J. O. (2010). Sand transport on an estuarine submarine dune field. *Geomorphology*, *121*(3–4), 257–265. https://doi.org/10.1016/j.geomorph.2010.04.022

Gong, W., Schuttelaars, H., & Zhang, H. (2016). Tidal asymmetry in a funnel-shaped estuary with mixed semidiurnal tides. *Ocean Dynamics*, *66*(5), 637–658. https://doi.org/10.1007/s10236-016-0943-1

Guo, L., Brand, M., Sanders, B. F., Foufoula-Georgiou, E., & Stein, E. D. (2018). Tidal asymmetry and residual sediment transport in a short tidal basin under sea level rise. *Advances in Water Resources*, *121*, 1–8. https://doi.org/10.1016/j.advwatres.2018.07.012

Guo, L., Wang, Z. B., Townend, I., & He, Q. (2019). Quantification of Tidal Asymmetry and Its Nonstationary Variations. *Journal of Geophysical Research: Oceans*, *124*(1), 773–787. https://doi.org/10.1029/2018JC014372

Hendershot, M. L., Venditti, J. G., Bradley, R. W., Kostaschuk, R. A., Church, M., & Allison, M. A. (2016). Response of low-angle dunes to variable flow. *Sedimentology*, *63*(3), 743–760. https://doi.org/10.1111/sed.12236

Herrling, G., Becker, M., Lefebvre, A., Zorndt, A., Krämer, K., & Winter, C. (2021). The effect of asymmetric dune roughness on tidal asymmetry in the Weser estuary. *Earth Surface Processes and Landforms*. https://doi.org/10.1002/ESP.5170

Hu, H., Yang, Z., Yin, D., Cheng, H., & Parsons, D. R. (2021). Hydrodynamics over low-angle dunes at the tidal current limit of the Changjiang Estuary. *Estuarine, Coastal and Shelf Science*, *253*, 107298. https://doi.org/10.1016/j.ecss.2021.107298

Hulscher, S. J. M. H., & Brink, G. M. van den. (2001). Comparison between predicted and observed sand waves and sand banks in the North Sea. *Journal of Geophysical Research : Oceans*, *106*(C5), 9327–9338. https://doi.org/10.1029/2001JC900003

Hulscher, S. J. M. H., & Dohmen-Janssen, C. M. (2005). Introduction to special section on Marine Sand Wave and River Dune Dynamics. *Journal of Geophysical Research: Earth Surface*, *110*(4). https://doi.org/10.1029/2005JF000404

Julien, P. Y., Klaassen, G. J., Brinke, W. B. M. Ten, & Wilbers, A. W. E. (2002). Case Study: Bed Resistance of Rhine River during 1998 Flood. *Journal of Hydraulic Engineering*, *128*(12), 1042–1050. https://doi.org/10.1061/(ASCE)0733-9429(2002)128:12(1042)

Laan, T. van der, Cleveringa, J., Mari, T., Preite, D. De, Ysebaert, T., & Wijnhoven, S. (2014). T2009-Rapport schelde-Estuarium. *Vlaams-Nederlandse Scheldecomissie*.

Langbein, W. B. (1963). The hydraulic geometry of a shallow estuary. *International Association of Scientific Hydrology. Bulletin*, *8*(3), 84–94. https://doi.org/10.1080/02626666309493340

Le Bot, S., & Trentesaux, A. (2004). Types of internal structure and external morphology of submarine dunes under the influence of tide- and wind-driven processes (Dover Strait, northern France).

Marine Geology, *211*(1–2), 143–168. https://doi.org/10.1016/J.MARGEO.2004.07.002

Lefebvre, A., & Winter, C. (2016). Predicting bed form roughness: the influence of lee side angle. *Geo-Marine Letters*, *36*(2), 121–133. https://doi.org/10.1007/s00367-016-0436-8

Leuven, J. R. F. W., Pierik, H. J., van der Vegt, M., Bouma, T. J., & Kleinhans, M. G. (2019). Sea-level-rise-induced threats depend on the size of tide-influenced estuaries worldwide. *Nature Climate Change*, *9*(12), 986–992. https://doi.org/10.1038/s41558-019-0608-4

Li, M., Ge, J., Kappenberg, J., Much, D., Nino, O., & Chen, Z. (2014). Morphodynamic processes of the Elbe River estuary, Germany: The Coriolis effect, tidal asymmetry and human dredging. *Frontiers of Earth Science*, *8*(2), 181–189. https://doi.org/10.1007/s11707-013-0418-3

McLaren, P. (1993). *Patterns of sediment transport in the western portion of the Westerschelde*. GeoSea Consulting.

Meire, P., Ysebaert, T., Van Damme, S., Van Den Bergh, E., Maris, T., & Struyf, E. (2005). The Scheldt estuary: A description of a changing ecosystem. In *Hydrobiologia* (Vol. 540, Issues 1–3, pp. 1–11). Springer. https://doi.org/10.1007/s10750-005-0896-8

Naqshband, S., Ribberink, J. S., Hurther, D., & Hulscher, S. J. M. H. (2014). Bed load and suspended load contributions to migrating sand dunes in equilibrium. *Journal of Geophysical Research: Earth Surface*, *119*(5), 1043–1063. https://doi.org/10.1002/2013JF003043

Németh, A. A., Hulscher, S. J. M. H., & De Vriend, H. J. (2002). Modelling sand wave migration in shallow shelf seas. *Continental Shelf Research*, *22*(18–19), 2795–2806. https://doi.org/10.1016/S0278-4343(02)00127-9

Nidzieko, N. J., & Ralston, D. K. (2012). Tidal asymmetry and velocity skew over tidal flats and shallow channels within a macrotidal river delta. *Journal of Geophysical Research: Oceans*, *117*(3), 3001. https://doi.org/10.1029/2011JC007384

Pope, J. (2000). Where and Why Inlet Channels Shoal: A Conceptual Geomorphic Framework. *ERDC/CHL CHETN-U.S. Army Corps of Engineers*.

Porcile, G., Blondeaux, P., & Vittori, G. (2017). On the formation of periodic sandy mounds. *Continental Shelf Research*, *145*, 68–79. https://doi.org/10.1016/J.CSR.2017.07.011

Postma, H. (1967). Sediment transport and sedimentation in the estuarine environment. *American Association of Advanced Sciences*, *83*, 158–179.

Powell, D. M., Reid, I., & Laronne, J. B. (2001). Evolution of bed load grain size distribution with increasing flow strength and the effect of flow duration on the caliber of bed load sediment yield in ephemeral gravel bed rivers. *WRR*, *37*(5), 1463–1474. https://doi.org/10.1029/2000WR900342

Pritchard, D. W. (1952). Salinity distribution and circulation in the Chesapeake ay estuarine system. *Journal of Marine Research*, *11*(2), 106–123.

Rijn, L. C. van. (2011). Tidal Phenomena in the Scheldt Estuary, part 2. *Deltares Rapport*.

Salvatierra, M. M., Aliotta, S., & Ginsberg, S. S. (2015). Morphology and dynamics of large subtidal dunes in Bahia Blanca estuary, Argentina. *Geomorphology*, *246*, 168–177. https://doi.org/10.1016/j.geomorph.2015.05.037

Savenije, H. H. G. (2012). Salinity and Tides in Alluvial Estuaries. In *Salinity and Tides in Alluvial Estuaries*. https://doi.org/10.1016/B978-0-444-52107-1.X5000-X

Stanev, E. V., Jacob, B., & Pein, J. (2019). German Bight estuaries: An inter-comparison on the basis of numerical modeling. *Continental Shelf Research*, *174*, 48–65. https://doi.org/10.1016/j.csr.2019.01.001

Stark, J. (2016). *Effects of intertidal ecosystems on estuarine hydrodynamics and flood wave attenuation: a multi-scale study*. https://doi.org/10.13140/RG.2.2.24404.19840

Streif, H. (2004). Sedimentary record of Pleistocene and Holocene marine inundations along the North Sea coast of Lower Saxony, Germany. *Quaternary International*, *112*(1), 3–28. https://doi.org/10.1016/S1040-6182(03)00062-4

Valle-Levinson, A. (2010). *Contemporary Issues in Estuarine Physics*. https://www.cambridge.org/nl/academic/subjects/earth-and-environmental-science/oceanography-and-marine-science/contemporary-issues-estuarine-

physics?format=HB&isbn=9780521899673
van der Mark, C. F. (2007). *A new and widely applicable tool for determining the geometric properties of bedforms*. *October 2016*. https://doi.org/10.13140/RG.2.2.17637.40161
van der Mark, C. F., Blom, A., & Hulscher, S. M. J. H. (2008). Quantification of variability in bedform geometry. *Journal of Geophysical Research: Earth Surface*, *113*(3), 3020. https://doi.org/10.1029/2007JF000940
van der Sande, W. M., Roos, P. C., Gerkema, T., & Hulscher, S. J. M. H. (2021). Gravitational Circulation as Driver of Upstream Migration of Estuarine Sand Dunes. *Geophysical Research Letters*, *48*(14), e2021GL093337. https://doi.org/10.1029/2021GL093337
Van Dijk, T. A. G. P., & Kleinhans, M. G. (2005). Processes controlling the dynamics of compound sand waves in the North Sea, Netherlands. *Journal of Geophysical Research: Earth Surface*, *110*(4). https://doi.org/10.1029/2004JF000173
van Dijk, T. A. G. P., Lindenbergh, R. C., & Egberts, P. J. P. (2008). Separating bathymetric data representing multiscale rhythmic bed forms: A geostatistical and spectral method compared. *Journal of Geophysical Research: Earth Surface*, *113*(4), 4017. https://doi.org/10.1029/2007JF000950
van Santen, R. B., de Swart, H. E., & van Dijk, T. A. G. P. (2011). Sensitivity of tidal sand wavelength to environmental parameters: A combined data analysis and modelling approach. *Continental Shelf Research*, *31*(9), 966–978. https://doi.org/10.1016/j.csr.2011.03.003
Vandenbruwaene, W., Plancke, Y., Verwaest, T., & Mostaert, F. (2013). Interestuarine comparison: . Interestuarine comparison: Hydrogeomorphology: Hydro- and geomorphodynamics of the TIDE estuaries Scheldt, Elbe, Weser and Humber. *WL Rapporten*, *February*, 1–77.
Venditti, J. G. (2013). Bedforms in Sand-Bedded Rivers. In *Treatise on Geomorphology* (Vol. 9, pp. 137–162). Elsevier Inc. https://doi.org/10.1016/B978-0-12-374739-6.00235-9
Vilas, F., Rubio, B., Rey, D., & Bernabeu, A. M. (2015). Estuary. In *Encyclopedia of Planetary Landforms* (pp. 725–730). Springer New York. https://doi.org/10.1007/978-1-4614-3134-3_621
Vroom, J., Vet, P. L. M. de, & Werf, .J. van der. (2015). Validatie waterbeweging Delft3D-NeVla model Westerscheldemonding. *Deltares Rapport*, *1210301–00*.
Wang, Z. B., Jeuken, M. C. J. L., Gerritsen, H., De Vriend, H. J., & Kornman, B. A. (2002). Morphology and asymmetry of the vertical tide in the Westerschelde estuary. *Continental Shelf Research*, *22*(17), 2599–2609. https://doi.org/10.1016/S0278-4343(02)00134-6
Wilbers, A. W. E., & Ten Brinke, W. B. M. (2003). The response of subaqueous dunes to floods in sand and gravel bed reaches of the Dutch Rhine. *Sedimentology*, *50*(6), 1013–1034. https://doi.org/10.1046/J.1365-3091.2003.00585.X
Winterwerp, J. C., Wang, Z. B., Stive, M. J. F., Arends, A. A., Jeuken, C., Kuijper, C., & Thoolen, P. M. C. (2001). A new morphological schematization of the Western Scheldt estuary, The Netherlands. *Symposium on River, Coastal and Estuarine Morphodynamics*, 1–10.
Zhou, J., Wu, Z., Zhao, D., Guan, W., Zhu, C., & Flemming, B. (2020). Giant sand waves on the Taiwan Banks, southern Taiwan Strait: Distribution, morphometric relationships, and hydrologic influence factors in a tide-dominated environment. *Marine Geology*, *427*, 106238. https://doi.org/10.1016/j.margeo.2020.106238

Appendix A

The missing data values in the topographic datasets are interpolated based on the neighbouring cells. Based on the largest cluster of missing data values, a neighbourhood of a 5x5 cell window is used to interpolate the missing data values. This window is kept consistent for all study sites, both in the Western Scheldt as well as in the Elbe. The missing data value is assigned the average of the 5x5 surrounding grid. This interpolation is performed by first using the conditional toolbox (Con) in ArcGIS to determine where the missing data values are located. After identifying which cells contain missing data, the cells are assigned the values obtained when creating a raster with the Focal Statistics toolbox. In the Focal Statistics toolbox, the neighbourhood is set to a rectangular window with a height and width of 5 cells and a statistics type of “MEAN”. A representation of the neighbouring cells included in the interpolation of the missing data is given in Figure 55.

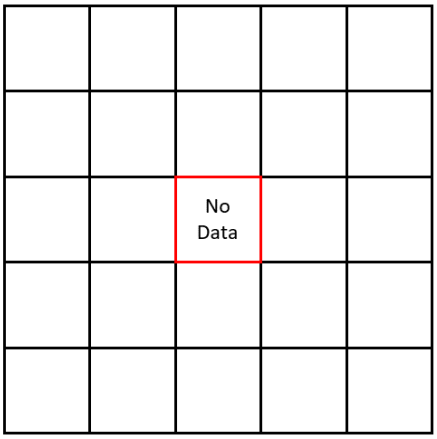

Figure 55: Neighbouring cells included in the interpolation of the missing data.

Appendix B

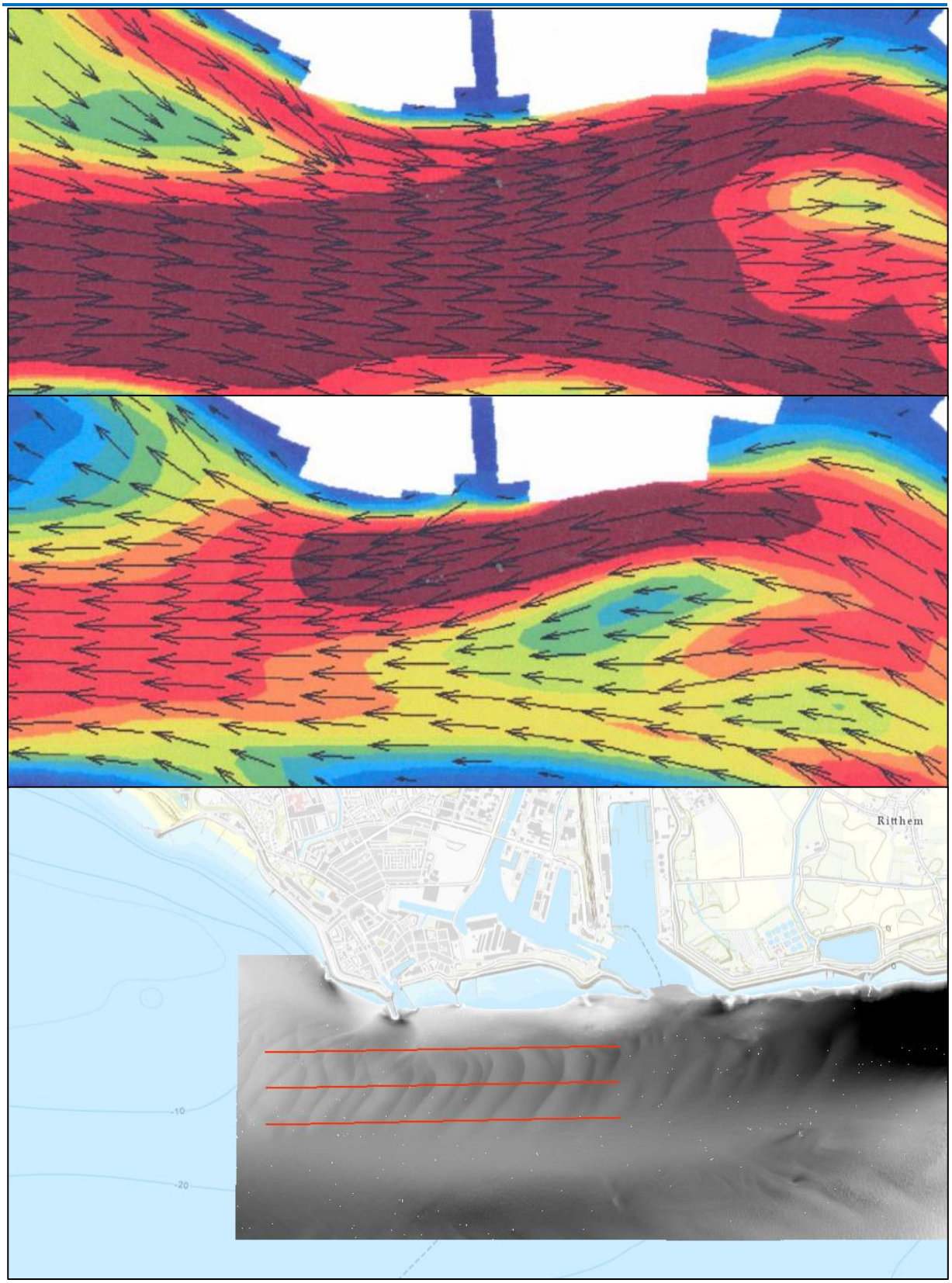

***Figure 56: Determining the direction of the transects for the Vlissingen study location (bottom) based on the depth-averaged flow direction at peak ebb-(middle) and flood (top) flow* (Rijn, 2011).**

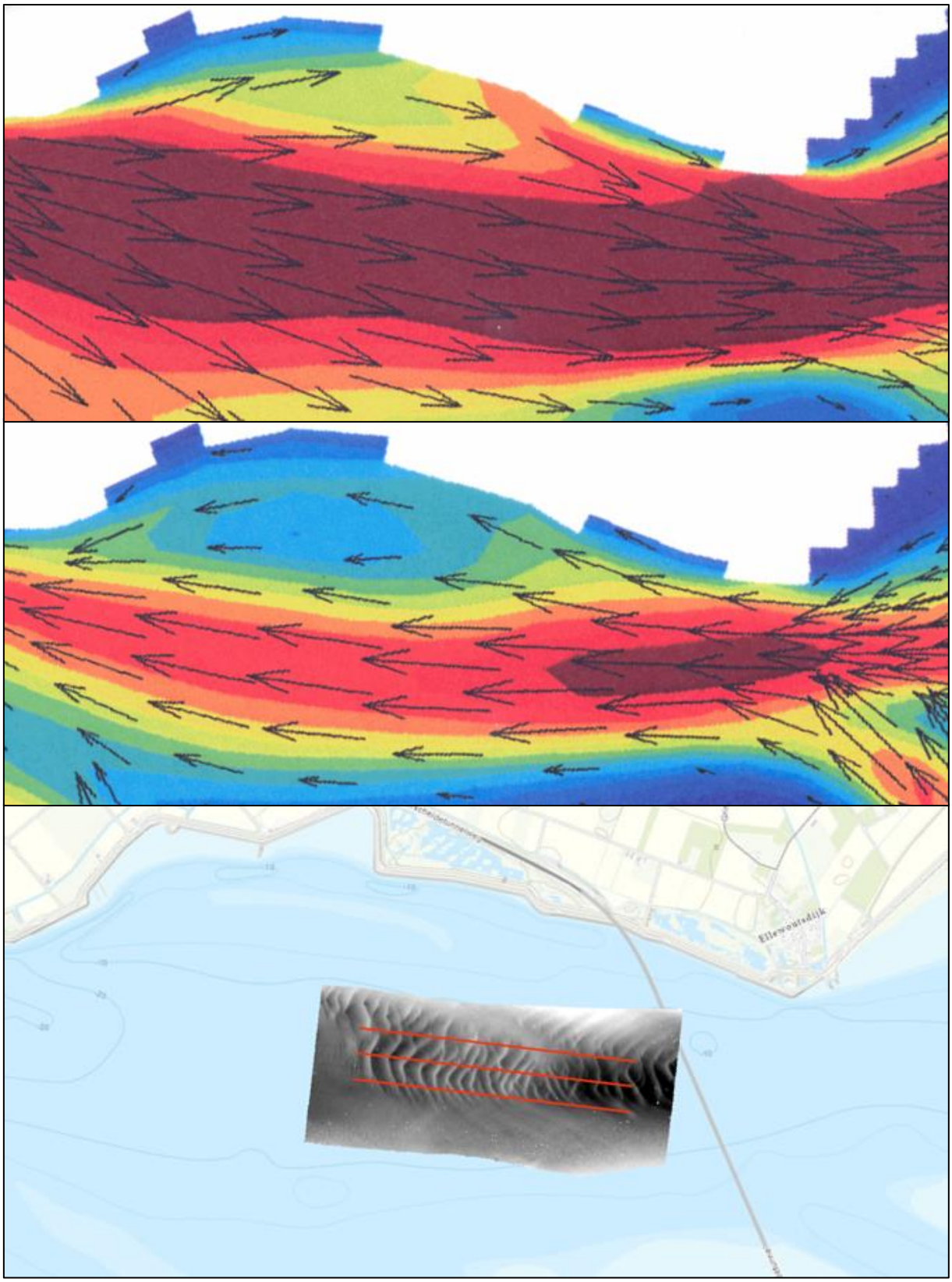

Figure 57: Determining the direction of the transects for the Borssele study location (bottom) based on the depth-averaged flow direction at peak ebb- (middle) and flood (top) flow (Rijn, 2011). Please note that the pictures are rotated to fit the page. I.e., upward direction does not denote north.

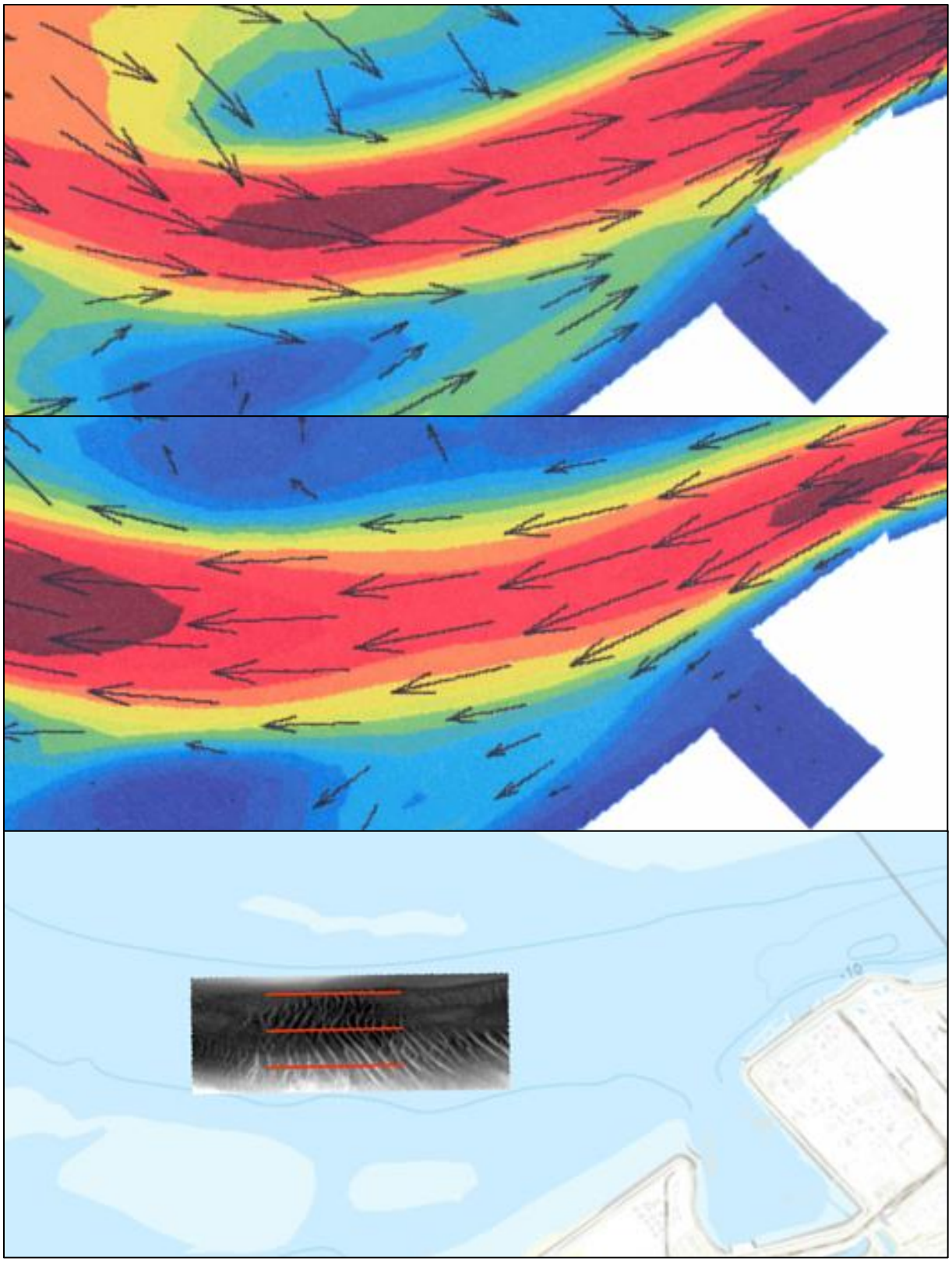

Figure 58: Determining the direction of the transects for the Terneuzen study location (bottom) based on the depth-averaged flow direction at peak ebb- (middle) and flood (top) flow (Rijn, 2011). Please note that the pictures are rotated to fit the page. I.e.., upward direction does not denote north.

Appendix C

A tool is developed in python which is able to extract bed elevation profiles over the width of the field and export them to Excel. This tool asks the user to input a shapefile containing three polylines: one identifying the centre axis of the dune field and two polylines identifying the edge of the study location on either side of the centre (Figure 59.1). All three of these polylines are in the direction as determined by in Appendix B. Furthermore, it is important to note that the polylines and the bed elevation profiles are always set up such that they are in the downstream direction. In other words, the first point of a polyline or extracted bed elevation profile is always the upstream end while the last point is always at the downstream end. Based on the three created polylines, the tool identifies which of the polylines is the left and the right side of the dune field. With the left and the right side, the four corners of the field can be determined (Figure 59.2). Then, using Pythagoras and the location of the dune field corners, equidistant points are created along the starting and ending edge of the dune field (Figure 59.3). These points have an intermediary distance equal to the grid size of the underlying grid. The first point along the starting edge is coupled with the first point on the ending edge. Again, Pythagoras is used to create equidistant points along the line connecting the starting and ending point with an intermediary distance equal to the grid size of the underlying raster. This is repeated for all couples of starting-ending points to create a matrix containing the equidistant points (Figure 59.4). A visualisation of this process just described is given in Figure 59.

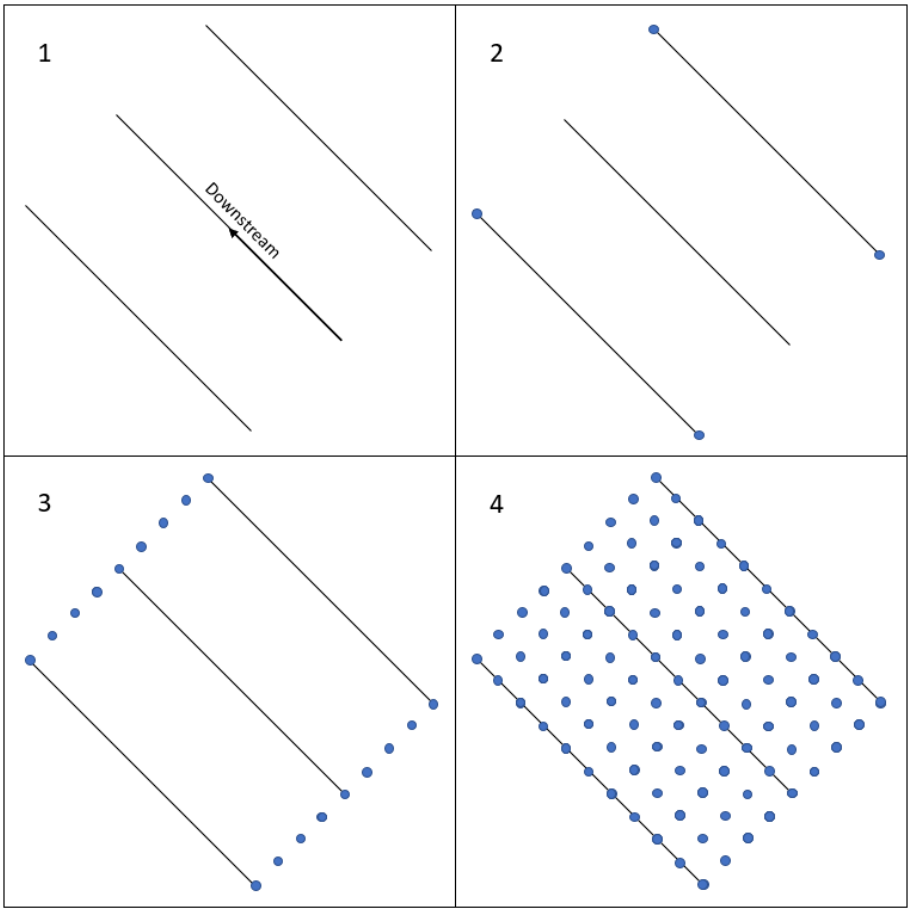

Figure 59: Schematic representation of the steps executed to extract the transects for the Western Scheldt study locations.

In the created matrix, the longitudinal and lateral location in the dune field is captured by the rows and columns, respectively. This matrix is used to extract the bed level values from the raster file. To accomplish this, the raster layer containing the bed level data is first converted into a matrix itself using the “raster to numpy array” toolbox. Combining the corner coordinate of the raster layer, the coordinates of the equidistant points and the cell size of the raster, the bed level at these equidistant points can be extracted. This results in a matrix containing the bed level values at the points which were created. Finally, this matrix is exported to Excel such that it can further be processed in Matlab. In essence, this Excel file contains a resampling of the dune field which is rotated to be in line with the streamwise direction as determined in Appendix B.

Appendix D

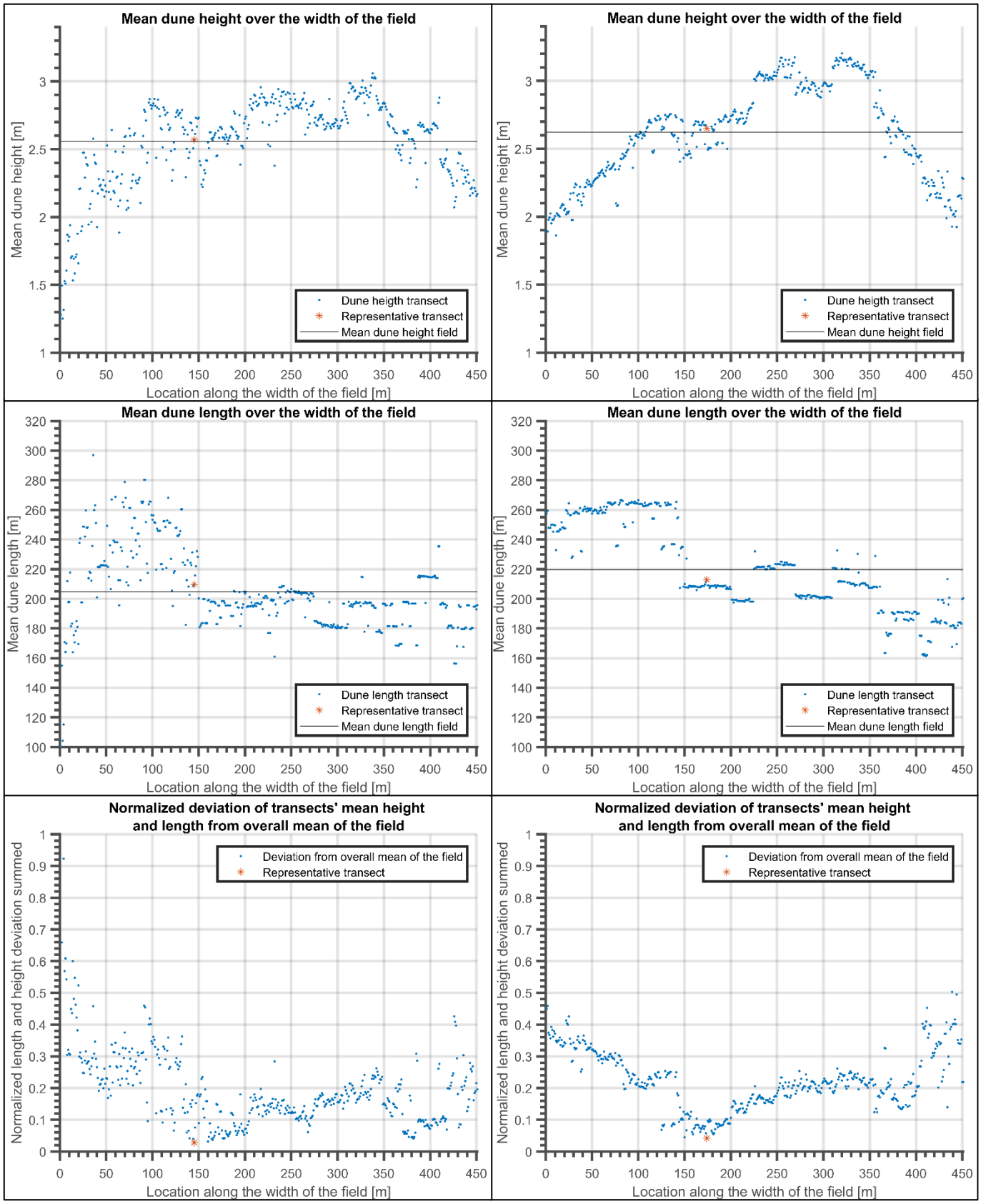

Figure 60: Determining the representative transect for the Vlissingen study area in 2018 (left) and 2019 (right).

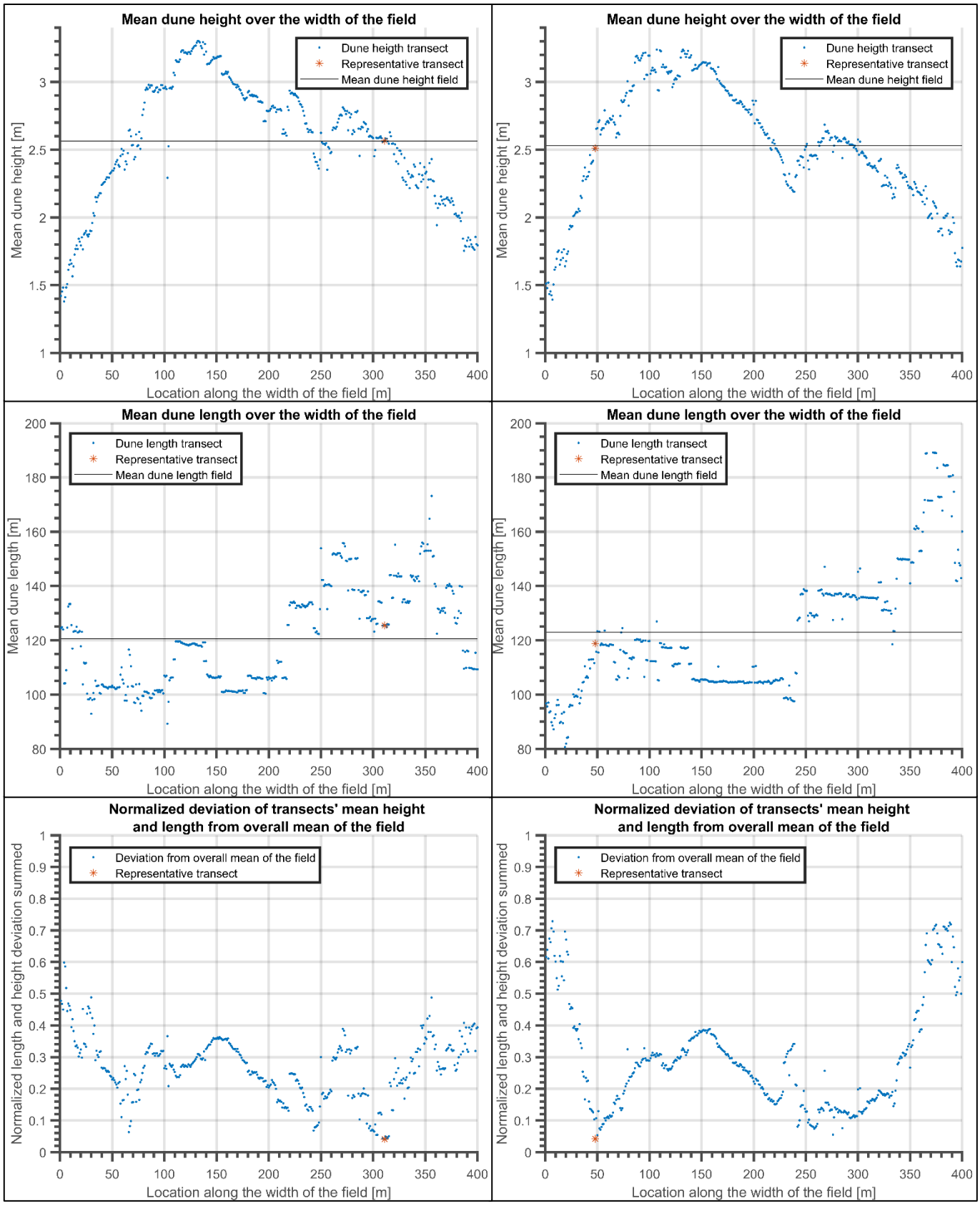

Figure 61: Determining the representative transect for the Borssele study area in 2017 (left) and 2019 (right).

Figure 62: Determining the representative transect for the Terneuzen study area in 2017 (left) and 2019 (right).